IMPROVING PERFORMANCE CHARACTERISTICS OF POLY (LACTIC ACID) (PLA) BASED NANOCOMPOSITES BY ENHANCED DISPERSION OF MODIFIED CELLULOSE NANOCRYSTALS (CNCS)

A Dissertation
Submitted to the Graduate Faculty
of the
North Dakota State University
of Agriculture and Applied Science

By

Jamileh Shojaeiarani

In Partial Fulfillment of the Requirements
for the Degree of
DOCTOR OF PHILOSOPHY

Major Department:
Mechanical Engineering

October 2018

Fargo, North Dakota

North Dakota State University
Graduate School

Title

Improving Performance Characteristics of Poly (Lactic Acid) (PLA) Based Nanocomposites by Enhanced Dispersion of Modified Cellulose Nanocrystals (CNCs)

By

Jamileh Shojaeiarani

The Supervisory Committee certifies that this ***disquisition*** complies with North Dakota State University's regulations and meets the accepted standards for the degree of

DOCTOR OF PHILOSOPHY

SUPERVISORY COMMITTEE:

Dilpreet S Bajwa
Chair

Ghodrat Karami

Long Jiang

Sreekala G Bajwa

Nicole M Stark

Approved:

11/2/2018 — Date

Dr. Alan R. Kallmeyer — Department Chair

ABSTRACT

Poly (lactic acid), (PLA) is a biodegradable and biocompatible polymer which has attracted significant attention as a promising substitute for petroleum-based polymers. To optimize the usage of PLA in a wide range of applications, different methods such as polymer blending and the incorporation of traditional and nanofillers have been extensively explored. Cellulose nanocrystals (CNCs), rod-like nanoparticles with a perfect crystalline structure, are considered as outstanding reinforcing agent owing to the excellent mechanical properties. The optimal characteristics of CNCs as a reinforcing agent in the polymer can be achieved through homogeneous dispersion within the polymeric matrix. However, the strong hydrophilic character of CNCs due to the presence of hydroxyl groups on the surface restricts the uniform dispersion of CNCs in the PLA matrix. In this work, three surface modification treatments along with two different mechanical preparation techniques were employed to improve the dispersion quality of CNCs in the PLA matrix. Polymer adsorption, green esterification, and time-efficient esterification were used as surface modification treatments. Solvent casting and spin-coating method were employed to prepare highly concentrated CNCs masterbatches. Nanocomposites were prepared using melt extrusion, followed by an injection molding process. The morphology of masterbatches indicated better CNCs dispersion through spin-coated thin films, suggesting a high evaporation rate and the effect of centrifugal force and surface tension in the spin-coating process decrease the possibility of CNCs aggregate through the film. Consequently, nanocomposites manufactured using spin-coated masterbatches exhibited higher mechanical strength in comparison with solvent cast ones. In the case of surface modification treatments, the most uniform CNCs dispersion was observed in the nanocomposites reinforced by valeric acid through esterification technique. Higher thermal stability was also achieved through the

application of esterification technique. This observation was related to the presence of DMAP on the surface of CNCs which turns into inert materials, prohibiting the thermal degradation. The higher molecular weight and lower molecular number observed in spin-coated samples in comparison with film cast nanocomposites led to the higher damping behavior in spin-coated nanocomposites. This observation indicated the more viscoelastic properties in spin-coated samples owing to the presence of more polymer chain freedom in spin-coated nanocomposites.

ACKNOWLEDGEMENTS

I am grateful for the support and funding from National Science Foundation, ND EPSCoR (grant No.11A1355466) for conducting this research.

I am deeply grateful to all of those with whom I have had the pleasure to work during my Ph.D. curriculum. The Members of my Dissertation Committee have provided me extensive personal and professional guidance and taught me a great deal about both scientific research and life in general. I would especially like to thank Dr. Dilpreet Bajwa, the major advisor of my committee. As my teacher and mentor, he has guided me and encouraged me to carry on through these years and has contributed to this thesis with a major impact. He has shown me what a good scientist (and person) should be. Thank you as well for guiding me, often with big doses of patience, through the subtleties of scientific writing.

I am also grateful to Ashkan Eslaminejad for his unfailing assistance and very valuable comments on this dissertation.

Nobody has been more important to me in the pursuit of this project than the members of my family. A very special word of thanks goes for my parents, Hossein and Pari, whose love and guidance are with me in whatever I pursue. I wish to thank my loving and supportive husband, Ali who provides unending inspiration and always shows how proud he is of me.

DEDICATION

To my Parents

To my Husband

To my Siblings

Thank you for your unconditional love and encouragement.

TABLE OF CONTENTS

LIST OF TABLES

LIST OF FIGURES

LIST OF ABBREVIATIONS

BA .....Benzoic Acid.

CNC .....Cellulose Nanocrystals.

CNF.....Cellulose Nanofibers.

DMA .....Dynamic Mechanical Analyzer.

DSC.....Differential Scanning Calorimetry.

DTG .....Derivative Thermogravimetric.

FTIR.....Fourier-Transform Infrared Spectroscopy.

GPC.....Gel Permeation Chromatography.

MFI .....Melt Flow Index.

M_n.....Molecular number.

M_w/M_n .....Dispersity Index.

M_w .....Molecular weight.

PEO.....Poly Ethylene Oxide.

pH.....potential Hydrogen.

PLA .....Poly(lactic acid).

RH.....Relative Humidity.

TGA .....Thermogravimetric Analysis.

THF.....Tetrahydrofuran.

LIST OF SYMBOLS

°C .....Celsius.

Eq .....Equation.

h.....Hour.

ΔH_c .....Crystallization enthalpy.

ΔH_m .....Celsius.

ΔH_m^0.....Celsius.

J/g .....Joule/gram.

kg .....kilogram.

kJ/m^2 .....kilojoule/square meter.

kN .....kilo Newton.

mm .....millimeter.

mm/min .....millimeter/minute.

MPa .....Mega Pascal.

T_{onset} .....Initial decomposition temperature.

T_{peak} .....Temperature of maximum weight loss rate.

T_g.....Glass transition temperature.

T_m .....Melting temperature.

W% .....Total weight loss.

wt% .....Weight percent.

X% .....Degree of crystallinity.

T_c.....Cold crystallization temperature.

T_{endset} .....Temperature at the end of the thermal degradation.

γ.....Shear rate.

η .....Viscosity.

G'..Storage modulus.

G''..Loss modulus.

1. INTRODUCTION

1.1. Motivation

Poly(lactic acid), (PLA) with Lactic acid as monomer is an aliphatic polyester obtained from renewable resources like corn, wheat, and potatoes (Figure 1.1). Lactic acid produced by carbohydrate fermentation or chemical synthesis has two optically active configurations, l-lactides and d,l-lactides [1]. Poly-condensation and ring opening polymerization are two chemical routes which have been developed to convert lactic acid to PLA. Considering the origin of PLA, there are three different isomeric forms of PLA. Poly(meso-lactide) or poly(DL-lactide) which is an amorphous grade of PLA (A-PLA) and the other two are poly (L-lactic acid) (PLLA) and poly (D-lactic acid) (PDLA), are homo-crystalline in nature [2].

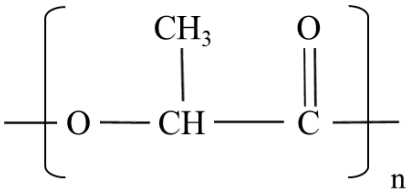

Figure 1.1. Chemical structure of PLA.

Amorphous PLA with glassy and transparent clarity can easily dissolve in most organic solvents such as tetrahydrofuran (THF), chloroform, acetonitrile, and benzene. While, crystalline PLA only can be dissolved in chlorinated solvents under the specific condition like high temperature [3].

PLA is considered as a biodegradable and viable substitute for petroleum-based synthetic polymers. It is the most widely used bio-based polyester due to its superior mechanical properties, thermal properties and processability compared to petrochemical polymers like polypropylene and polyethylene [4]. However, high crystallinity, high permeability, brittleness,

high cost, low availability, and limited molecular weight of PLA had limited its commercial application in industry [5].

PLA can be processed by different methods such as film extrusion, injection molding, melt processing, foam, blow molding, fiber spinning, and thermoforming. In which, the melt processing is the main conversion method for PLA. The thermal stability of the polymer in all different processing methods has the main role in preventing the degradation of the polymer [6]. PLA has a melting point and glass transition temperature of about 173 and 55 °C, respectively. Degradation at temperatures above 200 °C has been reported for PLA. In general, PLA degradation under environmental condition follows a complicated process and depends on different parameters such as molecular weight, temperature, moisture and residual catalyst or solvent [7].

To address PLA deficiencies, there are several PLA modification methods to optimize it for specific applications and to increase its ability in diverse applications. The most common methods are, polymer blending, and nanocomposite technology [8]. The blending of different polymers can result in miscible or immiscible solutions, depending on whether the polymer chains of the two components form a homogeneous single phase or phase separates into individual domains of the two components [9]. Miscible or compatible polymer blends properties follows the rule of the mixture in which the final properties of blends is typically an average of the properties of the individual components and consequently fewer issues of appearance, the directionality of properties, and rheology can be altered by blending the appropriate type and amounts of polymers [9]. Polyethylene oxide (PEO), polyolefin and polyvinyl acetate (PVA) are some examples of different polymers which have been used to blend PLA [10, 11].

The application of nanofillers is another method for improving the properties of PLA. In nanocomposite technology, nanofillers in the size range of 1–100 nm, with high specific surface area can be incorporated to PLA to enhance the mechanical properties of the nanocomposite [12]. In this method, the resin takes advantage of reinforcement application of nanomaterial [13]. The morphology of nanofillers dispersion has a significant role on the performance characteristics of the final composite and critically affects the physical and mechanical properties [14]. Hydrophobicity and polar nature of PLA limits the incorporation of different nanofillers and reinforcements and results in nonuniform dispersion [15]. Increasing the compatibility between PLA and different nanofillers have been studied and there are many published articles on improving nanofiller dispersion in PLA [16-19].

Facing the necessity to decrease the negative effects on the environment caused by the accumulation of petroleum-based polymer waste, the research efforts of material scientists have focused on the development of new nanofiller materials based on biopolymers, capable of degrading under natural conditions without leaving toxic or harmful waste in the environment.

Over the last several years, nanocellulose and in particular, cellulose nanocrystals (CNCs) have received much attention for the production of fully-renewable and biodegradable nanocomposites. CNCs exhibit a number of outstanding and encouraging properties in several applications, including packaging, automotive and biomedical sector.

CNCs are natural nanofillers derived from cellulose. Cellulose, a high molecular-weight (162 g/mol or more) linear homopolysaccharide, is the most abundant organic compound available on the earth and is the primary structural component of the cell wall of various plants, and many forms of algae and the oomycetes.

Cellulose is a complex ordered carbohydrate polymer in a hierarchical structure of elementary crystallites which forms the fibers via hydrogen bonding [20]. Regardless of the source, cellulose is a linear homopolymer composed of β-1,4-linked glucopyranose units; in which every monomer unit is corkscrewed at 180° with respect to the adjacent unit (Figure 1.2).

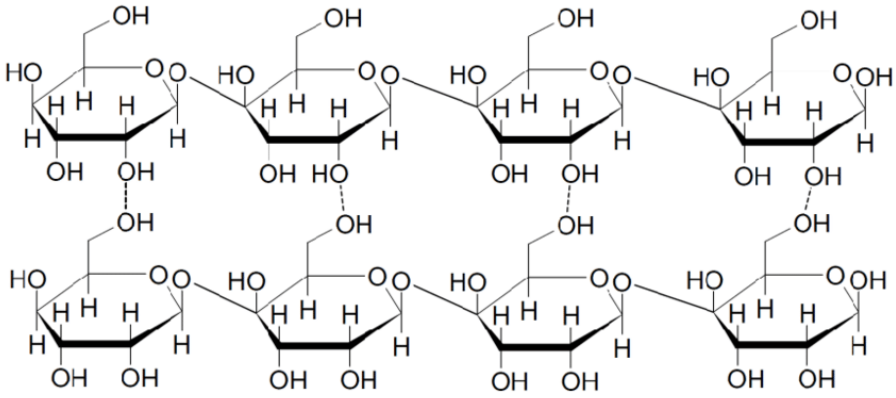

Figure 1.2. Schematic representation of a cellulose molecule.

Cellulose can be transformed into micro or nano-scale products with different shape and crystallinity using different methods such as acid hydrolysis, combined mechanical shearing and enzymatic hydrolysis [21-25]; in which, the amorphous or disordered regions of cellulose is hydrolyzed, and the crystalline regions with higher resistance to acid attack remain intact and results in cellulose nanocrystals (CNCs) [26-28]. Source of cellulose and acid hydrolysis conditions both influence the properties of CNCs [29, 30]. In general, CNCs with a strength over 10 GPa and the elastic modulus of 150 GPa [31] have attracted a lot of attention as a reinforcing agent and have been employed in nanocomposite, soft-tissue replacement, and food packaging industry for several decades [25, 32, 33]. Each glucopyranose unit within the CNCs chain carries three hydroxyl groups, which govern cellulose characteristic properties such as hydrophilicity (Figure 1.3). Hydroxyl group located at C_6 is primary alcohol and at C_2 and C_3 are secondary alcohols. It has been reported that the hydroxyl group located at position 6 as shown in Figure 1.3 has reactivity ten times higher than the other hydroxyl group [34].

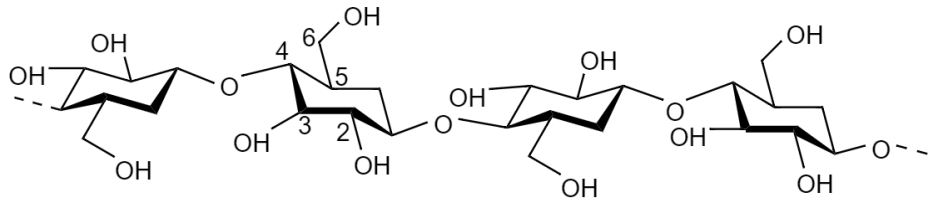

Figure 1.3. Hydroxyl group on the cellulose surface.

The strong hydrophilic character of cellulose nanocrystals due to the presence of free hydroxyl groups on the surface of CNCs restricts the application of different solvents processing medium for solution blending [35]. The dispersion of CNCs into hydrophobic and water insoluble polymer is a big issue. Several techniques have been experimented to decrease the affinity for moisture and improve the compatibility with a nonpolar polymer. The presence of hydroxyl groups on the surface of CNCs provides an opportunity to engineer its surface with different surface modification techniques and alter the hydrophilicity and improve the compatibility with different nonpolar polymer matrices [36, 37]. Much research has been devoted to moderate the hydrophilicity of CNCs using physical and chemical modifications [38].

1.1.1. Problem Statement

The incorporation of CNCs into the polymeric matrix is known to improve the mechanical properties of composites due to a large increase in the interfacial contact area between the polymeric matrix and CNCs. The presence of strong interfacial adhesion between nanocomposite components can contribute to an effective stress transfer from matrix to nanofillers and consequently lead to a highly improved mechanical strength of the resulting nanocomposites. In general, it is well known that the optimum improvement of PLA-CNC nanocomposites can be achieved through the uniform dispersion of CNCs in PLA matrix [15, 39, 40]. Thereby, CNCs dispersion and interaction with the polymer matrix are critical for reinforcement purposes. However, the strong hydrophilicity and the polar nature of CNCs

inhibits the homogeneous dispersion in the most nonpolar polymer matrices such as PLA. The formation of CNCs aggregates in PLA matrix and phase separation results from poor dispersion of CNCs which hinders the improvements in the mechanical performance of the nanocomposites [41, 42]. To overcome this problem, many different approaches have been extensively studied to promote the dispersion of CNCs within relatively hydrophobic PLA matrix and to improve the interfacial interactions between CNCs and PLA matrix. Most studies have focused on the improvement of the CNCs dispersion through the PLA matrix using CNCs surface modification methods [43-46]. In addition, several investigations showed improvement in the CNC's homogeneous dispersion through the polymeric matrix using different manufacturing process [47-50].

1.2. Research Approach

This research focused on the application of CNCs as a renewable nanofiller in improving the performance characteristics of PLA. The main emphasis was given to the dispersion quality of CNCs. This PhD. dissertation aims as investigating different CNCs surface modification treatments along with mechanical processing techniques for improving the dispersion quality of CNCs through PLA matrix. More specifically, this thesis is a study of three surface modification treatments on CNCs to decrease their hydrophilicity character and to improve the compatibility between PLA matrix and CNCs. The main focus was given to the application of green chemicals in CNCs modification.

Along with surface modification treatments, masterbatch approach was considered as a mechanical preprocessing technique to improve the CNCs dispersion through PLA matrix. Two different methods were employed for manufacturing CNCs masterbatches. This thesis will expand the existing knowledge in CNCs surface modification and mechanical preprocessing

techniques to potentially improve the performance characteristics of PLA by incorporating modified CNCs.

1.3. Hypothesis and Objectives

1.3.1. Thesis Goal

The goal of this project is to identify the most efficient CNCs functionalization methods and manufacturing process to improve the uniform dispersion of CNCs in PLA matrix, and consequently to improve the performance characteristics of PLA-based nanocomposite. The project was divided into three objectives. The objectives include surface functionalization of CNCs, manufacturing nanocomposites through two different processing techniques, and nanocomposite characterization. Particularly, the study has the following sub-objectives:

1.3.1.1. Sub-Objectives

1. To identify the chemical treatment which improves the uniform dispersion of CNCs through PLA matrix.
2. To prepare masterbatch films through two different methods (solvent casting and spin-coating methods) and manufacturing nanocomposite.
3. To characterize modified and unmodified CNCs, analyzing the effect of surface treatments on modified CNCs, masterbatches, and nanocomposite samples.
4. To study the effect of masterbatch approach on nanocomposites physical and mechanical properties.

1.3.1.2. Thesis Hypothesis

The research is based on the scientific hypothesis that:

1. The surface modified CNCs will uniformly disperse in the PLA matrix.
2. Incorporating modified CNCs into PLA can improve PLA performance characteristics.

3. Different masterbatch preparation methods can result in improved CNCs dispersion through PLA matrix with varying interactions between CNCs and PLA matrix.

1.4. Thesis Structure

This manuscript-based thesis is divided into seven chapters; Chapter one includes a general introduction and problem statement (Chapter 1), a general literature is presented in Chapter two, Chapters three to six of this thesis include the main findings of this research, and Chapter seven contains an overall discussion of the research related to the sub-objectives outlined above. A schematic for the organization of the thesis is presented in Figure 1.4.

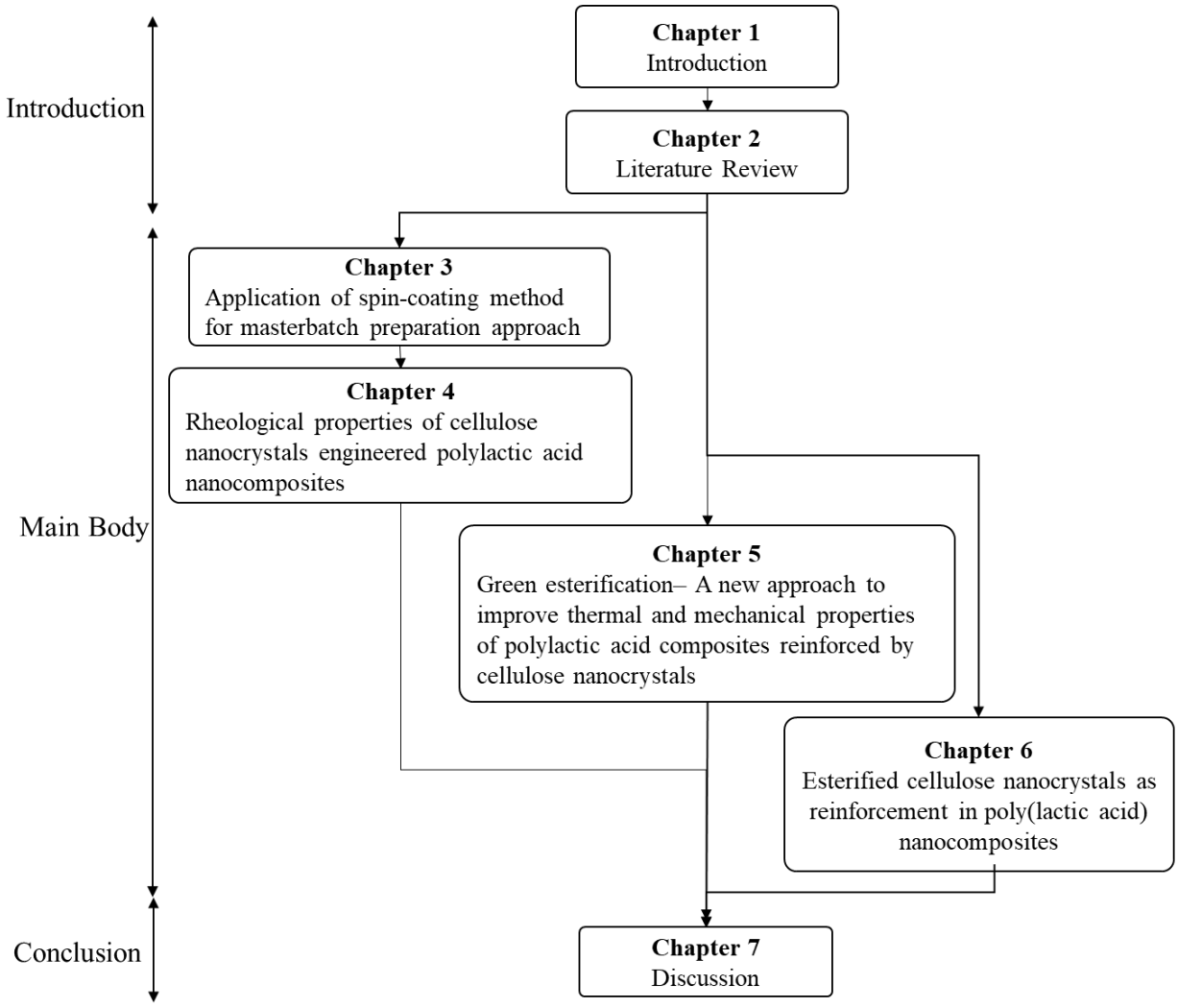

Figure 1.4. Thesis overview and organization of the chapters.

Chapter 1 offers a comprehensive introduction on poly(lactic acid) and cellulose nanocrystals as bio-based polymers. This chapter identifies the current challenges in the commercial application of PLA and CNCs. The objectives and hypothesis of the thesis are also defined.

Chapter 2 presents a comprehensive literature review, and scientific concepts of PLA and CNCs as promising alternatives for petroleum-based polymers. The parameters affecting the potential application of PLA and CNCs are reviewed.

Chapter 3 presents a paper published in *Carbohydrate Polymers 190 (2018), 139-147*. This chapter provides a comprehensive study on the application of different routes in manufacturing masterbatches. The morphology of masterbatches were evaluated using scanning electron microscopy to illustrate the formation of CNCs aggregates in masterbatch films. Further tests were conducted on corresponding nanocomposites to analyze the CNCs dispersion through PLA matrix.

Chapter 4 provides in-depth information on the rheological properties of PLA-CNCs nanocomposites manufactured through different routes. The effect of different masterbatches preparation techniques on polymer structure was studied in this chapter. The main focus has been given on studying the viscoelastic behavior of PLA-CNCs nanocomposites. A characterization of shear viscosity and flowability of nanocomposites were studied in this chapter. The findings of this chapter have been submitted to the journal of "*Composites Part B: Engineering".* (Conditionally accepted by the journal of *Composites Part B: Engineering*, October 2018).

Chapter 5 is based on a paper published in *Journal of Applied Polymer Science 135 (2018), 46468*. It presents a green esterification treatment method for CNCs surface modification. The application of green esterification method on the mechanical,

thermomechanical and thermal properties of nanocomposites was evaluated using tensile test, dynamic mechanical analyzer (DMA), and thermogravimetric (TGA).

Chapter 6 reports a case study to evaluate the performance characteristics of PLA-CNCs nanocomposites prepared using spin-coated masterbatches. In this study a time-efficient esterification technique was identified to decrease the hydrophilicity character of CNCs and to improve the compatibility between CNCs and PLA matrix. The results presented in this chapter has been submitted to the journal of "*cellulose"*. (Conditionally accepted by the journal of *Cellulose*, May 2018).

Chapter 8 includes significant conclusions including recommendation for further research on PLA– based nanocomposites reinforced by CNCs.

2. LITERATURE REVIEW

2.1. Bionanocomposites

The growing environmental awareness promotes academic and industrial attention in the development of biomaterials with low environmental impact at different applications. Among different type of biomaterials, poly(lactic acid, PLA) has received widespread attention over the last two decades, competing with petroleum-based polymers. A solution mainly developed over the past decade has consisted to incorporating nano-sized reinforcements through the polymer matrix, yielding so-called nanocomposite materials [51]. In this context, a promising number of investigations have been performed on the addition of CNCs into PLA matrix to improve PLA properties for commercial application in the market [42, 52].

Cellulose as the most abundant natural polymer on the earth, have attracted considerable attention [53].Cellulose nanocrystal (CNCs) with a renewable nature is the main structural building block of plant, and can be extracted from wood and plant fibers. Cellulose nanocrystals are ordered inherently in a crystalline structure. CNCs with glucose as monomer have three free hydroxyl groups on each anhydro glucose [54, 55]. The superior mechanical characteristics of rod-like shaped CNCs (approximately 50-60 nm long and 5-10 nm wide) make CNCs an interesting nano fillers in various polymer matrices as reinforcement and nucleation agent [30, 56, 57].

Beside the appealing intrinsic properties in CNCs such as high surface area, excellent mechanical properties, unique morphology, low density, and very low coefficient of thermal expansion, it has been claimed that, CNCs displays two main drawbacks, related to its intrinsic physical properties.

1. CNCs possess a hydrophilic character, due to the presence of large number of hydroxyl groups on its surface, which limits the application of CNCs in hydrophobic polymer matrices [58].
2. High hydrophilicity of CNCs results in a high tendency to form agglomerates in petro-chemical polymers.

On the other hand, inherent hydrophilic characteristics, and the presence of large number of hydroxyl groups on the surface of CNCs dictate the dispersion and self-aggregation of CNCs in different solvents [59]. In nanocomposite technology, the homogeneous dispersion of CNCs within the polymer matrix plays a key role in achieving the excellent performance characteristics [13]. To improve CNCs dispersion through different polymer matrix, the modification of CNCs surfaces has been extensively explored. Decreasing the surface energy of CNCs and improving its dispersion quality in different organic solvents have been intensively studied in recent decade to achieve the excellent thermal and mechanical properties in the final products [36, 60]. To improve the quality of CNCs dispersion through polymeric matrix, several surface modification treatments have been introduced [61-63]. As it mentioned before, the abundant hydroxyl groups on the surface of CNCs contribute to special characteristics that it has. In addition, the presence of a large number of hydroxyl groups on the surface, promote the ability of using different surface modification methods. Hydroxyl group located on the sixth position acts as the primary alcohol and most of the modification methods aim to make predominantly change on this hydroxyl group [64].

2.2. Surface Modification Treatment

The number of research studies highlighting the optimum characteristics of CNCs as reinforcing agent in PLA matrix has been growing markedly in recent years. It is reported that

the homogeneous dispersion of CNCs within the polymeric matrix is an essential step for achieving the superior properties of CNCs in composite materials [65, 66]. In addition, the dispersion of CNCs into hydrophobic polymer with water insoluble nature is a big issue. Therefore, several techniques have been experimented to decrease the affinity for moisture of the CNCs and to improve their compatibility with a nonpolar polymer. The presence of hydroxyl groups on the surface of CNCs provides an opportunity for application of different surface modification techniques to alter the hydrophilicity and improve the compatibility with different nonpolar polymer matrices [36, 37]. Much research has been devoted to moderate the hydrophilicity of cellulose nanocrystals using physical and chemical modifications [38].

The application of different chemical-oriented surface modification methods is the most common method to alter the hydrophobicity nature of CNCs and enhance the compatibility between CNCs and nonpolar polymer. There are several surface modifications methods, aim at avoiding irreversible agglomeration of CNCs during drying and aggregation in nonpolar matrices. It was shown that physical adsorption of polymer chains on the surface of CNCs improves dispersibility and thermal stability of nanocrystals as reinforcement in nanocomposites [67-69].

2.2.1. Physical Modification Treatment

Physical surface adjustment can frequently be performed under mellow response conditions, normally in water [70]. The interactions between the physically adsorbed polymer and CNCs are sufficiently strong to stand different conditions which it will be exposed to, such as wide temperature through melt processing and the chemical interaction with different solvents [70].

In polymer grafting method, the small molecules are attached on the surface of CNCs by covalent bounding. Polymer grafting method aims at increasing the polar characteristic of CNCs. In particular, the identical grafted chains and matrix used in grafted method can result in better compatibilization [71]. Gu et al., (2016) studied polymer grafting method and they have introduced Poly (ethylene glycol) (PEG) on the CNCs surface. They reported that PEG has a good compatibility with CNCs and they showed an improved flexibility in PEG coated CNCs as compared with pure CNCs [72]. Arias and his group used PEO aqueous solution to mix with CNCs and improve CNCs dispersion in PLA. They showed that physical adsorption of PEO on the CNCs improve the nano-level dispersion of CNC in the PLA matrix [73].

2.2.2. Chemical Modification Treatment

In the case of chemical functionalization methods, there are five different categories: esterification, oxidation, carboamination, Silylation and cationization. The introduction of small molecules onto CNCs surface is a common part in all five methods. Esterification reaction (Figure 2.1) is a reversible chemical reaction, in which acid anhydrides or acyl chlorides act as acetylating agents. In esterification method an ester functional group (O=C–O) is introduced on the surface of CNCs by condensation of a carboxylic acid group (COOH) and alcohol group (OH). The final reaction product is a less polar chemical [36, 46].

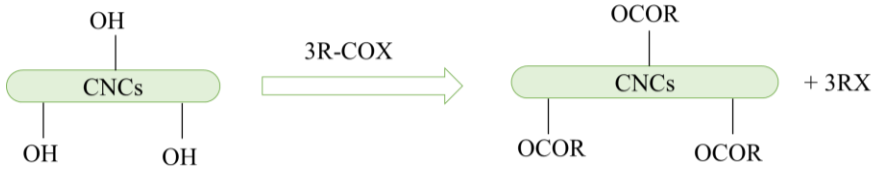

Figure 2.1. Pathway implemented to prepare modified CNCs using a typical esterification reaction.

Spinella et al., (2015) utilized modified CNCs through Fischer esterification as a reinforcement for PLA and they reported higher thermal stability of CNCs from lactic acid modification. Their results also showed higher storage modulus below and above PLA's glass transition temperature for nanocomposite samples [74].

In oxidation method, which was first used to improve the dispersibility of CNCs in aqueous solution, the TEMPO-mediated oxidation is always used to change the surface properties of CNCs and transform the surface hydroxyl groups to carboxyl groups. This transformation might be able to increase the CNCs compatibility with different solvents [75]. Spinella et al., (2016) modified CNCs with natural di- and tricarboxylic acids using two concurrent acid-catalyzed reactions. They observed different crystallinity, morphology in the modified CNCs compared to unmodified ones [46].

Through carboamination method, there is a reaction between isocyano group and hydroxyl group on the surface of CNCs. Using the isocyanate as coupling agent can increase the reaction rate. Phenyl isocyanate (PI), dimethylbenzyl (TMI) and n-octadecyl isocyanate ($C_{18}H_{37}NCO$) isocyanate are three main isocyanates that used for the CNCs modification.

Silylation reaction of CNCs consists on using alkyldimethylsilyl chlorides of different chain lengths with imidazole in toluene. Different organosilane with general formula of RR'R''SiX have been developed as coupling agent. The X functional group is the active component and is involved in the reaction with CNCs [38]. Pei et al., (2010) studied the crystallization and mechanical property of PLA by incorporating CNCs. They modified CNCs by partial silylation through reactions with n-dodecyldimethylchlorosilane in toluene. They claimed that their modified CNCs had a fine dispersion in organic solvents. Higher crystallization rate

and improved tensile modulus and strength of the nanocomposite were observed due to the addition of modified CNCs into PLA [19].

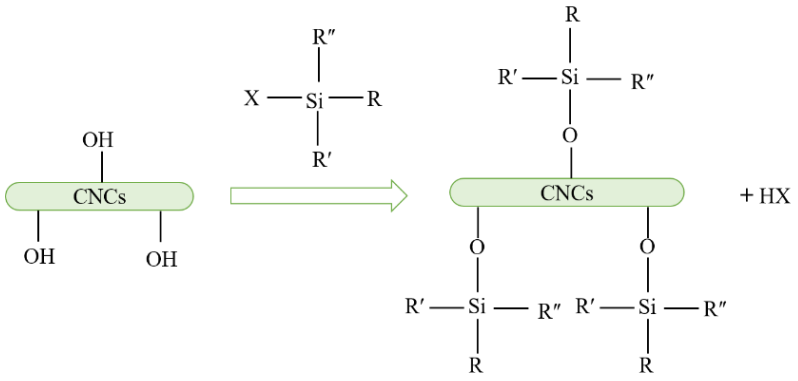

Figure 2.2. Schematic illustration of silylation reaction.

Cationization is another method for CNCs surface modification. In which a cationising agents would introduce to the surface of the CNCs. Glycidyltrimethylammonium chloride (GTMAC) or derivatives have been widely used in this method. The introduction of positive charges to CNCs could be accomplished by grafting ammonium-containing groups. It was reported that cationization method leads to a decrease in surface charge density of the cellulose nanocrystal [36]. It was also reported that cationization method can result in reverse surface charge while the charge density keeps content [76].

2.3. Mechanical Processing Techniques

The need for developing new manufacturing processes capable of scaling up motivated the academia to find out innovative processing techniques. In the literature, two innovative manufacturing processes can be found: the application of liquid feeding and the application of masterbatch approach.

2.3.1. Liquid Feeding

The application of extruder to shape thermoplastic materials dates back to 1935, when the first extruder machine was built by Paul Troester [77]. Since then, it has become the most broadly used processing technique through development of different types of extruders capable of serving in different fields. The dramatic growth in plastic processing industry make it essential to feed solid and liquid phases into extruders. In solid feeding extruders, the forces generate from rotating screw and the stationary barrel move the materials down in the screw channel. In Liquid feeding extruders, liquid can be fed into an extruder through a liquid injection nozzle.

It is reported that the drying process of cellulose nanocrystals results in the formation of irreversible aggregates which cannot be re-dispersed through extrusion process. The application of liquid feeding seems to be a possible option to limit the formation of cellulose nanocrystal agglomerates. The incorporation of liquid and solid phase in an extruder could be difficult and the liquid feed rate as well as liquid temperature need to be monitored carefully, since the liquid temperature can strongly influence the viscosity and the change in liquid viscosity can result in pellet slippage on the barrel wall and consequently form undesirable product [78].

The first report of liquid feeding application of cellulose nanofillers into a polymer was by Oksman in 2006 [79]. The extrusion process was implemented using an extruder equipped by a peridtalic pump which controlled the liquid feeding rate. Two different feeding methods were used: the dry materials were fed into the extruder from a top mounted hopper into the barrel taking advantage from gravimetric feeding and the aqueous cellulose nano whisker suspension was fed into the extruder using vacuum pump to ensure the constant liquid feeding rate. In the extrusion process the existing solvent in liquid phase was removed by atmospheric venting (Zones 7 and 8) as well as vacuum venting (zone 10) (Figure 2.3).

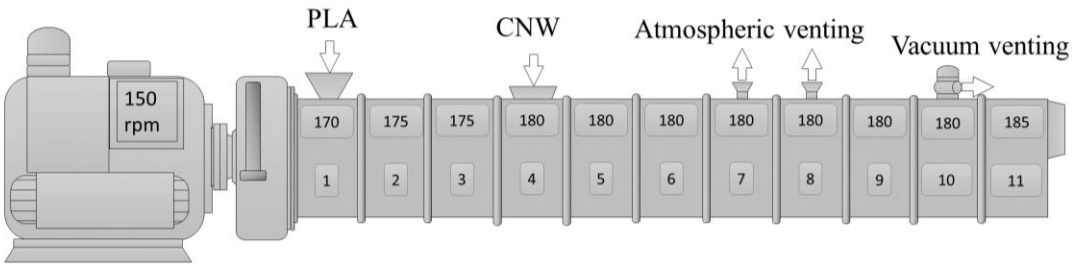

Figure 2.3. Schematic image of extrusion process with liquid feeding [79].

The elaboration of achieving uniformly dispersed cellulose nanowhisker in this work resulted in the generation of high amount of solvent vapor during extrusion process. TEM analysis of the composite samples exhibited partly dispersed cellulose nano whisker into matrix as well as thermal degradation of cellulose nano whisker [79].

In another work similar to cellulose nano whisker liquid feeding, cellulose nanofibers were fed into PLA in a liquid phase. The high viscosity of cellulose nanofiber suspension reduced the uniform dispersion thorough composite samples [48]. The need for a specific extruder capable of feeding liquid and dry matter was reported as an essential need for incorporating liquid cellulose nanofiber into polymer matrix.

2.3.2. Masterbatch Approach

The incorporation of cellulose nanocrystals into different polymer matrix in a step-wise manner is one of the most commonly used preprocessing techniques in nanocomposites preparation. It is reported that the application of masterbatch can maximize the dispersion of cellulose nanocrystals in polymer matrix, however, the time consuming nature is the main weakness of the masterbatch approach [80, 81]. In masterbatch approach, a selective polymer is employed as a carrier for cellulose nanocrystals. The polymer can be either the same or different than the host polymer in the nanocomposite [50, 82-85]. The highly concentrated masterbatches

can be diluted in the extrusion process by adding polymer using the let-down ratio or mixing ratio (CNCs: polymer, generally between 1:14 and 1:20). The let-down ratio is of paramount importance since high mixing ratio might limit the uniform dispersion of CNCs in polymer matrix [86]. Solvent casting and spin-coating are two methods employed in preparing CNCs masterbatches in literature.

Solvent casting has a widespread use in different applications owing to its simplicity and low cost processing [87]. Solvent casting technique contains solubilization, casting and solvent evaporation steps. In solvent casting method, polymer melt, or polymer solution is applied on a flat surface, the solvent is then evaporated leaving a solid film. The evaporation rate of the solvent depends on the boiling point of the solvent, the viscosity of the solution, the pressure and the ambient temperature [88]. The rheological properties of the polymeric solution are of huge importance since the film thickness and the roughness of the film depends on the viscosity of the solution.

The solvent casting is a century-old method for nanocomposite films production and is the most common method for preparing highly concentrated masterbatches. The application of solvent casting in composites manufacturing was reported for the first time by Favier et al., (1995) [89]. In that study a tunicin-based nanocrystals in a latex matrix of poly(styrene-co-butyl acrylate) was studied and the competitive mechanical properties in corresponding composites confirmed the capability of solvent casting technique in composite films preparation. The preparation of thin films with uniform thickness, maximum optical clarity, and low haze were some advantages reported for solvent casting technology [87, 90, 91]. In general, the literature regarding the preparation of cellulose nanoparticles masterbatches involve the solvent casting as the main technique [50, 66, 92]. In solvent casting method, a polymer is first dissolved in a

selective solvent either at room temperature or at elevated temperatures. The nanocelluloses are dispersed in either same or different solvent separately. The application of sonication and homogenization techniques can be used to increase the dispersion of nanoparticles through the solvent prior to the addition into the polymer solution [93]. The solution of polymer and CNCs suspension are then mixed together using magnetic stirrer and then poured into a flat-bottomed glass Petri-dishes and the solvent is evaporated and solidate the films (Figure 2.4).

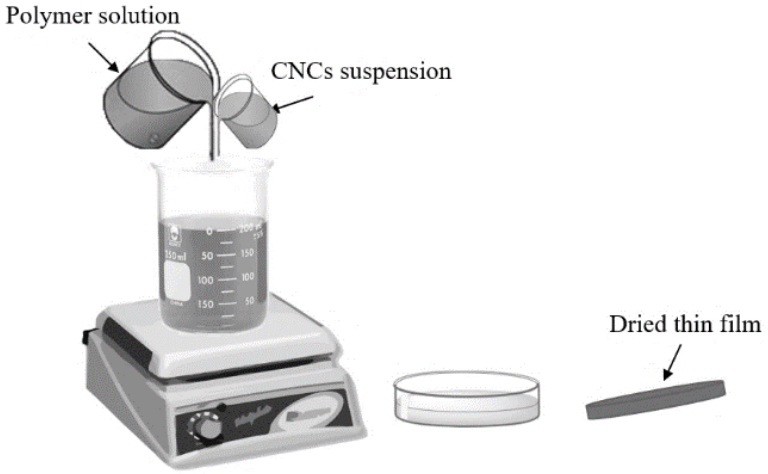

Figure 2.4. Schematic depicting of solvent casting method.

Spin-coating is a common method employed to prepare thin films with thickness in the order of micrometer to nanometers. In this method a liquid is deposited on a substrate which can either be static or rotating at a specific angular velocity [94-96]. The deposited liquid generally consists of volatile solvents and non-volatile solute, and the non-volatile solute forms a thin film after solvent evaporation. Spin-coating involves four consecutive stages: deposition, spin-up, spin-off, and evaporation with some overlap in spin-off and evaporation steps (Figure 2.5) [97]. During spin-off state, a film of liquid tends to spread with a uniform thickness, and after reaching a uniform thickness it tends to remain the uniform thickness. This behavior suggests that mixture viscosity does not depend on shear and it would be constant throughout the substrate [98]. The

equilibrium between centrifugal force generated from rotating substrate and the hydrodynamic (viscous) force evolving from the viscosity of mixture governs the efficiency of the formation of thin films with desirable thickness [86, 99]. In another word, the film forming procedure is mainly influenced by the solution viscosity and the spinning speed. In general, the uniformity of thin film depends on the spinning speed, the concentration of mixture, and the volatility of the solvent [100]. The desired film thickness can be achieved by adjusting the spinning time and speed [101].

The most common application of spin-coating method is in the field of microelectronic thin films preparation. This method was first used by Emil et al., who studied the thin film formation of Newtonian fluid on a rotating substrate [102]. The application of this method in polymer films has been investigated in several theoretical and experimental studies [99, 103, 104].

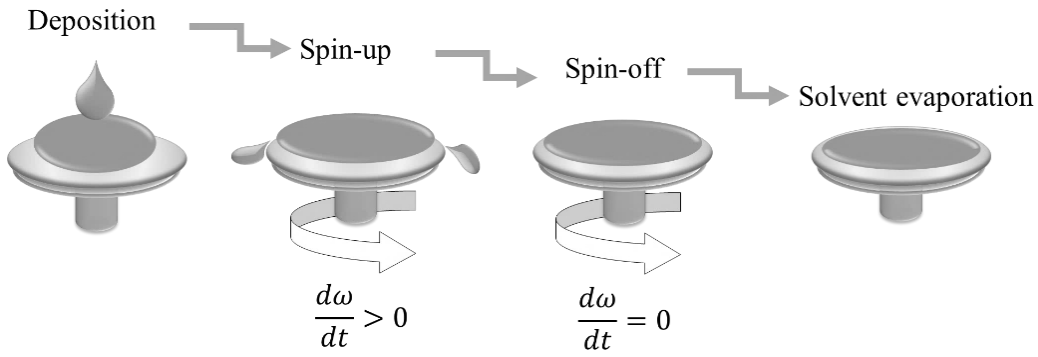

Figure 2.5. Schematic illustration of spin-coating method.

3. APPLICATION OF SPIN-COATING METHOD FOR MASTERBATCH PREPARATION APPROACH[1]

3.1. Abstract

This study systematically evaluated the influence of masterbatch preparation techniques, solvent casting and spin-coating methods, on composite properties. Composites were manufactured by combining CNCs masterbatches and PLA resin using twin screw extruder followed by injection molding. Different microscopy techniques were used to investigate the dispersion of CNCs in masterbatches and composites. Thermal, thermomechanical, and mechanical properties of composites were evaluated. Scanning electron microscopy (SEM) images showed superior dispersion of CNCs in spin-coated masterbatches compared to solvent cast masterbatches. At lower CNCs concentrations, both SEM and optical microscope images confirmed more uniform CNCs dispersion in spin-coated composites than solvent cast samples. Degree of crystallinity of PLA exhibited a major enhancement by 147% and 380% in solvent cast and spin-coated composites, respectively. Spin-coated composites with lower CNCs concentration exhibited a noticeable improvement in mechanical properties. However, lower thermal characteristics in spin-coated composites were observed, which could be attributed to the residual solvents in masterbatches.

Keywords: Poly(lactic acid); Cellulose nanocrystals; Masterbatch; Composites; Solvent casting; Spin-coating.

[1] The material in this chapter was co-authored by Jamileh Shojaeiarani, Dilpreet S. Bajwa, and Nicole M. Stark. Content in this chapter was published in Journal of Carbohydrate Polymers 190 (2018): 139-147. Jamileh Shojaeiarani had primary responsibility for performing the samples preparation and all of the tests. Jamileh Shojaeiarani also drafted and revised all versions of this manuscript. Dilpreet S. Bajwa and Nicole M. Stark served as proofreader, and Dilpreet S. Bajwa supervised the project.

3.2. Introduction

During the past decade, the use of biocompatible and biodegradable materials has grown, primarily motivated by environmental consciousness and use of renewable resources [105]. Among the bio-based polymers, polylactic acid (PLA), which is derived from renewable resource, is widely used for commercial products [1, 2, 106-108]. Its biocompatible nature, relatively high strength, great wrinkle resistance and low toxicity are some beneficial characteristics that make PLA a promising alternative to petrochemical plastics [109-111]. However, its shortcomings such as low impact strength, high brittleness, low tensile elongation, and low heat degradation temperature limit the application of PLA [112-115]. Therefore, numerous methods have been tried to overcome these aforementioned weaknesses by using multiple reinforcing agents [116-119].

Cellulose nanocrystals (CNCs) have attracted great interest due to their biocompatibility, low density, abundance, large surface area, and high strength in the composites field [58, 120, 121]. Incorporation of CNCs in a polymeric matrix is expected to improve the mechanical and barrier properties of the matrix [122-124].

One of the main problems related to the use of CNCs as reinforcing agents is their high hydrophilicity and strong tendency to form aggregates in hydrophobic media [125]. Therefore, several techniques have been experimented to improve the dispersion of CNCs in polymer matrices. The most extended approach to promote the dispersion of CNCs through PLA matrix is the use of surface modification methods. The most widely explored surface modification techniques are acetylation [58, 126], esterification [45, 46], silylation [127, 128] and carboxymethylation [44, 129].

In addition to surface modification methods, several manufacturing processes have been investigated to promote the uniform dispersion of cellulose nanocrystals into hydrophobic polymers. Liquid feeding of cellulose-based nanoparticles into the PLA polymer during the extrusion process and the application of masterbatch films with high nanofiller concentration have been studied to improve the dispersion of nanoparticles in polymer matrix [50, 79, 130].

High concentrated masterbatch is mostly prepared through solvent casting technique. Solvent casting is a century-old methodology for nanocomposite films production. In this method, a polymer is first dissolved in a solvent and then fibers or filler are added to the solution. The solvent is then evaporated leaving behind thin nanocomposite film. Thin films with uniform thickness, maximum optical clarity, and low haze are some advantages of solvent casting technology [87, 90, 91].

Spin-coating method is extensively employed for fabrication of smooth polymeric coatings on flat substrates. In this method, the polymer solution is applied on a substrate which can be either static or rotating at a low speed [94-96]. Spin-coating has also been used to prepare open films of cellulose nanoparticles on different substrates to examine the influence of the substrate on the nanoparticles sub-monolayer [131, 132]. In the spin-coating method, thin films with the thickness of the order of micrometers are spread evenly over the substrate surface owing to centrifugal force and the surface tension of the solution. In this method, solvent evaporates simultaneously as the solution is applied on the substrate [96].

In spite of the broad use of the spin-coating method in thin film preparation, to the best of our knowledge, no one has used this technique for preparing masterbatches. Spin-coating method was introduced for the first time in this paper as masterbatch preparation technique and solvent casting method was considered as the reference method. Modified CNCs were prepared through

physical attachment method introducing poly (ethylene oxide) to attach on the surface of CNCs. Composites were prepared using high shear melt compounding technique through extrusion followed by injection molding process. The agglomeration of cellulose nanocrystals in masterbatches and the corresponding composites were studied using scanning electron microscopy. In addition, crystallinity, thermal properties, and mechanical behavior of resultant composites were studied experimentally.

3.3. Experimental

3.3.1. Materials

Poly (lactic acid) (PLA 2002D, M_n= 98,000 g.mol^{-1}) was supplied by NatureWorks LLC (Minnetonka, MN, USA). Polyethylene oxide (PEO, M_n=106 g.mol^{-1}) was purchased from Sigma-Aldrich (St. Louis, MO, USA). Cellulose nanocrystals (CNCs, dimensions of 150 nm length and 7 nm width) were provided by USDA-Forest Service, Forest Products Laboratory (Madison, WI, USA).

3.3.2. Cellulose Nanocrystals Modification

Physical attachment method was used to improve the interfacial bonding between CNCs and PLA. Poly (ethylene oxide) was introduced as a third polymer component attached to the surface of CNCs. It has been shown that there is an acceptable compatibility between PLA and PEO and the latter can improve the bio-degradation of PLA [9]. Modified CNCs (p-CNCs) were made from an aqueous mixture of 4% CNCs and 1% PEO suspension with the weight ratio of 4:1 (CNCs: PEO). The mixture was then freeze-dried for further use [133, 134].

3.3.3. Preparation of Masterbatch

Chloroform was used as solvent in both methods to dissolve PLA and disperse p-CNCs. Masterbatch thin films with 15 wt% p-CNCs and 85 wt% of PLA were prepared through solvent casting and spin-coating techniques.

In both methods, PLA was dissolved in chloroform (30 wt%) under vigorous stirring at room temperature (24 ºC) until the PLA pellets were fully dissolved. The p-CNCs were dispersed in chloroform (7.5 wt%) using homogenizer (IKA T50 ULTRA-TURRAX, Wilmington, NC, USA) for 5 min and then transferred to an ultrasonic probe (Misonix sonicator 3000; 550W, 20 kHz, Vernon Hills, IL, USA) for 5 min to achieve a stable suspension. The dissolved PLA and dispersed p-CNCs solutions were then mixed together and stirred for 5 hours at room temperature. In solvent casting method, the mixture was directly poured into Petri dishes and chloroform was allowed to evaporate at ambient temperature for 30 hours.

In the second method, a spin-coater machine (WS-400-6NPP-LITE, North Wales, PA, USA) equipped with a vacuum chamber was used. The mixture was loaded in a syringe and injected through a needle (diameter= 500 μm) onto the center of the rotating glass substrate with 100 mm diameter and spread evenly by the combination of centrifugal force and surface tension. To achieve the desired and even thickness of the films, the spinning speed was kept constant at 400 rpm for 180 s. The spin-coated films were dried out simultaneously as the solution was injected onto the substrate. The ultimate thickness of both masterbatch films was approximately 1.12 mm.

3.3.4. Preparation of PLA Composite

Dried masterbatch films were chopped using a paper cutter (ACCO, Columbus, WI, USA) with the approximate size of 4 mm by 4 mm, pre-mixed with PLA pellets and then diluted

to final CNC concentrations of 1, 3, and 5 wt% using a twin-screw extruder (Krauss-Maffei Co., Florence, KY, USA). The barrel temperature for eight zones was set at 157, 157, 165, 162, 162, 162, 160, 160 °C (feed throat to die end), respectively, and the screw speed was set at 170 rpm. The extruded pellets were dried in an oven (Binder ED, Binder Inc., Bohemia, NY, USA) set at 80 °C for 24 h prior to processing in an injection molding machine. Injection molding machine (Technoplas Inc. model SIM-5080) was used to prepare composite samples. Samples were molded for tensile and impact tests according to ASTM D790 and ASTM D638 standards, respectively [135, 136]. All samples including pure PLA and composites went through the same extrusion and molding cycles. The samples obtained from injection molding machine with different material designations and compositions of PLA and p-CNCs are summarized in Table 3.1.

Table 3.1. Codes and composition details of composite samples.

Sample code	PLA (wt%)	CNCs (wt%)	PEO (wt%)	Method
PLA	100	0	0	Virgin
PLA-1CNC-so	99	0.94	0.06	Solvent casting
PLA-3CNC-so	97	2.8	0.2	Solvent casting
PLA-5CNC-so	95	4.7	0.3	Solvent casting
PLA-1CNC-sp	99	0.94	0.06	Spin-coating
PLA-3CNC-sp	97	2.8	0.2	Spin-coating
PLA-5CNC-sp	95	4.7	0.3	Spin-coating

3.3.5. Scanning Electron Microscopy (SEM) of Masterbatch

The dispersion of p-CNCs in each masterbatch films was evaluated using scanning electron microscope (JSM-7600F, USA Inc., Peabody, MA, USA) operating at 15 kV. The SEM images were taken at a magnification of 500 from the cross section of masterbatches.

3.3.6. Scanning Electron Microscopy (SEM) of Composites

The morphology of the impact-fractured surface of composites was examined using a scanning electron microscope (JSM-6010LA, USA Inc., Peabody, MA, USA) with an accelerating voltage of 10.0 kV at a magnification of 100. All samples were attached to the aluminum mounts using carbon adhesive tabs and coated with a conductive layer of carbon in a high-vacuum evaporative coater (Cressington, Ted Pella Inc., Redding, CA, USA).

3.3.7. Optical Light Microscopy

The dispersion quality and degree of self-aggregation of p-CNCs at composite samples was investigated using an optical microscope (Axiovert 40MAT, Carl Zeiss, Dublin, CA, USA). The average size of p-CNCs aggregates through PLA matrix was studied through iSolution DT software. For preparing thin films for the optical microscope, the composite extruded pellets were melted on a glass slide at 150 °C for 10 min and another glass slide was put on the melted samples as a cover glass to prepare a flat thin film for each formulation.

3.3.8. Differential Scanning Calorimeter (DSC)

DSC measurements were performed on DSC Q200 (TA Instruments, New Castle, DE, USA) over a temperature range from 25 to 200 °C at a heating rate of 1 °C/min and then held for 5 min, and then samples were cooled down to 25 °C at a cooling rate of 5 °C/min. The second heating was performed at the same range and heating rate to determine glass transition temperature (T_g), crystallization temperature (T_c), melting temperature (T_m). The Degree of crystallinity of samples were calculated using Eq. 3.1.

$$X_c = \left[\frac{\Delta H_m - \Delta H_c}{\Delta H_m^c}\right] \times \frac{100}{W_{PLA}} \quad (3.1)$$

where ΔH_m, ΔH_c, and ΔH_m^c are the melting enthalpy, cold crystallization enthalpy, and melting heat for pure crystalline PLA (93.6 $J.g^{-1}$) respectively. W_{PLA} is the weight fraction of PLA in the composite sample [137].

3.3.9. Dynamic Mechanical Analysis (DMA)

Thermomechanical behavior of PLA and composite samples were studied using a DMA Q800 (TA Instruments, New Castle, DE, USA) following ASTM D4065 [138]. Measurements were carried out from 25 to 90 °C at a heating rate of 1 °C/min, with a fixed frequency of 1 Hz in a dual cantilever mode.

3.3.10. Mechanical Properties of Materials

Mechanical properties of composites including ultimate tensile strength, elongation at break, and modulus of elasticity were obtained from tensile test. The tensile testing was performed following ASTM D638 standard using an Instron universal testing machine (Model 5567, Norwood, MA, USA) [136]. Since the concentration and dispersion quality of CNCs in the PLA matrix can influence the toughness of the composites, the toughness of samples was calculated following ASTM D256 standard [139]. The tests were conducted on unnotched impact specimens using an Izod impact tester (Tinius Olsen, Model Impact 104, PA, USA).

3.3.11. Statistical Analysis

The mean values and standard deviations of the mechanical properties of the samples were statistically analyzed by ANOVA and Tukey's test (α=0.05). The data was analyzed using Minitab software version 17 (Minitab Inc., State College, PA, USA). Eight replicates were used for each test.

3.4. Results and Discussion

3.4.1. Scanning Electron Microscopy (SEM) of Masterbatch

The prepared masterbatches through solvent casting and spin-coating techniques and their corresponding cross-sectional SEM micrographs are shown in Figure 3.1. The SEM images show that spin-coated masterbatch films exhibited smaller and well-dispersed p-CNCs aggregates in comparison with solvent cast masterbatches in which micrometric CNC aggregates can be observed (Figure 3.1). This behavior can be attributed to the application of centrifugal force through rotating substrate and surface tension against the attractive forces between p-CNCs in spin-coating process which inhibited the formation of p-CNCs aggregates.

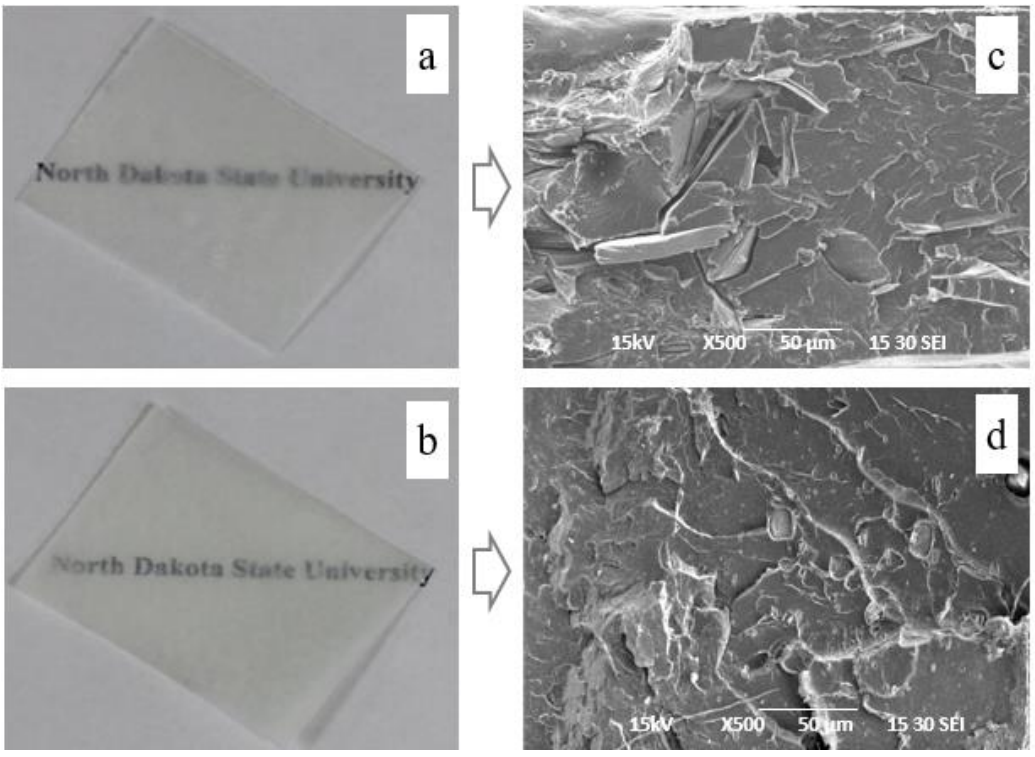

Figure 3.1. Masterbatch films prepared from different methods: (a) solvent casting, (b) spin-coating, and SEM images of masterbatch films: (c) Solvent cast, (d) Spin-coated.

The high evaporation rate and low essential time for vaporizing the solvent from thin films in spin-coating method, limited the movement of p-CNCs through PLA matrix and

inhibited their assembly into micro-sized aggregates. Slower evaporation rate in solvent casting technique allows solvent molecules to exclude the nanoparticles and pushing them into closer proximity and leading to the formation of strong agglomerates. It was also observed that high evaporation rate in spin-coated masterbatches accelerated the drying process and consequently resulting in the formation of the air bubble on the surface of the masterbatch films.

3.4.2. Scanning Electron Microscopy (SEM) of Composites

The impact-fractured surfaces of PLA composites were evaluated using SEM images (Figure 3.2). Some small spherical particles can be observed on the fractured surfaces of solvent cast composites and PLA-5CNC-sp, indicating poor dispersion of p-CNCs through PLA matrix and low interaction between p-CNCs and PLA. However, a good dispersion was achieved in spin-coated composites with low p-CNC contents (1 and 3 wt%). Particularly, no aggregation was detected on the fracture surface of PLA-1CNC-sp (Figure 3.2d). Given that the higher concentration of CNCs can result in greater aggregates [74, 117], we hypothesize that non-uniform dispersion of p-CNCs at the higher concentration can be attributed to inadequate shear or lower residence time in the twin screw extruder. Another factor that contributed to uneven dispersion is evaporation of the residual solvent and high viscosity of p-CNCs as reported in a recent study. It is reported that dispersion of CNCs in liquid feeding is influenced by percentage liquid phase, and liquid feeding rate [48, 140]. In this work, the presence of high amount of residual solvent associated with a large volume of spin-coated masterbatche pellets inhibited the uniform dispersion of 5% p-CNC in PLA matrix during the extrusion process.

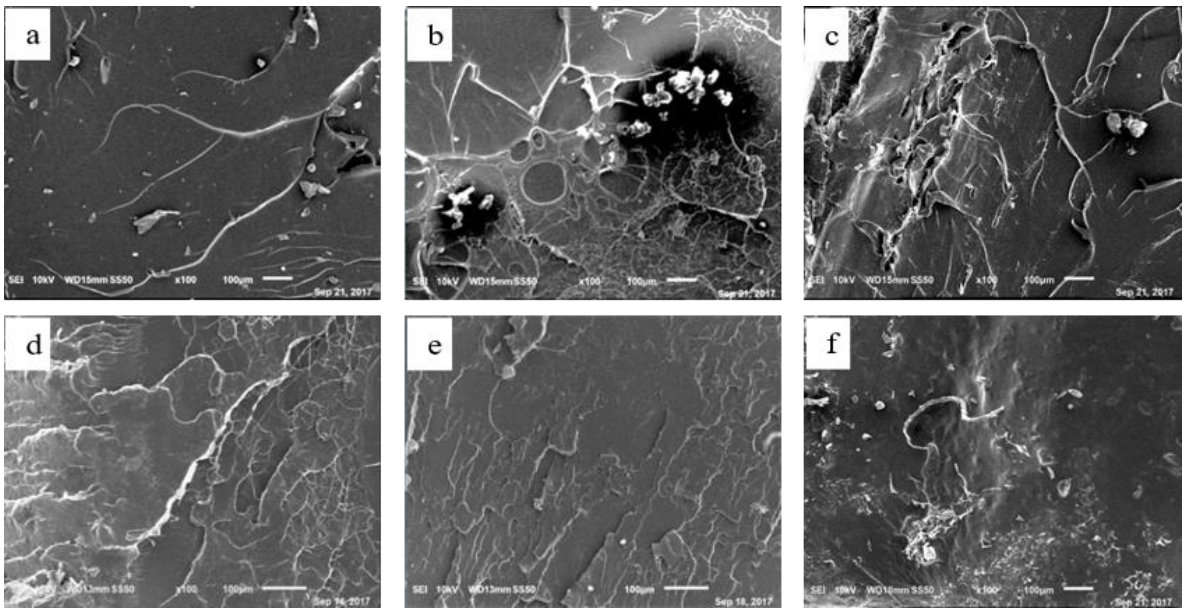

Figure 3.2. SEM micrographs of PLA-CNC composites: a) PLA-1CNC-so, b) PLA-3CNC-so, c) PLA-5CNC-so, d) PLA-1CNC-sp, e) PLA-3CNC-sp and f) PLA-5CNC-sp.

The fractured surface corresponding to PLA-1CNC-sp and PLA-3CNC-sp was rougher and more irregular as compared to solvent cast composites with the same p-CNCs content. In general, the mechanical properties of samples can be correlated with the morphology of the composites and the rough and irregular impact-fractured surface can be an indication of tough materials. The presence of plenty of fracture lines on the impact fractured surface of PLA-1CNC-sp and PLA-3CNC-sp, can be considered as an indication of high toughness in materials [141, 142]. To have more information on samples toughness, impact strength was also studied.

3.4.3. Optical Light Microscopy

Optical microscopy images are illustrated in Figure 3.3. The average size of p-CNCs aggregates increased with increasing the p-CNC loading in composites. The number of relatively big aggregates (>2.5 μm) increased with increasing p-CNC content in composite samples prepared via solvent casting and spin-coating routes.

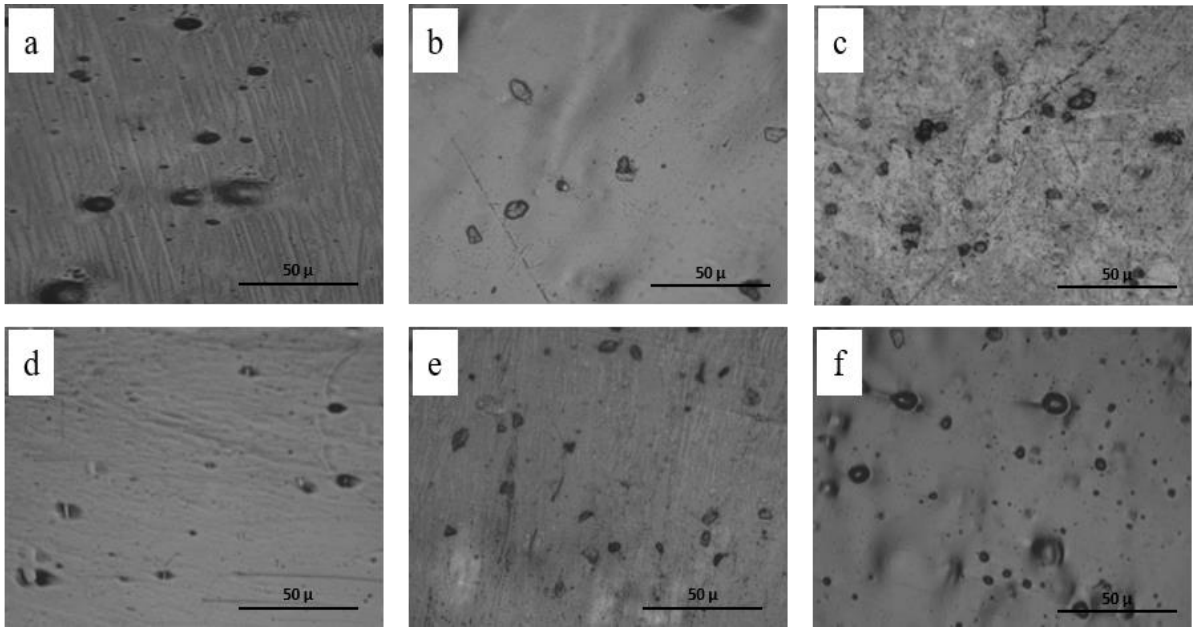

Figure 3.3. Optical micrographs of PLA-CNC composites: a) PLA-1CNC-so, b) PLA-3CNC-so, c) PLA-5CNC-so, d) PLA-1CNC-sp, e) PLA-3CNC-sp and f) PLA-5CNC-sp.

With respect to the agglomeration size, spin-coated composites with 1 and 3% p-CNCs contents exhibited smaller p-CNCs aggregates in comparison with composites prepared using solvent cast masterbatch. This observation can be attributed to well-embedded p-CNCs in masterbatch films which lowered the possibility of forming p-CNCs aggregates in composites during extrusion process (Figure 3.1). However, dispersion was slightly better in solvent cast composites with 5% p-CNCs loading.

3.4.4. Differential Scanning Calorimeter (DSC)

Figure 3.4 illustrates the DSC heating scan thermograms of PLA and composite samples observed from second heating scans. The DSC thermograms show that there is a variation in the exothermic peak value and position related to cold crystallization for different samples confirming that different samples acquire different mobility to rearrange their crystal structure. All samples possessed single crystallization temperature (T_c), proving the presence of single homogeneous phase through the heating process. Interestingly, all samples except PLA-3CNC-sp

and PLA-5CNC-sp possessed melting endotherms with two distinct peaks which can be attributed either to different crystal structures in the composite sample or the melt-recrystallization mechanism [143-145]. The corresponding DSC thermal parameters are listed in Table 3.2. It can be observed that the glass transition temperature (T_g) was shifted to higher values in all composites compared to pure PLA and the average T_g in solvent cast and spin-coated composites increased by 6% and 4%, respectively. The observed differences in the thermal characteristics between composite samples and pure PLA can be attributed to the influence of incorporating p-CNC and chloroform on the actual composition and characteristics of the final products.

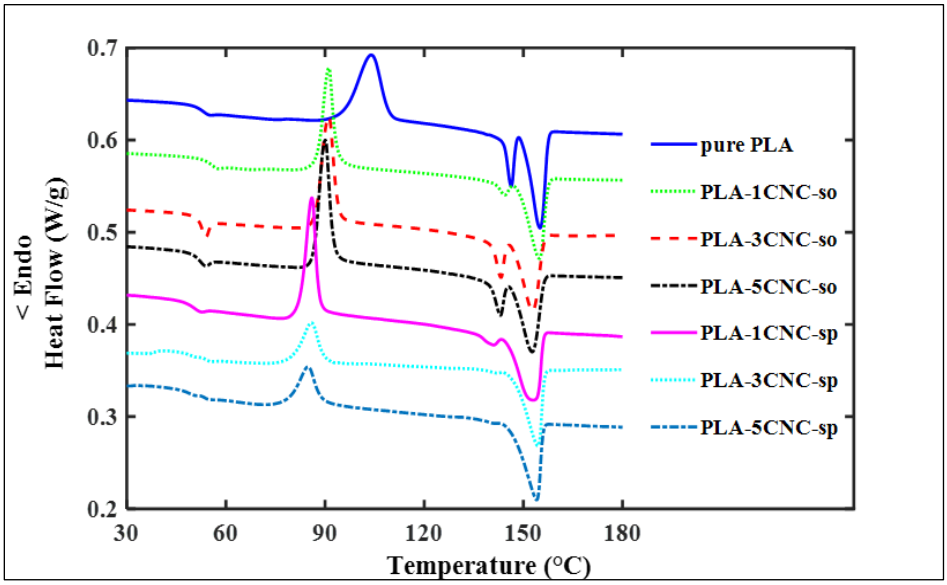

Figure 3.4. DSC curves during the second heating scan of PLA and composites.

The average crystallization peak temperature decreased by 13% and 18% for solvent cast and spin coated composites, respectively. The observed decreases in T_c could be attributed to the influence of PEO incorporation and the presence of residual solvent in the specimens. Amount of residual solvent in each masterbatch right before the extrusion process were measured and the

results showed the presence of 8.65% residual solvent in spin coated masterbatches compared to 1.37 % in solvent cast masterbatches.

Higher decline in T_c was observed in spin-coated composites as compared to solvent cast samples. This behavior can be attributed to the application of well dispersed p-CNCs through PLA matrix as heterogeneous nucleus in lowering the cold crystallization temperature and facilitating the formation of organized structure [146, 147]. In addition, considering the drying process, spin-coated masterbatches dried in less time compared to solvent cast masterbatches, therefore, more decrease in T_c was observed in spin-coated composites.

Table 3.2. Thermal properties of PLA and composite samples.

Sample code	T_g (ºC)	T_c (ºC)	T_m (ºC)	X%
PLA	50.16	103.98	155.06	3.99
PLA-1CNC-so	53.66	91.15	154.88	9.82
PLA-3CNC-so	52.77	91.08	152.84	12.49
PLA-5CNC-so	53.24	90.05	152.68	7.21
PLA-1CNC-sp	50.70	84.29	150.28	11.34
PLA-3CNC-sp	52.33	85.41	155.02	26.38
PLA-5CNC-sp	53.65	84.92	154.52	19.97

For all composite samples, the degree of crystallinity increased significantly with an increase in the p-CNCs content. In solvent cast and spin-coated composites the average degree of crystallinity increased by 147% and 380% in comparison with pure PLA, respectively.

The observed improvement in degree of crystallinity in composites was due to the presence of the p-CNCs and their nucleation effect [148]. In each set of samples, the highest degree of crystallinity was observed in composites with 3 wt% p-CNCs and decreased with increasing p-CNCs content, suggesting the formation of p-CNCs aggregates at PLA-5CNCs.

The observation of higher crystallinity in spin-coated composites as compared to solvent cast samples were in agreement with another research that reported partial crystallization of amorphous molecules in the solvent cast films [91]. More uniform dispersion of p-CNCs in spin-coat composites led to the formation of higher attraction of p-CNCs in PLA matrix and induced a higher nucleation agent effect [18, 111, 149]. As the optical micrographs suggested, the smaller CNCs aggregates in spin-coated composites resulted in a high number of nucleating sites and improving the degree of crystallinity. At solvent cast composites, lower degree of crystallinity was due to p-CNCs' agglomeration in PLA matrix (Figure 3.3).

3.4.5. Dynamic Mechanical Analysis (DMA)

Figure 3.5 illustrates the storage modulus and tan δ as a function of temperature for pure PLA and composites. All samples exhibited a typical behavior of a semi-crystalline polymer with a large drop in storage modulus corresponding to their glass transition region (T_g). It can be observed that the addition of p-CNCs led to an improvement in the storage modulus of composites as compared to pure PLA in the glassy state. In lower p-CNCs contents (1 and 3 wt%), spin-coated composites exhibited higher storage modulus in comparison with solvent cast composites. In particular, storage modulus was increased by 29%, 21%, and 31% with increasing the p-CNCs content in solvent cast samples, and in the case of spin-coated composites it was improved by 49%, 24%, and 4% as compared to pure PLA. These results were in a good agreement with the microscope observations and confirming the better p-CNCs dispersion in spin-coated composites at lower p-CNCs contents.

From DMA results, tan δ peak temperature indicates the glass transition temperatures (T_g) of materials. It can be observed that the addition of p-CNCs slightly shifted the tan δ peaks toward higher temperature, however, the addition of p-CNCs did not have a significant effect on

T_g and all samples exhibited T_g in the regions between 64-67 ºC. In particular, the average T_g increased by 5% and 3% for solvent cast and spin-coated composites. The results on T_g showed that T_g from DSC and DMA observations methods had the same trend.

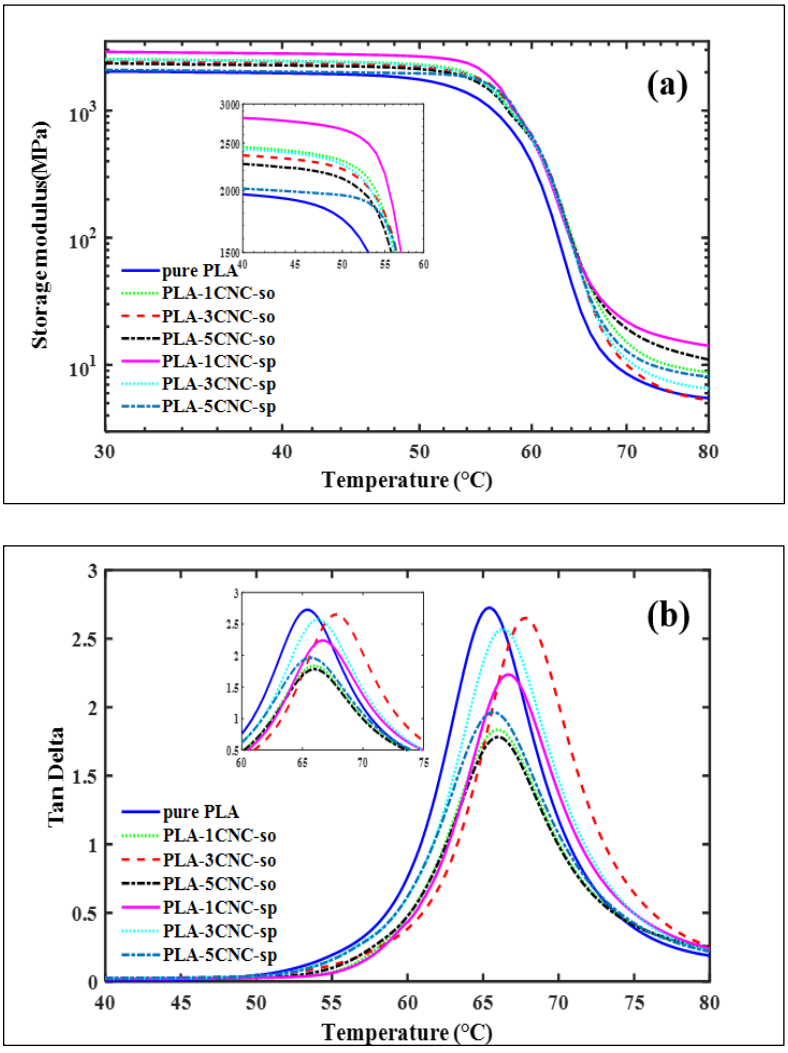

Figure 3.5. Storage modulus (a) and Tan δ (b) as a function of temperature of PLA and composites.

The viscoelastic behavior of samples was examined through the peak values of the tan δ curves in Figure 3.5b. The peak values of the tan δ exhibits the viscoelastic behavior of materials and the dissipated energy by sample through deformation [150]. In composites the lower tan δ peak values indicates the enhancement in interfacial bonding between fibers and matrix [151].

All composites exhibited lower peak value for tan δ as compared to pure PLA. The average peak value for tan δ decreased by 18% and 22% for solvent cast and spin-coated composites, respectively. This result can be attributed to the restrictive effect of p-CNCs through PLA matrix to the segmental motions of the polymer molecules during the transition and resulting in more elastic response of materials [152].

3.4.6. Mechanical Characteristics

In general, the incorporation of p-CNCs increased Young's modulus, tensile strength, elongation at break, and impact strength, although, no significant improvement was observed in the case of Young's modulus and tensile strength for solvent cast composites. Significantly higher Young's modulus and ultimate tensile strength in PLA-1CNC-sp and PLA-3CNC-sp demonstrated that more uniform p-CNCs dispersion in spin-coated composites with lower p-CNCs loadings (i.e. 1 wt% and 3 wt%) has formed a stronger interfacial adhesion between PLA and p-CNCs and resulted in an improvement in mechanical properties of spin-coated composites (Figure 3.2). Similar findings were reported where more uniform CNCs dispersion resulted in higher tensile stress and Young's modulus in PLA- based nanocomposites [80, 153] (Figure 3.6). As already observed on DSC analysis, the incorporation of p-CNCs improved the polymer crystallization in composites and resulted in an enhancement of Young's modulus and tensile strength because the composites' rigidity also improved. In general, the higher the degree of crystallinity, the harder the composite. These results are consistent with previous published works on electrospun bio-nanocomposite mats from PLA and CNCs [117] and PLA-lignin coated CNCs nanocomposites [111], which indicated the same correlation between composite crystallinity and strength.

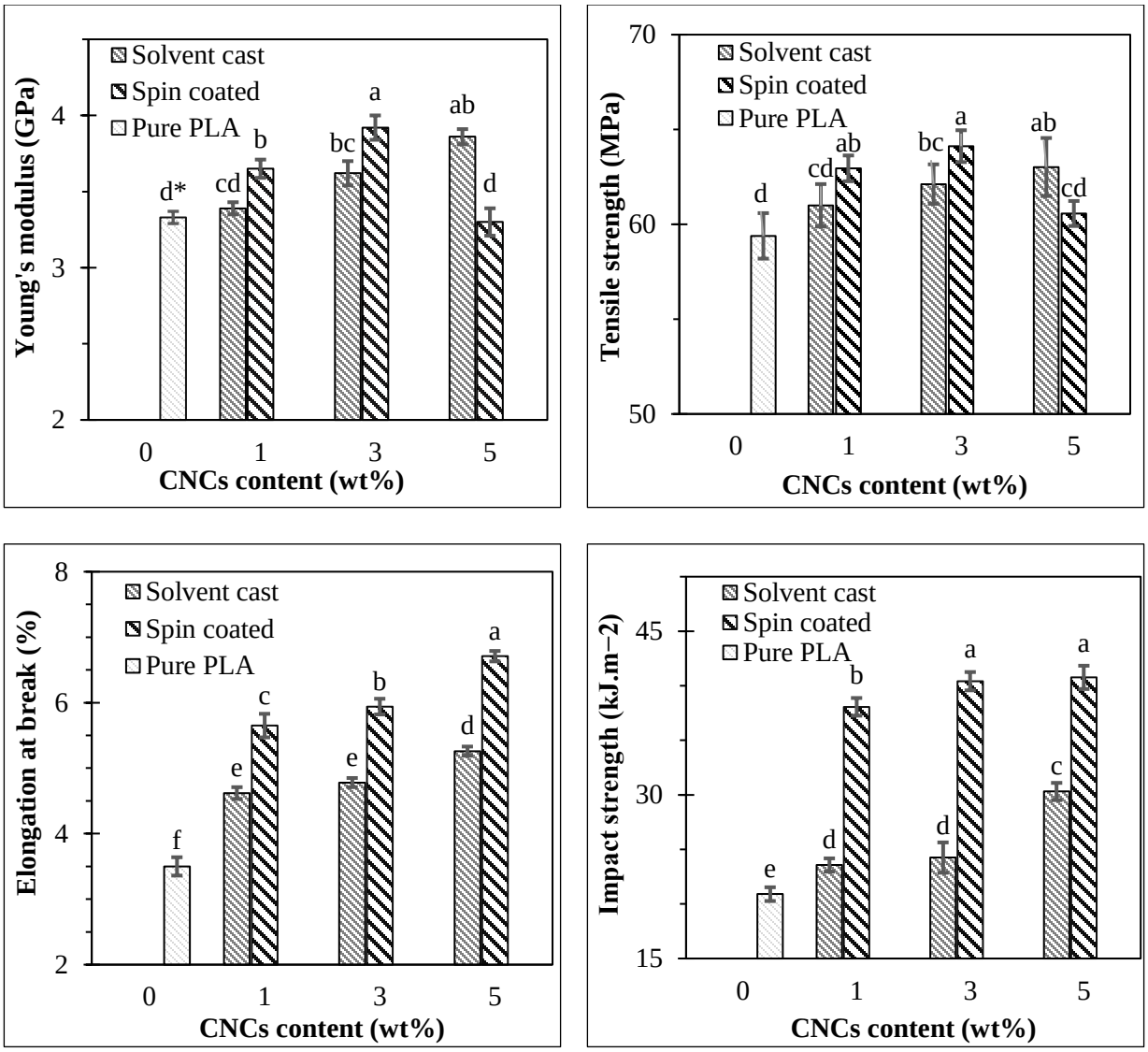

Figure 3.6. Mechanical properties of PLA and composite samples.
(*bars in each graph sharing same superscript letter are not significantly different at 5% significance level).

There was a significant improvement in the elongation at break and impact strength for all composites prepared via spin-coating and solvent casting routes as compared to pure PLA. It is difficult to describe why incorporation of p-CNCs in PLA had so large influence on elongation at break and impact strength since different factors such as structure and incorporation of PEO could affect the mechanical properties of samples. However, similar results have reported by adding cellulose nanowiskers to PLA [79]. In particular, spin-coated composites possessed

higher elongation at break and impact strength than solvent cast composites at all p-CNCs loadings. These results confirmed the previous conclusion drawn from rough and irregular fractured surface in spin-coat composites observed in SEM images.

3.5. Conclusions

We have described a versatile spin-coating technology for masterbatch preparation. Modified cellulose nanocrystals were successfully incorporated in PLA by preparing masterbatch through spin-coating and solvent casting methods. SEM micrographs of masterbatches revealed more homogenous and uniform p-CNCs dispersion in PLA-CNC-sp samples compared to PLA-CNC-so with low CNCs concentrations. The SEM investigations on fracture surface confirmed the difference in fracture surfaces in solvent cast and spin-coated composite. The difference can be attributed to the effect of masterbatch preparation methods on p-CNCs distribution and their interaction with PLA matrix. DSC results confirmed the increase of the crystallinity for nanocomposite samples compared to pure PLA; in which the spin-coated composites exhibited higher degree of crystallinity than solvent cast samples. This behavior can be attributed to partial crystallization of amorphous molecules in the solvent cast films. Spin-coated composites exhibited higher mechanical properties and storage modulus at lower p-CNCs contents (1 and 3%) and higher ductility for all samples. The presence of air bubbles on the surface of spin-coated masrterbatches observed in optical microscopy images resulted from high evaporation rate of the solvent in spin-coating process. Lower thermal characteristics in spin-coated composites resulted from the residual solvent in composites was due to short time for drying process. In general, these results show huge potential for using different manufacturing methods along with chemical modification methods to overcome the major obstacles to producing PLA-CNCs composites on a commercial scale.

4. RHEOLOGICAL PROPERTIES OF PLA REINFORCED WITH CELLULOSE NANOCRYSTALS[1]

4.1. Abstract

Ecofriendly materials such as polylactic acid (PLA) and cellulose nanocrystals (CNCs) are widely sought as potential substitute for petrochemical-based plastics. Uniform dispersion of cellulose nanocrystals in polymer matrices has inhibited their wide-spread application. In this study the influence of masterbatch preparation techniques on molecular structure, melt strength, rheological and dynamic mechanical properties of nanocomposite were systematically analyzed. Film casting and spin-coating methods were used to prepare masterbatches. Nanocomposites were obtained by masterbatch dilution via melt compounding followed by injection molding process. The higher molecular weight and lower molecular number were observed in spin-coated samples in comparison with film cast nanocomposites. The spin-coated nanocomposites exhibited higher storage modulus than film cast samples in the glassy state. However, tan δ curves exhibited higher peak value in spin-coated nanocomposites, which were in good agreement with higher dispersity index of spin-coated samples. The complex viscosity of PLA and nanocomposites exhibited non-Newtonian behavior at a low shear rate, followed by shear thinning phenomenon. The spin-coated nanocomposites demonstrated higher complex viscosity than film cast samples, which was attributed to higher molecular weight in spin-coated samples. The shear-thinning tendency in spin-coated samples was higher than film cast nanocomposites.

[1] The material in this chapter was co-authored by Jamileh Shojaeiarani, Dilpreet S. Bajwa, Nicole M. Stark, and Sreekala G. Bajwa. Jamileh Shojaeiarani conceived and carried out the experiments and analyzed the observed results. Jamileh Shojaeiarani wrote this chapter in consultation with Dilpreet G. Bajwa, Nicole M. Stark, and Sreekala G. Bajwa. Dilpreet G. Bajwa supervised findings of this work.

Keywords: Poly(lactic acid); Cellulose nanocrystals; Masterbatch; Molecular structure; Rheological properties;. Thermal stability.

4.2. Introduction

The growing concern over ecologically friendly materials is pushing the academia and industries to seek versatile and bio-based materials for various applications. Biopolymers are considered as convenient substitutes for synthetic plastics and have received a substantial attention owing to their advantages over traditional and petroleum-based analogs. Among various biodegradable polymers, PLA which is derived from renewable resources such as sugar beet, and maize has received considerable attention as a promising polymer for packaging applications [154]. However, PLA application is still limited as a result of some inherent drawbacks like low thermal stability and low melt strength [155]. The melt strength of polymers indicates the chain resistance to untangling under shear strain. The linear chain structure in PLA results in low melt strength, sagging, and necking which limits its processing [156]. Thus, the considerable efforts have been directed to overcome the weaknesses in PLA polymer. Several studies have focused on incorporating the bio-based nanofillers such as cellulose fibrils, fibers and nanocrystals to strengthen PLA [157, 158].

Cellulose nanocrystals (CNCs) have attracted a huge attention as reinforcing agent in polymeric matrices. CNCs are cellulose-based, non-toxic, and biodegradable nanoparticles isolated from bulk cellulose of woody and non-woody plants [13]. The high mechanical and barrier properties in CNCs suggest the competitive potential for the application as reinforcing agent in polymeric materials [159]. It has been observed that the optimal performance of CNCs as reinforcing agent in polymeric matrix is ascribed by the dispersion quality of CNCs through

polymeric matrix. For optimal improvement, uniform dispersion of CNCs in polymers is required [125].

Rheological properties in composite materials play a significant role in improving the processability of composites as the processing operation such as extrusion and injection molding involve high shear rates [160]. Cellulose nanocrystals have been reported to be a good rheological modifier for different polymers because they surround themselves between polymer chains, providing high stability to the polymer network [161]. A significant change in the melting behavior and rheological properties of nanocomposites has been observed by the incorporation of nanofillers [111, 162]. Musa et al., studied the effects of incorporating CNCs on the rheological behavior of nanocomposites. They found that the high interfacial area resulting from inter-particle interactions governs the rheological properties of nanocomposites [159].

Different studies have shown that well-dispersed CNCs can enhance the performance characteristics of PLA through improvement in the level of crystallinity and formation of matrix-nanofiller network [42]. Therefore, improving the CNCs dispersion in PLA has been extensively explored though different chemical surface modification techniques and mechanical processing [66, 86, 160].

It was reported that the application of masterbatch approach can enhance the dispersion quality of CNCs in host polymer [86]. The highly concentrated masterbatches are diluted using extrusion process considering the let-down ratio or mixing ratio (masterbatches: polymer ratio) [86]. The time-intensive film casting is the most commonly used technique in preparing masterbatches [9]. Long time drying process in film casting process favored the formation of micro-sized CNC aggregates through polymer matrix [15]. Spin-coating is a newly introduced

method for fabricating highly concentrated masterbatches. The short drying time in spin-coating deposition technique hindered the formation of CNCs aggregates in polymer matrix [15].

In this study, the impact of two different masterbatch preparation methods on the molecular structure, rheological, viscoelastic, and thermal properties of nanocomposites were evaluated. Nanocomposites were manufactured by diluting film casted and spin-coated masterbatches via melt compounding followed by injection molding process. The modified CNCs were prepared using poly(ethylene oxide) through physical attachment method.

4.3. Experimental

4.3.1. Materials

Poly(lactic acid) grade 2003D manufactured by Nature Works LLC (Minnetonka, MN, USA) with the glass transition of 55- 60ºC and melt flow of 6 g/10 min was used as a biopolymer. USDA-Forest Service, Forest Products Laboratory (Madison, WI, USA) provided cellulose nanocrystals (CNCs) with dimensions of 10-15 nm. Analytical grade chloroform manufactured by Sigma-Aldrich (St. Louis, MO, USA) was used in this study. Polyethylene oxide (PEO) with the molecular number of 106 $g.mol^{-1}$ and a purity of 99% was obtained from Sigma-Aldrich (St. Louis, MO, USA).

4.3.2. Surface Modification Treatment

CNCs were treated using poly(ethylene oxide) to decrease the hydrophilicity character of CNCs and to enhance the compatibility between CNCs and PLA matrix. An aqueous suspension of CNCs (4 wt%) and a suspension of PEO (1 wt%) were separately prepared and then were mixed together with the ratio of 4:1 (CNCs: PEO). The freeze-dried mixture was used as modified CNCs (p-CNCs) [133, 134].

4.3.3. Scanning Electron Microscopy of Masterbatches

The formation of CNC aggregates through the thickness of the thin film masterbatches were studied through scanning electron microscopy (SEM) images. A JSM-7600F scanning electron microscopy (USA Inc., Peabody, MA, USA) operating at 15 kV was used to take the images with the magnification of 500 and 1000.

4.3.4. Preparation of Nanocomposites

Film casting and spin-coating methods were used to prepare highly concentrated CNCs masterbatches (15 wt%), following the method which was reported in the previous work [86]. The nanocomposites with different p-CNCs contents (1%, 3%, and 5%) were prepared using a co-rotating twin-screw extruder (Leistritz, Mic 18/GL-40D, Somerville, NJ, USA) and injection-molding machine (Technoplas Inc. SIM-5080). Prior to injection molding, the extruded pellets were placed in an oven (Binder ED, Bohemia, NY, USA) for 24 h at 60 °C to remove the excess moisture from the pellets. Table 4.1 shows the processing condition and material codifications.

Table 4.1. Composition of the nanocomposite materials.

Materials code	Composition		Methods
	PLA (wt%)	p-CNCs (wt%)	
PLA	100	0	-
F-PLA1	99	1	Film casting
F-PLA3	97	3	Film casting
F-PLA5	95	5	Film casting
S-PLA1	99	1	Spin-coating
S-PLA3	97	3	Spin-coating
S-PLA5	95	5	Spin-coating

4.3.5. Gel Permeation Chromatography (GPC)

The weight average molecular weight (M_w) and the number average molecular weight (M_n) were measured using a gel permeation chromatography (EcoSEC HLC-8320GPC, Tosoh Bioscience, Japan) equipped with a differential refractometer (DRI) detector. Nanocomposite solutions (1 mg/ml) were prepared in tetrahydrofuran solvent and filtered using filter disk (0.2 μm pore size) prior the testing. The column temperature was maintained at 40 ºC, and the solvent flow rate was set at 0.35 ml/min.

4.3.6. Dynamic Mechanical Analysis (DMA)

Dynamic mechanical analysis was used to study the molecular relaxation behavior of PLA and nanocomposites. Measurements were recorded using a DMA Q800 (TA Instruments, New Castle, DE, USA) following ASTM D4065 standard procedure [138]. Data were recorded in the temperature range of 25 to 90 °C with a scanning rate of 1 °C/min, and a fixed frequency of 1 Hz in a dual cantilever mode. The storage modulus and tan δ as a function of temperature were reported.

4.3.7. Rheological Properties

The flow properties (rheological properties) of materials were measured using a Rheometer AR 2000 (TA Instruments, New Castle, DE, USA). The rheological properties of PLA and nanocomposites were measured in an oscillatory mode. The sample weighing 5 gr was placed between two parallel plates with 25 mm diameter and a gap of 1 mm at 170 ºC. Prior to testing, samples were dried in a vacuum oven set at 65 ºC for 8 hours to avoid a significant decline in viscosity.

4.3.8. Thermogravimetric Analysis (TGA)

Thermal stability of pure PLA and nanocomposites were studied using thermogravimetric analyzer Q500 (TA, New Castle, DE, USA). A 5-7 mg of each formulation was placed in an aluminum pan and temperature range was set in the range of 25 to 600 °C with a scanning rate of 10 °C/min. The corresponding TGA and derivative thermogravimetry (DTG) curves were recorded.

4.4. Results and Discussion

4.4.1. Scanning Electron Microscopy of Masterbatches

The distribution of CNC aggregates through the thickness of the thin film masterbatches were studied and Figure 4.1 illustrates the concentration of CNC in the masterbatches. The individual CNCs are hardly distinguishable, however, the presence of CNC aggregates (spotted by arrows) can be observed for both set of samples (i.e. solvent cast and spin coated masterbatches). Due to the relatively low evaporation rate in the solvent casted masterbatch, the concentration of CNCs varies vertically along with the thickness of the masterbatch and the highest CNCs concentration happens close to the free surface. The increasing CNCs concentration can lead to the formation of CNC aggregates (Figure 4.1a). However, in the spin-coated masterbatch, the CNC aggregates with perpendicular orientation with respect to the film thickness are scattered throughout the masterbatch thickness (Figure 4.1b). These observations confirm the lower CNCs mobility in the spin-coated masterbatch as a result of high evaporation rate of the solvent as well as the centrifugal force generated from rotating substrate [86]. During time-intensive solvent evaporation process in solvent cast thin films, solvent molecules exclude the CNCs molecules and assist in drawing the CNCs closer. This allows for the formation of

CNC aggregates with relatively larger size in comparison with time-efficient solvent evaporation in spin-coated thin films.

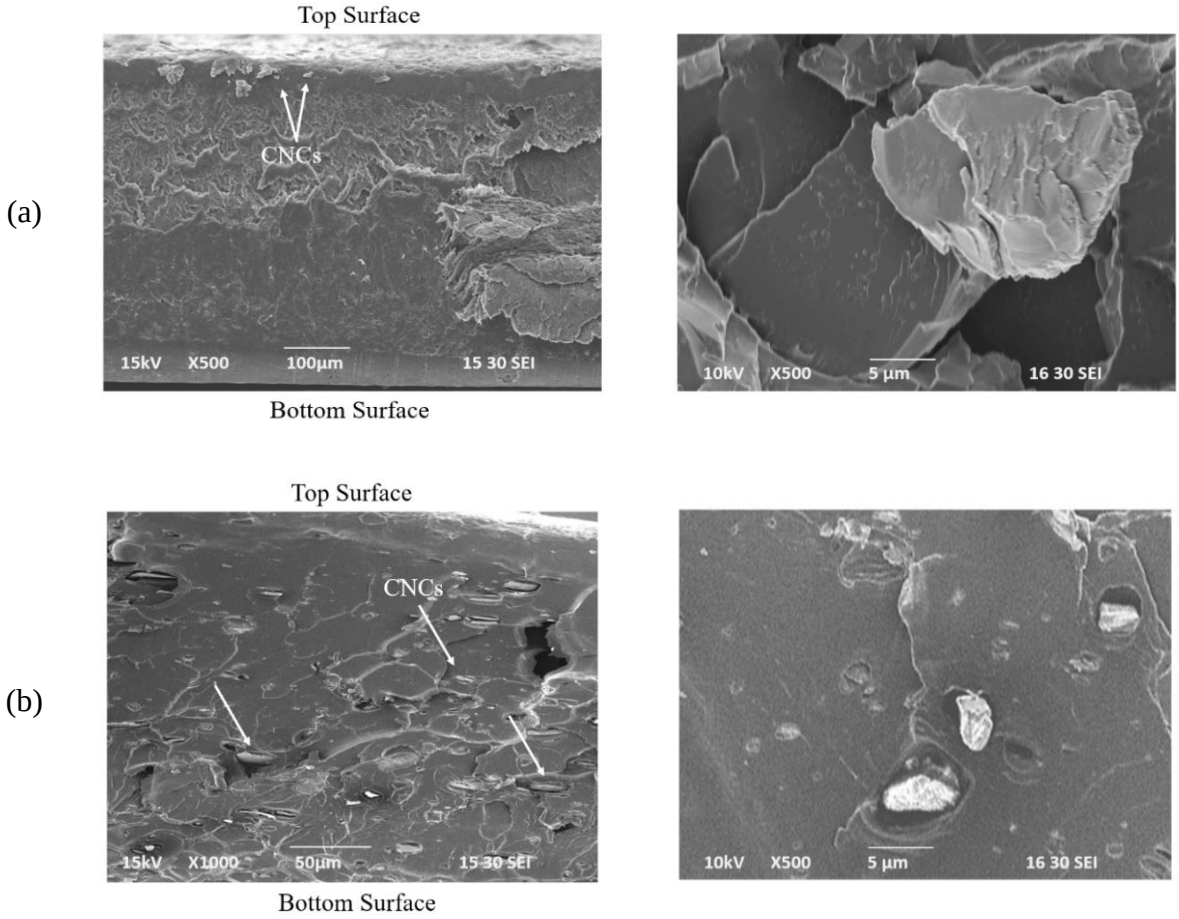

Figure 4.1. The comparison of CNCs aggregates formation in the masterbatches: a) solvent cast, b) spin-coated.

4.4.2. Gel Permeation Chromatography (GPC)

The number average molecular weight (M_n) and the weight average molecular weight (M_w) are two important properties in polymers, which influence different behaviors such as melt viscosity, mechanical properties and processability. PLA with linear chain is so sensitive to manufacturing processes, revealing a rapid reduction in M_n and M_w as a result of thermal degradation under high shear [163, 164]. A significant decline in the molecular weight of PLA was reported in different studies due to the addition of different nanofillers [165-167]. Table 4.2

shows the values of M_w, M_n and dispersity index (M_w/M_n) of PLA and nanocomposites after extrusion process. All nanocomposites exhibited a decline in M_w, M_n as compared to pure PLA, suggesting the presence of p-CNCs provoked the degradation of PLA during composite preparation, and the drop was linearly correlated to the nanofillers loadings. The observed results were in good agreement with another study reporting PLA chain degradation due to the incorporating nanofillers [168].

Table 4.2. The average molecular weight, the average molecular number, and the dispersity index (DI) of samples.

Materials code	M_n* (g/mol)	M_w (g/mol)	DI
PLA	97245	202517	2.08
F-PLA1	95081	193776	2.03
F-PLA3	83444	144434	1.73
F-PLA5	82423	137880	1.67
S-PLA1	94148	201791	2.14
S-PLA3	57226	183241	3.20
S-PLA5	52532	170335	3.24

*M_n: Number average molecular weight and M_w: Weight average molecular weight.

The number average molecular weight (M_n) refers to the colligative properties of polymers and the spin-coated nanocomposites exhibited lower M_n as compared to film cast samples. It was reported that polymer chain cleavage can happen when heat or high pressure are generated during processing [169]. The lower M_n in spin-coated nanocomposites can likely be attributed to the high pressure caused by injection during the masterbatch preparation technique, which interrupted molecular chains. In addition, it has been claimed that the presence of residual solvent in the samples could result in a decrease in M_n of polymers [164].

Due to the short drying time in the spin-coating method, the solvent did not evaporate completely, and some residual solvent was trapped in the masterbatches. The amount of residual solvent in each masterbatches before feeding into extruder was found to be 8.65 wt% and 1.37 wt% in spin-coated and film cast masterbatches, respectively. Therefore, the lower M_n in spin-coated samples could probably be a result of both the higher residual solvent in spin-coated masterbatches and the high injection pressure during spin-coated masterbatch preparation process.

Higher M_w was observed in spin-coated samples in comparison with their film cast counterparts. This observation suggested that the M_w favored spin-coating method. The higher M_w in spin-coated nanocomposites can be attributed to the strong interactions between PLA and CNCs. In general, the higher the molecular weight, the greater the degree of chain entanglement [170].

The dispersity index (DI) or heterogeneity index is a ratio of M_w to M_n, measuring the distribution of molecular mass in a polymer. Polymers with higher DI have wider molecular weight distribution. The dispersity index depends on the reaction condition and manufacturing process. It strongly affects polymer performance and the processing characteristics [171]. In general, polymers with lower DI are difficult to process as the shear-thinning tendency is low. In general, polymeric materials with broader molecular weight distribution tend to thin at lower temperatures and make molding and extrusion process easier. In spin-coated samples, DI constantly increased with p-CNC loading level. However, film cast samples exhibited narrower DI. The shorter polymer length for the higher molecular weight can be considered a result of high injection pressure in spin-coating masterbatch preparation technique.

4.4.3. Dynamic Mechanical Analysis (DMA)

The viscoelastic properties of polymers are strongly associated with the molecular structure and molecular relaxation motion. The viscoelastic properties of nanocomposites directly govern the load bearing capability of materials and attribute towards the interfacial bonding between matrix and nanofillers.

The storage modulus of PLA and nanocomposites at two different temperatures in glassy and rubbery states are shown in Table 1. It can be observed that all the composite samples exhibited higher storage modulus in comparison with PLA in the glassy state. The improved storage modulus in nanocomposites can be attributed to the growth in the stiffness of the PLA matrix owing to reinforcing effect imparted by p-CNCs that led to a greater degree of stress transfer at the PLA-p-CNCs interface. Particularly, the spin-coated nanocomposites reinforced with 1 wt% and 3 wt% p-CNCs exhibited higher storage modulus in the glassy and rubbery states in comparison with film cast samples. It is reported that a slight decrease in storage modulus in S-PLA5 is associated with the presence of residual solvent [86].

The better interaction between matrix and nanofillers provides a clear explanation for the increase in storage modulus with increasing M_w in spin-coated nanocomposites. In general, polymers with low M_w possess low number of long flexible chains. The lack of long flexible chain in the polymers would decrease the strength and elastic modulus in polymer materials [172]. In this work, S-PLA1 with highest M_w among nanocomposites (Table 4.3) exhibited the highest storage modulus followed by F-PLA1 in glassy state.

Tan δ curve is associated with the segmental motion in molecular chains. The position of tan δ peak reveals the glass transition temperature (T_g) in polymeric materials [173, 174]. The glass transition temperature of PLA and nanocomposites are shown in Table 3. The incorporation

of p-CNCs into PLA slightly increased T_g. As expected from Flory-Fox equation (Eq. 4.1) , the spin-coated nanocomposites with smaller M_n exhibited lower T_g than film cast samples [175] (Table 4.2).

$$T_g = T_{g\infty} - \frac{K}{M_n} \tag{4.1}$$

in which, T_g is glass transition and $T_{g\infty}$ reveals the maximum glass transition temperature occurs theoretically for the polymer with an infinite molecular weight. K is an empirical constant and associated with the free volume in the polymer chains.

Table 4.3. The viscoelastic properties in PLA and nanocomposites.

Materials	Storage modulus (MPa)		T_g (ºC)	Tan δ peak intensity
	35 ºC	85 ºC		
PLA	2001	7.01	65.16	2.72
F-PLA1	2500	9.09	65.92	1.83
F-PLA3	2397	5.43	67.8	2.65
F-PLA5	2300	10.46	65.99	1.78
S-PLA1	2849	14.68	65.18	2.23
S-PLA3	2467	7.41	67.05	2.57
S-PLA5	2056	8.54	65.71	1.96

The lower glass T_g in spin-coated nanocomposites can be attributed to more freedom in molecular mobility in PLA-CNC-sp. In general, the polymers with lower M_n possess more free volume at the end of each polymer chain and this, in turn, leads to higher chain mobility. In another word, slightly higher T_g in film cast samples can be related to the decreased mobility of the matrix chain, due to the higher M_n in film cast samples.

The intensity of tan δ indicates the mobility of polymer chain segments at the corresponding temperature [176]. In addition, the way in which the materials absorb or disperse

the energy during deformation can be observed from tan δ intensity. A higher tan δ intensity indicates that more energy is dissipated, and the material exhibits more viscous behavior. However, the lower tan δ value points out the behavior that is more elastic. The tan δ peak value decreased in all composite samples as compared to pure PLA, owing to the presence of p-CNCs. This observation was probably due to the decrease in the mobility of the polymer molecular chains as restricted by p-CNCs. As expected, spin-coated nanocomposites exhibited higher tan δ peak value in comparison with film cast samples. This observation was in good agreement with smaller M_n in spin-coated samples.

4.4.4. Thermogravimetric Analysis (TGA)

Thermal stability of samples was studied through weight loss and the corresponding derivative curves (DTG) (Figure 4.2). Thermal properties of PLA and nanocomposites including initial decomposition temperature (T_{onset}), decomposition temperature at 50% weight loss (T_{50}), maximum decomposition (T_{peak}), and final degradation temperatures (T_{endset}) are reported in Table 4.4.

Considering the weight loss profiles for pure PLA and PLA nanocomposites (Figure 4.2b), thermal decomposition of all samples except S-PLA5 happened in a typical one-step degradation pattern. The observation of one step degradation suggested the simultaneous degradation in all components [177]. The presence of two separate peaks in S-PLA5 might be a result of incorporating high amount of CNCs and the corresponding non-uniform dispersion as shown in previous study [86].

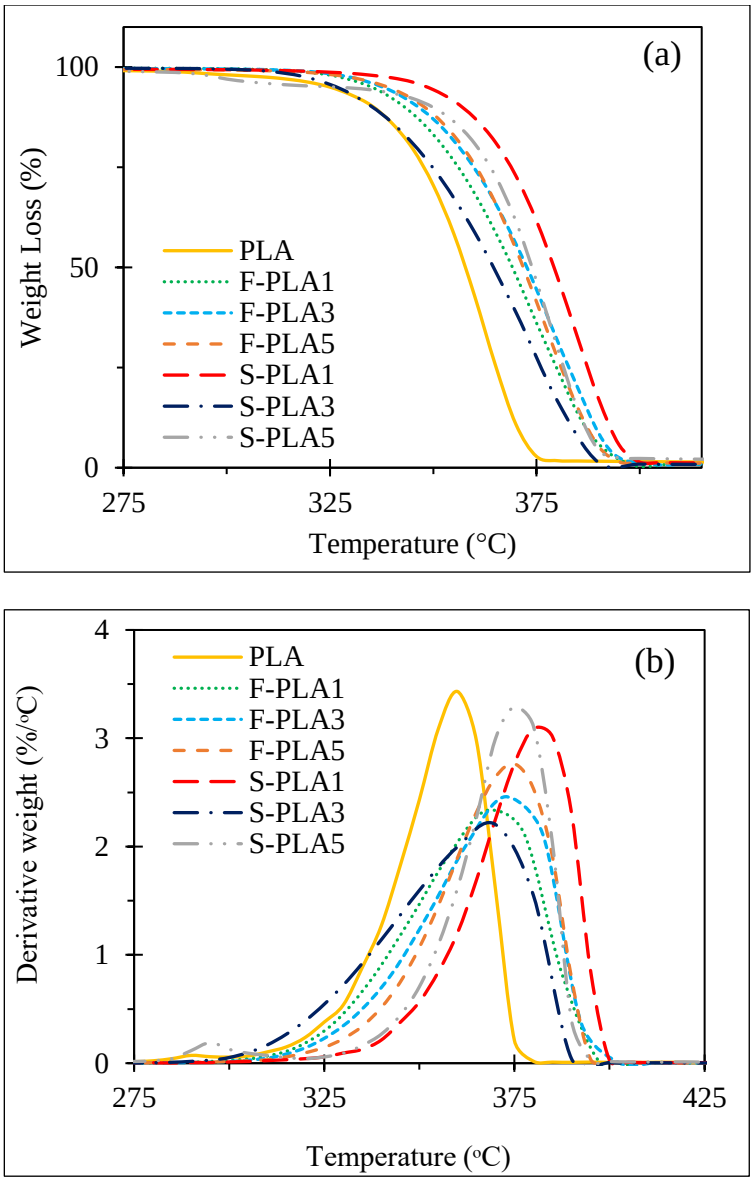

Figure 4.2. Representative thermogravimetric (TGA) and Derivative (DTG) thermograms of pure PLA and nanocomposites.

The total mass loss values for the nanocomposites containing modified CNCs are slightly lower than pure PLA. However, no significant change in the char yield was observed for PLA composite samples as compared with pure PLA.

Table 4.4. Thermal properties of PLA and PLA-PCNCs nanocomposites.

Sample code	T_{onset} (°C)	$T_{50\ wt.\%}$ (°C)	T_{peak} (°C)	T_{endset} (°C)	Weight Loss (%)
PLA	301.13	328.34	332.24	380.39	99.73
F-PLA1	311.22	359.37	345.32	397.72	99.37
F-PLA3	319.18	358.86	344.8	402.89	99.47
F-PLA5	310.72	358.05	345.24	395.71	99.61
S-PLA1	335.72	399.65	375.25	400.62	99.43
S-PLA3	316.30	355.07	372.1	385.72	99.54
S-PLA5	314.18	357.82	370.82	395.04	99.37

4.4.5. Rheological Properties

The dynamic oscillatory shear measurements were carried out to study the response of PLA and PLA-CNC nanocomposites to the dynamic shearing. Figure 4.3 depicts a representative curve for complex viscosity in PLA and nanocomposites.

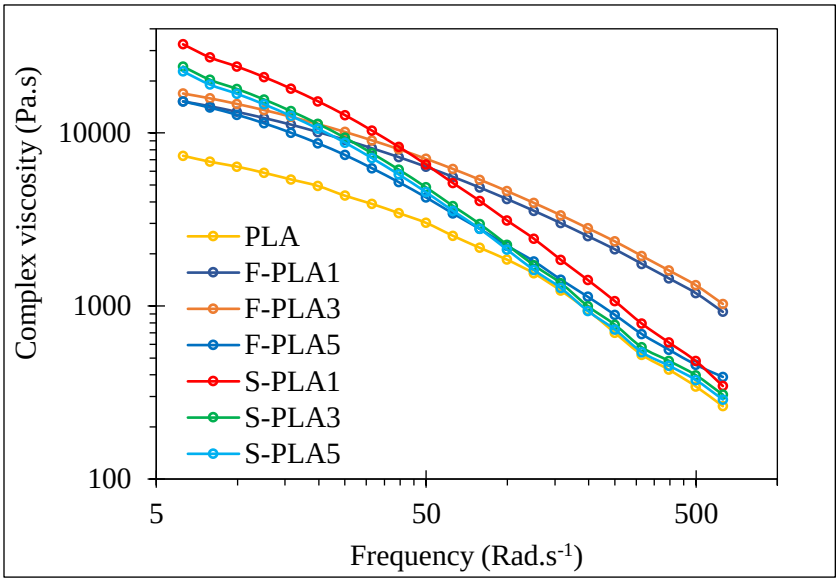

Figure 4.3. Complex viscosity for PLA and nanocomposites.

The complex viscosity of pure PLA and nanocomposite samples decreased with increasing frequency, exhibiting non-Newtonian behavior. The addition of p-CNCs into PLA through both masterbatch preparation routes increased the melt strength of nanocomposites. This

behavior indicates the formation of interconnected network-like structure in the composite samples because of the interaction between matrix and nanofillers. A similar observation was reported by Kamal et al., (2015), in which a significant improvement in complex viscosity was reported by the addition of CNCs into PLA matrix [159]. The high viscosity of nanocomposites was caused by the flow restrictions of PLA chains in the molten state due to the presence of p-CNCs. The polymer chain structure significantly governs the rheological properties and the processability of the polymer.

The molten viscosity and the molecular weight of polymers are correlated to each other based on Mark-Houwink equation (Eq. 4.2) [178].

$$[\eta] = KM_w^a \tag{4.2}$$

where a and K are Mark-Houwink constants and depend on the nature of polymer and solvent.

The higher viscosity in S-PLA1 was attributed to the higher M_w. All samples exhibited shear-thinning behavior, which was more predominant in spin-coated nanocomposites. The shear thinning behavior in polymers is associated with the disentanglement of polymer chains during flow. The onset of shear thinning in polymers is the point, in which, the rate of externally applied movement overcomes the rate of formation of entanglements in polymer chains. In shear thinning phenomenon the crosslink density of the network decreases, resulting in a decline in the viscosity [179]. The samples with higher M_w experienced more disentanglement during flow at higher shear rate, exhibiting more tendency for shear thinning at higher frequencies. Shear thinning in spin-coated samples could speed up the polymer flow and decrease heat generation and energy consumption through processing [180].

Network structure of PLA and nanocomposites was also studied through storage and loss moduli as a function of angular frequency at 170º C (Figure 4.4). The storage modulus increased

with increasing the angular frequency, but the rate of increment in modulus reduced as the frequency increased. In general, at lower frequencies, the interactions between PLA and p-CNCs overcome the applied shear. However, at higher frequencies, the interfacial bonding between PLA and p-CNCs cannot resist the external shear. This in turn, can result in a reduction in the slope of storage modulus. The storage modulus in PLA exhibited an improvement upon addition of p-CNCs, submitting the formation of interfacial bonding between PLA and p-CNCs, which led to more stress transfer from matrix to nanofillers. In particular, the highest storage modulus was observed in S-PLA1 followed by F-PLA1. This observation was in good agreement with an earlier reported study, in which, polymer with higher molecular weight exhibited higher storage modulus [181]. However, the lower storage modulus in PLA was probably due to the reduction in molecular entanglements in the pure PLA over the high frequency rate.

The loss modulus of PLA and nanocomposites exhibited a trend like storage modulus at different p-CNC contents (Figure 4.3b); however, the deviation from pure PLA was more pronounced in loss modulus. The incorporation of p-CNCs in PLA resulted in a substantial increase in the loss modulus, indicating a further increased entanglement density in PLA-CNC nanocomposites in comparison with pure PLA. These observations are in good agreement with the results reported by Hassan et al., They observed a similar trend in storage and loss modulus of PLA and PLA blends with increasing frequency [152].

In addition, all samples exhibited higher storage modulus than loss modulus over the entire range of frequency. This was an indication of the dominance of solid-like relaxation behavior typically found in strong gels [182].

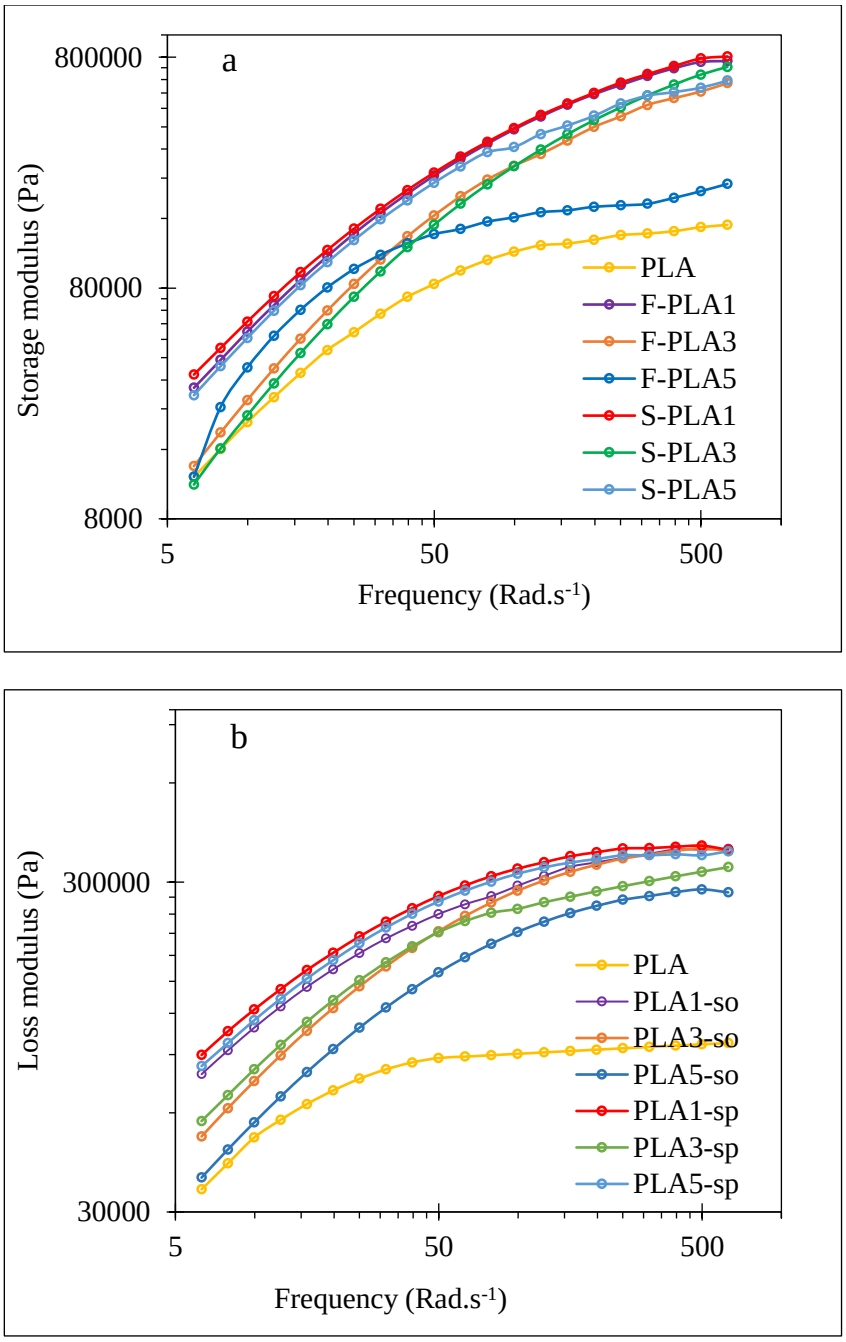

Figure 4.4. (a) Storage modulus and (b) loss modulus as a function of frequency of PLA and nanocomposites.

4.5. Conclusions

PLA-p-CNC nanocomposites were prepared through diluting masterbatches of film casted and spin-coated films, using melt compounding followed by injection molding. The

molecular structure, dynamic mechanical, thermal stability, and rheological properties of PLA and nanocomposites were studied. The GPC results suggested that the samples prepared using spin-coating method exhibited higher molecular weight with a wide distribution of chain lengths. This observation could probably be due to high injection pressure during spin-coated masterbatch preparation process. The viscoelastic and rheological properties of the nanocomposites demonstrated a close relationship with the number average molecular weight and the weight average molecular weight. The addition of p-CNCs into PLA resulted in an improvement in storage modulus as p-CNCs imparted reinforcing effect on the nanocomposites. The spin-coated nanocomposites with higher molecular number had higher storage modulus as compared to their film cast counterpart. This study shows that PLA nanocomposite characteristics can be engineered through different mechanical processing technique and the spin-coating method is a promising approach for masterbatch preparation method to improve the properties of the PLA-CNC nanocomposites.

5. GREEN ESTERIFICATION– A NEW APPROACH TO IMPROVE THERMAL AND MECHANICAL PROPERTIES OF POLYLACTIC ACID COMPOSITES REINFORCED BY CELLULOSE NANOCRYSTALS[1]

5.1. Abstract

Cellulose nanocrystal (CNCs) - reinforced poly(lactic acid) (PLA) nanocomposites were prepared using twin screw extrusion followed by injection molding. Masterbatch approach was used to achieve more efficient dispersion of CNCs in PLA matrix. Modified CNCs (b-CNCs) were prepared using benzoic acid as a nontoxic material through a green esterification method in a solvent-free technique. Transmission electron microscopy images didn't exhibit significant differences in the structure of b-CNCs as compared with unmodified CNCs. However, a reduction of 6.6 to 15.5% in the aspect ratio of b-CNCs was observed. The fracture surface of PLA-b-CNCs nanocomposites exhibited rough and irregular pattern which confirmed the need of more energy for fracture. Pristine CNCs showed a decrease in the thermal stability of nanocomposites, however, b-CNCs nanocomposites exhibited higher thermal stability than pure PLA. The average storage modulus was improved by 38% and 48% by addition of CNCs and b-CNCs in PLA, respectively. The incorporation of b-CNCs increased Young's modulus, ultimate tensile stress, elongation at break and impact strength by 27.02 %, 10.90 %, 4.20 % and 32.77 %, respectively, however, CNCs nanocomposites exhibited a slight decrease in ultimate strength and elongation at break.

[1] The material in this chapter was co-authored by Jamileh Shojaeiarani, Nicole M. Stark and Dilpreet S. Bajwa. Content in this chapter was published in Journal of Applied Polymer Science 135.27 (2018): 46468. Jamileh Shojaeiarani performed the experiments and processed the experimental data. Jamileh Shojaeiarani also drafted and revised all versions of the manuscript. Nicole M. Stark and Dilpreet S. Bajwa aided in interpreting the results and worked on the manuscript. Dilpreet Bajwa supervised the work.

Keywords: Poly(lactic acid); Cellulose nanocrystals; Green esterification; Mechanical properties; Thermal stability.

5.2. Introduction

Polylactic acid (PLA) is one of the most promising biodegradable polymers and is currently produced on a large industrial scale (over 140,000 tons per year) [1, 2, 50, 125]. PLA has become an attractive sustainable alternative to petroleum-based plastics due to its processability, relatively high strength, UV stability, and low toxicity [109, 111]. However, slow crystallization, low thermal resistance, and excessive brittleness limit PLA potential applications [183-185]. Improving the performance characteristics of PLA by incorporating cellulose nanocrystals (CNCs) is the subject of considerable attention, due to CNCs' nanoscale dimensions, widespread availability, superior mechanical, and thermal properties [186, 187]. CNCs with high crystalline structure, high aspect ratio, and large surface area are considered as one of the ideal reinforcing agents for polymer matrices in nanocomposite industry [188, 189].

Generally, the incorporation of CNCs into the polymeric matrix through a homogeneous dispersion results in the formation of a network of matrix-CNCs with an enormous amount of interfacial contacts between polymeric matrix and CNCs owing to large surface area of CNCs [190]. The strong interfacial adhesion between nanocomposite components leads to an effective stress transfer from matrix to CNCs and consequently strengthens the resulting nanocomposites [191]. Specifically, the optimal improvement in performance characteristics of PLA-CNCs nanocomposites can be achieved through the uniform dispersion of CNCs in PLA matrix [15, 40]. Therefore, CNCs dispersion and their corresponding interaction with the polymer matrix are critical factors for reinforcement purposes. However, the strong hydrophilicity of the CNCs and the presence of abundant hydroxyl groups on the surface of CNCs inhibit the homogeneous

dispersion of CNCs in the most hydrophobic polymeric matrices such as PLA [192]. The formation of CNCs aggregates results in a poor dispersion in PLA matrix and impedes the improvements in the mechanical performance of the nanocomposites [41, 42].

To overcome the major problem of non-uniform dispersion of CNCs in hydrophobic PLA matrix, many chemical and mechanical approaches have been extensively studied. Most of the works have focused on improving interfacial interactions between CNCs and PLA matrix using chemical-oriented surface modification methods. In a sialylation technique introduced by Gousse et al., alkylchlorosilanes was applied onto the surface of cellulose whisker as silylating agents. The modification technique required 16 h of vigorous stirring at room temperature. The results showed a good dispersion of modified cellulose whisker in solvents of low polarity (not lower than 2.37) [43]. Yuan et al., introduced alkyenyl succinic anhydride aqueous emulsion onto the surface of cellulose whiskers to improve their solubility in different solvents. The process involved freeze drying of the suspension and then heating to 105 ºC for different times (5 to 240 min). They reported good dispersion of modified cellulose whisker in solvent of low polarity such as 1,4-dioxane[45]. Acetate and lactate modification of CNCs was performed by dual acid application (organic acid and HCl), in which acid hydrolysis and Fischer Esterification occurred in tandem. The suspension was maintained at 150 ºC in a convention oven for 3 h and then the resulting CNC slurries were freeze dried overnight and then dried for at least 12 h to produce nanofiller powder [74].

In another work which has been performed by Yoo et al., two esterification routes were used to prepare fatty acid and PLA grafted CNCs through adding DL-lactic acid syrup and zinc acetate dehydrate catalyst. The final product was dried in this study at 50 ºC for 24 h in a vacuum

oven. It was claimed that the simplicity and ecofriendly aspects of their method can meet the industrial demand for scaling up the surface modification method [193].

In most of the chemical surface modification techniques, hazardous and toxic solvents and reactants are used to alter the hydrophilicity character of the CNCs. In addition, a small number of studies have reported some improvement in the CNCs dispersion through the polymeric matrix using different manufacturing process [47, 48, 194].

In the current study, the influence of incorporating pristine and modified CNCs on thermal and mechanical properties of the PLA-based nanocomposite was evaluated. Modified CNCs were prepared by introducing benzoic acid as grafting agent and solvent media onto the surface of CNCs. Benzoic acid with a broad application in food industry as a nontoxic and recyclable substance, was applied onto the surface of CNCs through a solvent-free and catalyzer free technique not only to integrate the green chemistry and diminishing the environmental footprint of the chemicals but also for improving the economic feasibility [195]. Dispersion–centrifugation process was performed to remove the untreated benzoic acid from the mixture with an excess of ethanol. Modified CNCs were then solvent exchanged in a stepwise manner from ethanol to chloroform without drying in order to decrease the aggregation of CNCs. A masterbatch approach was considered to ensure the uniform dispersion of CNCs in PLA matrix. The nanocomposites were manufactured using high shear co-rotating twin screw extrusion followed by injection molding. The structure of b-CNCs and the morphology of the fractured surface of the nanocomposites were studied using electron microscopes. The effects of CNCs and b-CNCs and their concentration on mechanical, thermomechanical, and thermal properties of nanocomposites were examined.

5.3. Experimental

5.3.1. Materials

Poly(lactic acid) (PLA 2002D, M_n= 98,000 $gmol^{-1}$) was supplied by NatureWorks LLC (Minnetonka, MN, USA). The specific gravity (SG) was 1.24, and the melting point (T_m) was 210 ^oC. Benzoic acid at 99.5% (p.a. quality) was purchased from Sigma-Aldrich (St. Louis, MO, USA). Cellulose nanocrystals (dimensions of 150 nm length and 7 nm width) were obtained from USDA-Forest Service (Forest Products Lab., Madison, WI, USA). CNCs were extracted from wood-based cellulose by sulfuric acid hydrolysis. Analytical grade ethanol manufactured by Sigma-Aldrich (St. Louis, MO, USA) was used in the experiments.

5.3.2. Surface Modification of Cellulose Nanocrystals

Modified CNCs (b-CNCs) were obtained through a green surface modification method using an acid ester of benzoic acid (BA) in a ratio of 1/10 (CNCs/BA) (Figure 5.1). In this method, benzoic acid was used as grafting agent on the surface of CNCs and solvent media above its melting point. CNCs suspension in water (10%, wt%) was sonicated for 5 min and the pH was fixed to 4 by applying hydrochloride acid (HCl, 0.1 mol. L^{-1}). Benzoic acid pellets were added to the aqueous suspension of CNCs and the suspension was stirred vigorously at 130 ^oC for 20 hours. Dispersion–centrifugation process was then repeated for 6 cycles to remove the untreated benzoic acid from the mixture (10,000 rpm) with a large excess of ethanol [195]. Modified CNCs were then solvent exchanged in a stepwise manner from ethanol to chloroform, a liquid medium without drying (to avoid aggregation) for the further application.

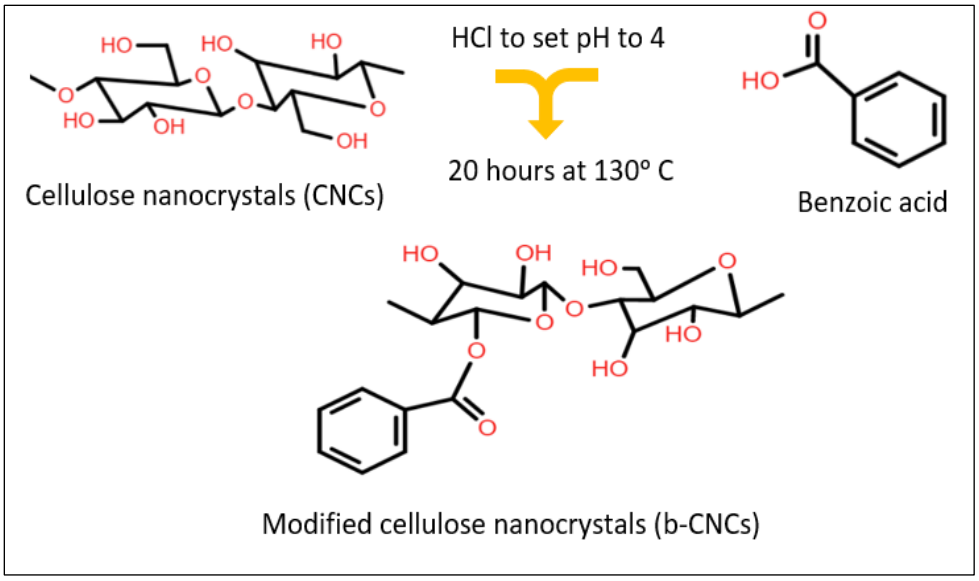

Figure 5.1. Esterification process to form modified CNCs (b-CNCs).

5.3.3. Preparation of Nanocomposites

In this work, masterbatch films with 15 wt% of cellulose nanocrystals (CNCs and b-CNCs) and 85 wt% of PLA were prepared using solvent casting method and chloroform as the solvent. PLA pellets were dissolved in chloroform under vigorous stirring at room temperature (~25 ^{o}C) for 12 hr. Cellulose nanocrystals (CNCs and b-CNCs) were added to chloroform separately and to improve the dispersion of cellulose nanocrystals in chloroform, the suspension was exposed to homogenizer (IKA T50 Ultra-Turrax, Wilmington, NC, USA) for 6 min and sonication (Misonix sonicator, Vernon Hills, IL, USA) for 5 min in an ice bath. The cellulose nanocrystals solution was then added to PLA solution, stirred for 5 hours, and was cast onto the Petri dishes and put to dry at ambient temperature for approximately 30 hours.

The dried masterbatch films with 15 wt% CNCs or b-CNCs were chopped using a paper cutter (ACCO, Columbus, WI, USA) with the approximate size of 4 mm by 4 mm and then diluted to nanocomposite extruded pellets with 1, 3 and 5 wt% of cellulose nanocrystals through the melt extrusion process. The chopped master batch and PLA polymer were fed into co-

rotating twin screw extruder (Krauss-Maffei Co., Florence, KY, USA) fitted with high shear elements. The barrel temperature for eight zones of extruder was set at 157, 157, 165, 162, 162,162, 160, 160 °C (feed throat to die end) respectively, and the screw speed was set at 170 rpm. The extruded pellets were placed in an oven (Binder ED, Binder Inc., Bohemia, NY, USA) set at 60 °C for 24 h prior to injection molding process (Technoplas Inc. SIM-5080). The final composition and codification of the samples obtained from injection molding are shown in Table 5.1.

Table 5.1. Compositions of the nanocomposite materials.

Material Designation	Composition		
	PLA (wt%)	CNCs (wt%)	b-CNCs (wt%)
PLA	100	-	-
PLA-1CNCs	99	1	-
PLA-3CNCs	97	3	-
PLA-5CNCs	95	5	-
PLA-1b-CNCs	99	-	1
PLA-3b-CNCs	97	-	3
PLA-5b-CNCs	95	-	5

5.3.4. Morphology and Dimensions

The morphology and aspect ratio of CNCs and b-CNCs were investigated using a transmission electron microscopy (TEM) (JEOL Inc., Peabody, MA, USA) operating at 2 kV. The CNCs and b-CNCs suspensions were deposited using an aqueous dispersion on a carbon-coated copper (300-mesh) TEM grids. The samples were subsequently stained to enhance the microscopic resolution.

5.3.5. Fractured Surface Morphology

The morphology of impact fractured surface of the nanocomposites was observed using scanning electron microscope (SEM) with an accelerating voltage of 20 kV (JEOL Inc., Peabody, MA, USA) at a magnification of 100X. The fractured surface of the tested specimens was sputter-coated with gold prior to SEM examination to avoid specimen charging.

5.3.6. Thermal Stability

Thermal stability is an important factor in bio-based nanocomposites as melt processing requires elevated temperatures. Inherently, bio-based nanocomposites suffer from low thermal stability which limits their application [196]. The thermal decomposition properties of pure PLA and nanocomposites were studied using thermogravimetric analyzer (TGA Q500, TA Instruments, New Castle, DE, USA) over a temperature range of 25 to 600 °C and a heating rate of 10 °C/min. The initial thermal decomposition temperature (T_{onset}), the maximum decomposition temperature (T_{peak}) and the final degradation temperatures (T_{endset}) were recorded.

5.3.7. Dynamic Mechanical Analysis (DMA)

The viscoelastic properties of PLA and nanocomposites were studied using dynamic mechanical analyzer (DMA Q800, TA Instruments, New Castle, DE, USA) following ASTM D4065. The bending method was used with a frequency of 1 Hz. The temperature was swept at a heating rate of 1 °C/min from 25 to 90 °C and the dynamic storage modulus (E'), loss modulus (E″), and the tan δ (=E″/E') of each sample as a function of temperature were determined. Four replicates of each formulation were used in the DMA test.

5.3.8. Mechanical Property

The mechanical properties of PLA and nanocomposites are governed by microstructural parameters of matrix and nanofillers, the distribution of nanofiller in the matrix, and interfacial bonding between nanofillers and matrix [197]. Mechanical characteristics of PLA and nanocomposites were studied through tensile and impact tests. The tensile test was carried out using an Instron universal testing machine (Model 5567, Norwood, MA, USA) following the ASTM D638 standard. Instron machine was equipped with a 30 KN load cell and the crosshead speed was set at 5 mm/min. An Izod impact tester (Tinius Olsen, Model Impact 104, PA, USA) was used to run the impact tests and to calculate the impact strength of unnotched specimens following ASTM D256 standard.

5.3.9. Statistical Analysis

The mechanical properties data were statistically analyzed using one-way ANOVA and Tukey's tests. All statistical analyses were performed with a significance level of 5%. The data were analyzed by Minitab software version 17 (Minitab Inc., State College, PA, USA). Eight replicates were used for each test.

5.4. Results and Discussion

5.4.1. Morphology and Dimensions

The morphology of CNCs plays a critical role in nanocomposite properties and it is very important to ensure that the morphology of b-CNCs is not affected as a result of the surface modification. The morphological features of the modified and pristine CNCs after the dispersion in water were investigated using TEM images (Figure 5.2).

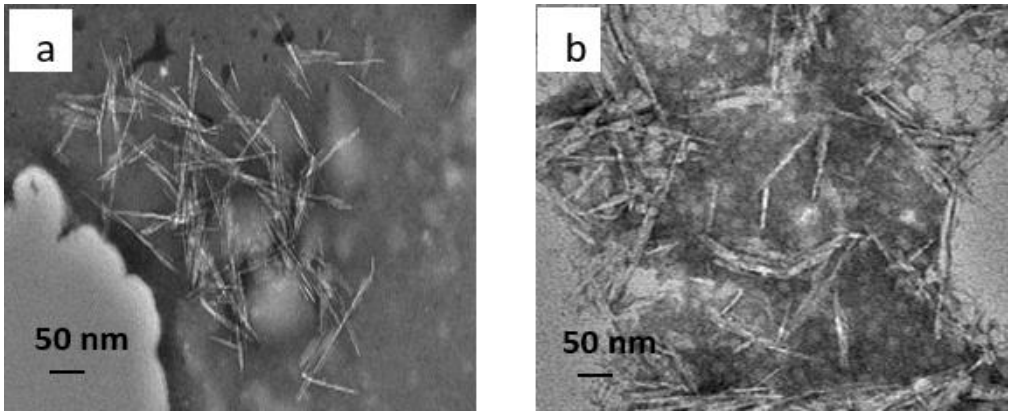

Figure 5.2. TEM images of (a) pristine CNCs and (b) modified CNCs.

It was observed that modified CNCs maintained their elongated morphology with the mean values in the range of 150 to 200 nm in length and 10 to 12 nm in width. The b-CNCs are thicker than CNCs and the results showed a reduction of 6.6 to 15.5% in the aspect ratio of b-CNCs.

5.4.2. Fractured Surface Morphology

The presence of CNCs aggregates and fracture pattern of nanocomposites were inspected through SEM images (Figure 5.3).

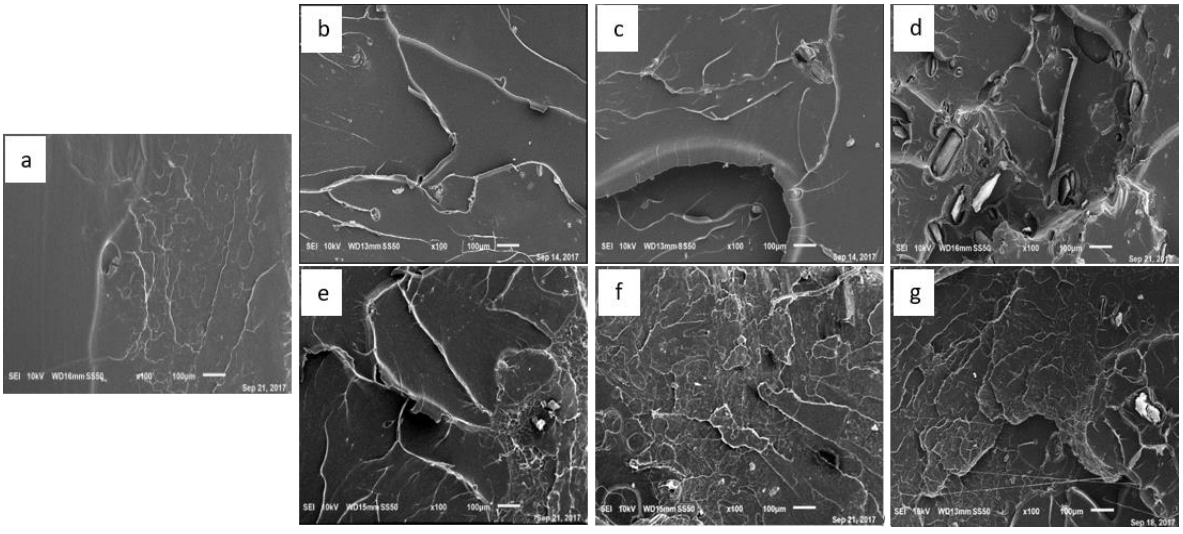

Figure 5.3. SEM images of fractured surface of a) pure PLA, b) PLA-1CNCs, c) PLA-3CNCs, d) PLA-5CNCs, e) PLA-1b-CNCs, f) PLA-3b-CNCs, and g) PLA-5b-CNCs.

The smooth fractured surface of pure PLA exhibited some distinct river markings confirming the brittle character of PLA. The observed clean and smooth impact fractured surface in nanocomposites with low content of pristine CNCs (1 and 3 wt%) indicated the inherent stiffness and brittle fracture pattern in PLA-1CNCs and PLA-3CNCs. However, nanocomposites with 1 and 3 wt% b-CNCs exhibited rough and irregular surfaces, suggesting the ductile fracture mechanism in PLA-1b-CNCs and PLA-3b-CNCs nanocomposites. In general, the fractured surface can illustrate the impact resistance of the materials [141, 198, 199]. The rough and irregular fractured surface in PLA-b-CNCs nanocomposites indicated more required work for impact fracture as compared with PLA-CNCs nanocomposites. It also suggested the higher impact resistance in PLA-b-CNCs nanocomposites than PLA-CNCs nanocomposites. Spherical voids, and cavities around visible CNCs aggregates mostly were observed in PLA-1CNCs, as shown in Figure 5.3c. This behavior was an evidence of the interfacial debonding between PLA and CNCs owing to poor interfacial adhesion in PLA-CNCs nanocomposites [200].

5.4.3. Thermal Stability

The influence of incorporating CNCs and b-CNCs into PLA on thermal stability of nanocomposite was investigated through thermogravimetric (TGA) and derivative thermogravimetry (DTG) curves (Figure 5.4).

Thermal degradation through a one-step process was observed for pure PLA, PLA-1CNCs and PLA-bCNCs nanocomposites, indicating simultaneous degradation for all components. However, two distinct peaks were observed in PLA-3CNCs and PLA-5CNCs. This behavior can be attributed to the CNCs' isolation technique. The CNCs which used in this study were isolated from cellulose by a controlled hydrolysis using sulfuric acid (H_2SO_4).

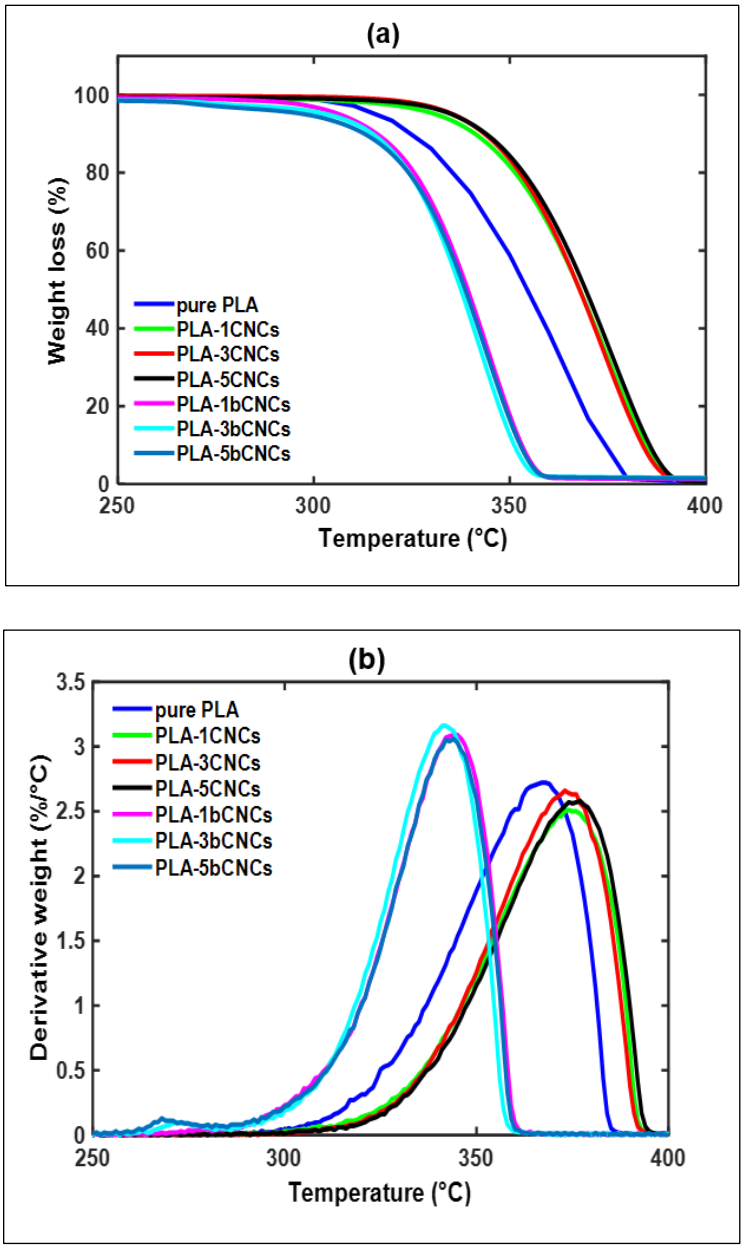

Figure 5.4. Representative (a) TGA and (b) DTG curves of PLA and nanocomposites.

The presence of two endothermic peaks confirmed that the sulfuric acid hydrolysis impacted the thermal stability of unmodified CNCs [201].The first peak observed between 250 and 300 °C was small and the second peak which dominated the overall process occurred between 290 and 350 °C. The first peak was related decomposition of the negatively charged sulfate groups on CNCs and the second peak can be related to depolymerization of cellulose in

competition with dehydration. These observations are corroborated by another study on cellulose nanomaterials treated with sulfuric acid [194, 202, 203]. Table 5.2 presents thermal characteristics of PLA and nanocomposites obtained from TGA and DTG curves.

The results on thermal properties of nanocomposites showed that PLA-b-CNCs nanocomposites were more thermally stable as compared with pure PLA, however, no significant change was observed with increasing b-CNCs content. The observed improvement in thermal stability of PLA-b-CNCs nanocomposites was likely due to the increased dispersion of b-CNCs and the formation of stable hydrogen bonded networks between PLA and b-CNCs which hindered the degradation process of PLA-b-CNCs nanocomposites components [74, 204]. PLA-CNCs nanocomposites exhibited an approximate decrease of 10% in thermal stability as compared with pure PLA. The application of sulfuric acid in CNCs isolation led to a lower temperature of thermal degradation for unmodified CNCs. It has been reported that treating cellulose with sulfuric acid can result in a reduction in thermal stability of CNCs, and an increase in char formation at the end of degradation process [205, 206].

Table 5.2. Thermal properties of PLA and nanocomposites.

Sample code	T_{onset} (°C)	T_{peak} (°C)	T_{endset} (°C)	Weight loss (%)
PLA	291.21	370.10	391.34	99.75
PLA-1CNCs	285.48	344.27	361.27	99.44
PLA-3CNCs	283.27	342.01	359.95	99.12
PLA-5CNCs	286.28	344.58	360.14	99.00
PLA-1b-CNCs	308.87	375.21	394.87	99.46
PLA-3b-CNCs	310.37	373.44	393.16	99.11
PLA-5b-CNCs	311.29	375.68	395.08	99.31

5.4.4. Dynamic Mechanical Analysis (DMA)

The interaction between polymer molecular chains and organic nanoparticles as they are subjected to periodic loading under a range of temperatures can be illustrated using dynamic mechanical analysis (DMA). Figure 5.5 illustrates the effect of CNCs and b-CNCs concentrations on storage modulus at elevated temperatures.

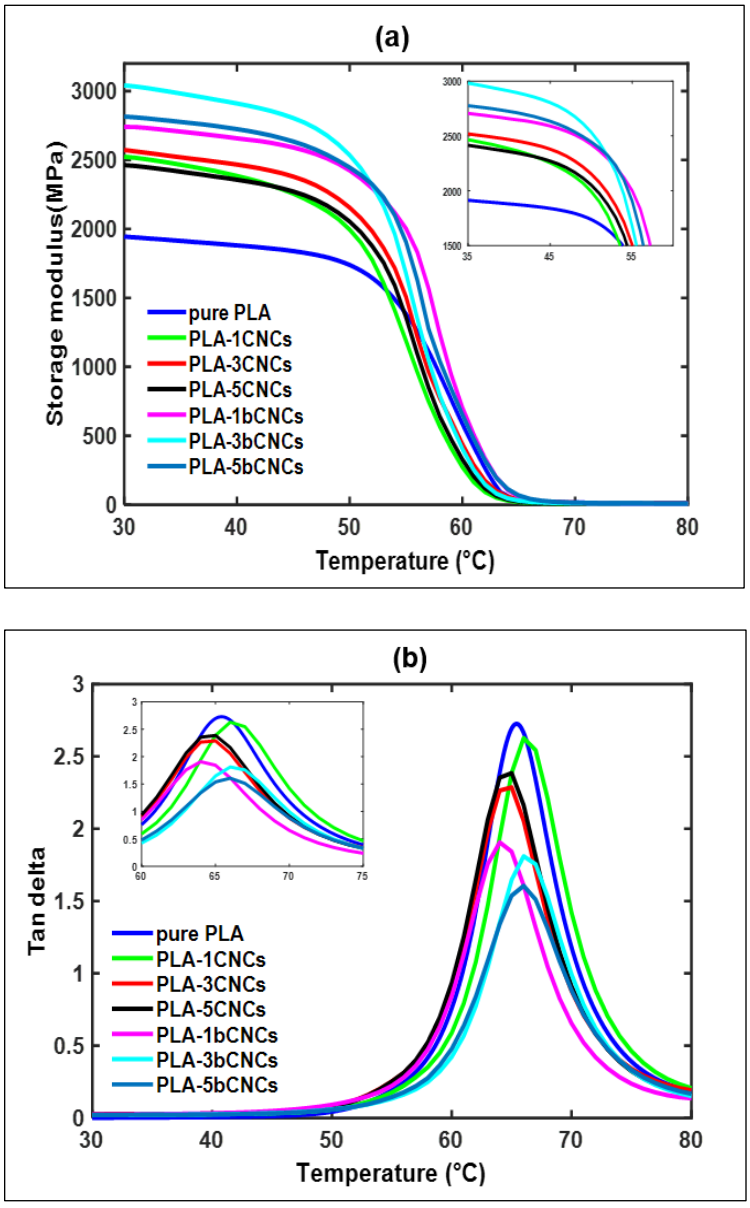

Figure 5.5. Representative (a) storage modulus and (b) tan δ vs. temperature curves of PLA and nanocomposites.

It was observed that the storage modulus of nanocomposites steadily increased with the incorporation of CNCs and b-CNCs as compared with pure PLA, which indicates the reinforcing effect of organic nanoparticles [207]. In particular, the storage modulus of PLA-b-CNCs nanocomposites was higher as compared with PLA-CNCs nanocomposites in the glassy state. This behavior was more likely due to the enhanced interfacial bonding between PLA and b-CNCs which resulted in better stress transfer from PLA matrix to b-CNCs. The maximum improvement in storage modulus was observed in PLA-3b-CNCs, however, with further increase in b-CNCs concentration to 5 wt%, storage moduli reduced owing to poor dispersion and agglomeration formation of b-CNCs in PLA matrix (Figure 5.3f).

The tan δ curves as a function of temperature for PLA and nanocomposites are shown in Figure 5.5b. The value of tan δ peak is an indication of viscoelastic behavior in nanocomposite and gives some information on the mobility of chain segments. The higher tan δ peak value typically means more energy dissipation potential in materials [176].

The tan δ peak value of nanocomposites reinforced with b-CNCs exhibited lower values probably due to less viscous and more elastic behavior in PLA-b-CNCs nanocomposites as compared with PLA-CNCs nanocomposites. These results revealed better interfacial bonding between PLA matrix and b-CNCs.

The tan δ peak value, glass transition temperature (T_g), and storage modules in the glassy and rubbery states (below and above the T_g of samples) are summarized in Table 5.3. The temperature at the peak value of tan δ curve is assigned as glass transition temperature (T_g) of the material. Glass transition temperature is a complex property in the amorphous region of polymers and is governed by several factors such as chain flexibility and intermolecular interactions. DMA results show that the addition of CNCs or b-CNCs into PLA matrix does not

noticeably affect the glass transition temperature of nanocomposites. The results implied that the interaction between PLA and cellulose nanocrystals slightly restricted the molecular mobility of the chains in polymer [208].

Table 5.3. Dynamic mechanical properties of PLA and nanocomposites obtained from DMA.

Sample	Tg (°C)	Peak tan δ	Storage Modulus (MPa)	
			30 °C	70 °C
PLA	64.05	2.72	1944±56.7e	15.62±0.44a
PLA-1CNCs	66.77	2.62	2524±12.17d	8.69±0.03c
PLA-3CNCs	65.12	2.15	2708±14.53c	15.99±0.48a
PLA-5CNCs	65.48	2.38	2463±14.11d	9.29±0.12c
PLA-1b-CNCs	64.23	1.90	2740±28.21bc	11.54±0.12b
PLA-3b-CNCs	66.29	1.81	3041±32.00a	11.48±0.09b
PLA-5b-CNCs	66.58	1.60	2815±24.60b	15.72±0.14a

* The different letters indicate a significant difference in the sample mean at $\alpha = 0.05$.

5.4.5. Mechanical Property

The mechanical behavior of PLA and nanocomposites were evaluated through tensile and impact tests and the results are presented in Table 5.4. It was observed that the addition of b-CNCs had a stiffening effect on PLA matrix and improved Young's modulus, most likely due to the uniform dispersion of b-CNCs and improved interfacial adhesion between b-CNCs and PLA matrix. Similarly, an increase in the ultimate tensile strength was observed in PLA-b-CNCs nanocomposites in comparison with PLA-CNC nanocomposites with the same CNCs content. These results were in a good agreement with the SEM observations which showed more micro-size CNCs aggregates in PLA-CNCs nanocomposites compared with PLA-b-CNCs nanocomposites.

No significant differences were observed in elongation at break for nanocomposites reinforced with b-CNCs as compared with pure PLA, however, lower elongation at break was observed for PLA-CNCs nanocomposites. The observed reduction in the elongation at break for PLA-CNCs can be attributed to the weak interaction between PLA and CNCs. In the other words, the formation of relatively big CNCs aggregates in PLA-CNCs as shown in Figure 5.3, confirmed the weak interaction between PLA and CNCs and resulted in lower elongation at break. Higher values of impact strength were observed for all nanocomposite samples as compared with neat PLA which was more pronounced in the case of PLA-b-CNCs nanocomposites. Higher impact strength in PLA-b-CNCs can be attributed to the better interfacial interaction between PLA and b-CNCs and higher absorption of energy during impact test as compared with PLA-CNCs. This behavior was supported by a rough and irregular fractured surface in PLA-b-CNCs nanocomposites observed from SEM images (Figure 5.3). Similar results were reported by Gao et.al who showed higher impact strength for PLA-based nanocomposites with a rougher fractured surface [141].

Table 5.4. Mechanical properties of PLA and nanocomposites.

Sample code	Young's modulus (GPa)	Ultimate strength (MPa)	Elongation at break (%)	Impact Strength (kJ m^{-2})
PLA	$3.33\pm0.04^{f*}$	57.39 ± 1.20^{bc}	3.5 ± 0.14^{a}	20.90 ± 0.63^{c}
PLA-1CNCs	3.29 ± 0.19^{f}	52.76 ± 4.56^{d}	2.82 ± 0.51^{bc}	21.15 ± 2.01^{c}
PLA-3CNCs	3.37 ± 0.29^{df}	55.36 ± 4.21^{cd}	2.23 ± 0.31^{c}	21.22 ± 1.48^{c}
PLA-5CNCs	3.46 ± 0.30^{d}	55.57 ± 3.12^{cd}	2.47 ± 0.35^{c}	22.95 ± 0.25^{c}
PLA-1b-CNCs	4.74 ± 0.32^{c}	59.91 ± 2.18^{bc}	3.64 ± 0.25^{a}	24.15 ± 1.93^{b}
PLA-3b-CNCs	4.23 ± 0.39^{a}	63.66 ± 2.89^{e}	3.53 ± 0.35^{ab}	27.37 ± 2.35^{ab}
PLA-5b-CNCs	4.17 ± 0.16^{ab}	61.58 ± 2.01^{f}	3.65 ± 0.23^{a}	27.75 ± 1.39^{a}

* The different letters indicate a significant difference in the sample mean at $\alpha = 0.05$.

5.5. Conclusions

The study compared the dispersion of pristine CNCs and esterified (b-CNCs) as a reinforcement in PLA matrix. Modified CNCs were prepared using a nontoxic and recyclable material through a solvent free and catalyzer free esterification technique. Nanocomposites were prepared by twin screw extrusion followed by injection-molding using masterbatch approach. Morphological properties of b-CNCs after esterification were studied using TEM images and no significant difference in the structure and shape of b-CNCs was observed as compared with unmodified CNCs. The fractured surface of PLA-b-CNCs showed increased surface roughness and contained fewer micro-size cellulose nanocrystal aggregates. These observations were further confirmed by the higher impact strength in PLA-b-CNCs nanocomposites as compared with PLA-CNCs. Higher thermal stability in PLA-b-CNCs nanocomposites was observed and can be attributed to of the esterification of CNCs which resulted in making b-CNCs more thermally stable. Although, a small reduction in the aspect ratio of b-CNCs was observed, higher mechanical properties in PLA-b-CNCs confirmed the treatment effect was more pronounced than the effect of aspect ratio of CNCs. The incorporation of b-CNCs improved the Young's modulus and ultimate tensile stress in PLA-bCNC nanocomposites by 27.02 % and 10.9 % respectively, however, the incorporation of pristine CNCs into PLA did not result in any significant change in the mechanical properties on PLA-CNC nanocomposites.

6. ESTERIFIED CELLULOSE NANOCRYSTALS AS REINFORCEMENT IN POLY(LACTIC ACID) NANOCOMPOSITES[1]

6.1. Abstract

Biopolymers are of huge interest as they carry potential to minimize the environmental hazards caused by synthetic materials. Poly(lactic acid) (PLA) reinforced by cellulose nanocrystals (CNCs) has shown promising results. To obtain the optimum characteristics of PLA-CNC nanocomposites, a superior compatibility between PLA and CNCs is paramount. The application of chemical surface modification technique is an essential step to improve the interaction between hydrophilic CNCs and hydrophobic PLA. In this study, a time-efficient esterification technique using valeric acid was introduced to improve the compatibility between CNCs and PLA. Masterbatches were prepared using spin-coating method to ensure the maximum dispersion of CNCs through PLA and to decrease the drying time. Nanocomposites were prepared using extrusion and injection molding. The degree of substitution for modified CNCs was calculated as 0.35. Transmission electron microscopy exhibited esterified CNCs (e-CNCs) in the nanoscale with rod shape structure. Thermal stability improved by 15% in nanocomposites containing 3% e-CNCs, whereas untreated CNCs didn't alter the thermal stability to a notable extent. A substantial increase of 200% was observed in crystallinity of nanocomposites reinforced with 3% e-CNCs. The incorporation of CNCs into PLA resulted in an increase in storage modulus and a decrease in tan δ intensity which was more profound in PLA-e-CNCs. The tensile strength of PLA-e-CNCs composites was found to be superior to

[1] The material in this chapter was co-authored by Jamileh Shojaeiarani, Dilpreet S. Bajwa, and Kerry Hartman. Jamileh Shojaeiarani developed the idea and processed the experimental data. Jamileh Shojaeiarani performed the analysis, drafted the manuscript and designed the figures. Dilpreet S. Bajwa provided critical feedback and supervised the project. Kerry Hartman helped supervise the project.

composites reinforced with untreated CNCs. The results confirmed that a combination of time-efficient esterification and spin-coated masterbatch was a successful approach to uniformly disperse CNCs in PLA matrix.

Keywords: Poly(Lactic Acid); Cellulose Nanocrystals; Esterification; Masterbatch; Mechanical properties.

6.2. Introduction

In the last few decades, the growing interest on environmental health and limited fossil fuel resources has contributed to a huge attention to bio-based polymers. Biopolymers synthesized from renewable natural resources are moving to the main stream owing to their sustainable nature and potential to decrease the reliance on fossil fuels and the availability [209].

Poly(lactic acid, PLA) as a biodegradable and biocompatible thermoplastic polymer is widely used in different industries such as food packaging, medical applications, and automotive applications, due to its competitive mechanical properties [210]. Currently, PLA holds a small fraction of the total global plastic market [211] and its application is restricted by its intrinsic low ductility and low thermal stability. Polymer melt blending, copolymerization and the addition of nano-sized fillers are some modification techniques, which have been used to improve the performance characteristics of PLA [212-214].

In the case of addition of nano-sized fillers, natural fibers have several advantages over synthetic fibers like low weight, CO2 neutrality, and biodegradability. Among different nanofillers, cellulose nanocrystals (CNCs) have shown a great potential in different applications owing to the availability and excellent mechanical properties. CNCs are typically stiff rod-shaped fibers with an approximate length of 10-1000 nm and the diameter of 1-100 nm depending on their origin and the isolation conditions [13]. The addition of CNCs into a wide

range of polymer matrices is of significant research interest. The critical issue to achieve the optimum performance characteristics in nanocomposites is the capability of obtaining well-dispersed hydrophilic CNCs in hydrophobic polymers like PLA [215].

Although the application of CNCs as nanofillers in PLA matrix has been extensively studied for several years, PLA-CNCs nanocomposites still suffer from the formation of CNCs aggregates throughout the matrix. The non-homogeneous dispersion of CNCs as a result of CNCs' aggregates leads to the discontinuity of interfacial interaction between CNCs and PLA [111] and weakens the resultant nanocomposites. To increase the hydrophobicity of CNCs and to facilitate the uniform dispersion CNCs through PLA matrix, different chemical-oriented surface modifications such as esterification, etherification, and oxidation have been extensively explored [216-220]. The time-consuming character is one of the main drawbacks of chemical- oriented modification techniques. It was reported that increasing the reaction time in esterification process could result in destroying the crystalline structure in cellulose nanocrystals [126]. In a Fisher esterification technique, which was introduced by De Paulu (2015), hydrolysis was performed for 72 h at 55 °C. They applied one pot modification method using sulfuric and trimethylactic acid to reduce the hydrophilic character of CNCs surface [220]. Tingaut et al., employed a heterogeneous catalytic method and solvent exchange to acetylate the surface of nano-fibrillated cellulose [221]. The introduced acetylation method was performed for 72 h.

In the present work, an attempt was made to develop a time-efficient esterification method for manufacturing PLA reinforced by modified CNCs. The application of catalyst as one of the esterification parameters was considered to reduce the hydrolysis time to 4 h. Valeric acid was used in this study to modify the surface of CNCs. Valeric acid can be obtained from renewable resources like lignocellulose [222]. Valeric acid is also considered safe as a food

additive by the World Health Organization and it is used in food industry as a flavor enhancer for synthetic flavor [223]. From an environmental point of view, there is no hazardous impact regarding valeric acid application owing to its complete aerobic degradation in a few days that restricts it from reaching the ground water.

The main objective of this study was to modify the surface of CNCs using valeric acid as safe material in an effective and time efficient esterification method. The modified CNCs was compounded as reinforcement to the PLA matrix. To overcome the problem of non-uniform dispersion of CNCs into PLA matrix, masterbatch approach was considered. The spin- coating mothed was used to prepare masterbatches. Nanocomposites with different nanofiller contents were manufactured using twin-screw extrusion followed by injection molding. The modified CNCs were studied using Fourier transformed infrared spectroscopy and transmission electron microscopy. The fracture surface of nanocomposites was studied by microscopic observations. The thermal, thermomechanical, and mechanical performance of nanocomposites were evaluated thoroughly.

6.3. Experimental Section

6.3.1. Materials

Poly (lactic acid, 2003D) with the average molecular number of 98,000 $gmol^{-1}$ was purchased from NatureWorks LLC (Minnetonka, MN, USA). Unmodified cellulose nanocrystals (CNCs) were extracted from wood-based cellulose through sulfuric acid hydrolysis by USDA-Forest Service (Madison, WI, USA). Analytical grade chloroform manufactured by Sigma-Aldrich (St. Louis, MO, USA) was used in the experiments. Valeric acid (99%), N, N-Dimethylformamide (DMF, 99.8%), 4-(Dimethylamino) pyridine (DMAP, 99%) were puchased

from Sigma-Aldrich (St. Louis, MO, USA). All materials were used as received without further purifications.

6.3.2. Surface Modification Treatment of Cellulose Nanocrystals

The chemical surface modification treatment of CNCs by valeric acid was performed using 4- Dimethylamino pyridine. A 50 mg dried CNCs were added to a 500 ml round flask, containing a solution of DMAP (50 mg) and N, N-Dimethylformamide (DMF, 6.25 mg). The mixture was subjected to sonication (Misonix, Vernon Hills, IL, USA) for 5 min in an ice bath to achieve a homogenous mixture. Then valeric acid (25 mg) was added into the mixture and mixture was mechanically stirred with the help of magnetic stirrer for 4 h at room temperature (~25 ^{o}C). The mixture was then subjected to centrifugation for four times to purify the esterified CNCs (e-CNCs) using chloroform by consecutive centrifugations at 10000 rpm for 4 min each. To avoid the drying of CNCs which results in irreversible aggregation, the modified CNCs were stored in chloroform for further use. An illustration of the reaction is illustrated in Figure 6.1.

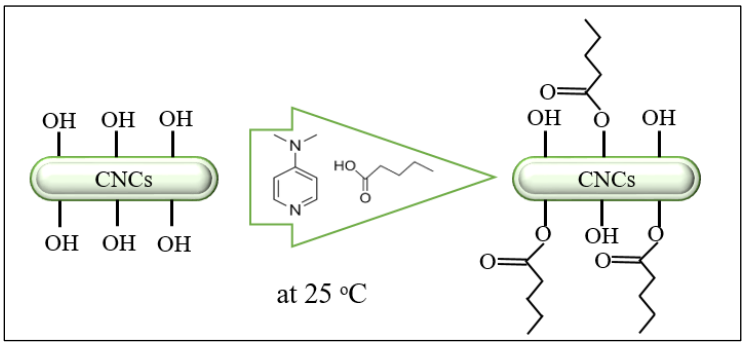

Figure 6.1. Proposed reaction schematic of esterification.

Elemental analysis was carried out to measure carbon, oxygen, hydrogen, and sulfur contents of CNC and e-CNCs. The degree of substitution (DS) of the hydrocarbon chains on the modified CNCs with the relative precision of the 1% was calculated using Eq. 6.1. This equation is employed for DS calculation in CNCs' surfacfe esterification techniques [224].

$$DS = \frac{6-13.42\times C}{(1.17\times n\times C)+(1.16\times C)-n} \quad (6.1)$$

where n is the number of carbons in the substituent molecule and C denotes the percentage of carbon in the modified CNCs (mass %).

6.3.3. Nanocomposite Preparation

Masterbatch approach was employed to increase the dispersion quality of CNCs through PLA matrix. The masterbatches, containing 15 wt% e-CNCs (or CNCs), were prepared using a similar method described in previous study [86]. PLA solution were prepared by dissolving PLA pellets in chloroform (15 wt%) using vigorous mechanical stirring at room temperature. The suspension of e-CNCs (or CNCs) in chloroform (10 wt%) were subjected to homogenizer (IKA T50, Wilmington, DE, USA) for 5 min and then sonicated for 3 min using a sonication probe (Misonix, Vernon Hills, IL, USA) in an ice bath to control the temperature rise. A predetermined amount of e-CNCs (or CNCs) suspension was added into PLA solution described earlier and the mixture was vigorously stirred for 20 min and subjected to homogenizer for 5 min. The solution was injected through a syringe onto the rotating glass substrate using a vacuum spin-coating machine (VTC, MTI Co., Richmond, CA, 200 rpm) for 240 s. The solvent was evaporated from the masterbatches surface immediately as the mixture was injected onto the rotating petri dishes. The solvent in the masterbatches was removed completely by drying the masterbatches in a vacuum oven set at 65 ºC for 4 h. The thickness of masterbatches was kept constant in the range of 1.8-2.1 mm.

Masterbatches were shredded and a paper cutter (ACCO, Columbus, WI, USA) was used to chop up the master batches into small pieces (approximately 4 mm by 4 mm). The masterbatch pieces were then blended with PLA matrix using an extruder to produce

nanocomposites with final concentrations of 1 and 3 wt% e-CNCs (or CNCs). The extrusion was conducted using a twin-screw extruder fitted with high shear elements (Leistritz, Mic 18/GL-40D, Somerville, NJ, USA). Extrusion temperature profile ranged from 155°C (zone 1) to 160°C (zone 7), die temperature was set at 160°C and the screw RPM was 170. Nanocomposite extruded pellets were oven dried at 60 °C for 4 h prior to injection molding process. Injection molding process was carried out using an injection molding machine (Technoplas Inc. SIM-5080). The injection molder had four feeding zones and an injection nozzle. The temperature for the feeding zones was 180 °C, 175 °C, 170 °C, and 165 °C, respectively. The nozzle temperature was set at 175 °C. Pure PLA samples were manufactured in the same method as nanocomposites without adding CNCs or e-CNCs. Table 6.1 summarizes the compositions of nanocomposite materials and the corresponding codes in this work.

Table 6.1. Sample codes of the extruded PLA and nanocomposites.

Material Designation	Composition		
	PLA (wt %)	CNCs (wt %)	e-CNCs (wt %)
PLA (control)	100	-	-
PLA-1CNC	99	1	-
PLA-3CNC	97	3	-
PLA-1e-CNC	99	-	1
PLA-3e-CNC	97	-	3

6.3.4. Fourier Transformed Infrared Spectroscopy (FTIR)

FTIR measurement of CNCs and e-CNCs was carried out to monitor the modification of CNCs in absorbance mode in the range of 400 and 4000 cm^{-1} at a spectral resolution of 4 cm^{-1}. A Thermo Nicolet 8700 spectrometer (Thermo Fisher, Waltman, MA, USA) equipped with an

attenuated total reflectance (ATR) sampling accessory with a diamond crystal was used to record the spectra. Each sample was scanned 64 times.

6.3.5. Morphology and Dimensions

The morphology of CNCs and e-CNCs were investigated using a transmission electron microscopy (TEM) (JEOL Inc., Peabody, MA, USA) operating at 2 kV. A drop of a 0.001 wt% suspension of CNCs and e-CNCs in chloroform were deposited on a carbon-coated copper (300-mesh) TEM grids. To enhance the microscopic resolution, the TEM samples were stained using phosphotungstic acid prior to capturing.

6.3.6. Fractured Surface

The morphology of PLA and nanocomposites was studied using scanning electron microscopy (SEM). The impact-fractured surface was studied using SEM (JEOL Inc., Peabody, MA, USA) working with an accelerating voltage of 20 kV at a magnification of 500X. The samples were sputter-coated with a fine layer of gold before SEM examination to avoid specimen charging.

6.3.7. Thermogravimetric Analysis (TGA)

Thermal stability is an important parameter in materials since the processing temperature restricts the choice of polymer. Inherently, biopolymers possess lower thermal stability than petroleum-based polymers [196]. The thermal degradation profile of pure PLA, pristine CNCs, e-CNCs, and nanocomposites was evaluated using thermogravimetric analyzer (TA Instruments, New Castle, DE, USA). All treatments were tested in triplicates, about 10 mg of the sample was placed in the platinum TGA pan. The samples were kept in a vacuum oven set at 80 ºC prior to

TGA test. The thermographs were recorded in the temperature range of 25 to 600 °C with a scanning rate of 10 °C/min.

6.3.8. Differential Scanning Calorimetry (DSC)

DSC experiments were conducted using a TA Instrument Q200 calorimeter (New Castle, DE, USA) in the temperature range of 25 to 200° C at a heating rate of 5° C/min, and then followed by a cooling process up to 25° C with a cooling rate of 5° C/min. Three replications were run for each formulation and for each run, a small amount of samples (< 20 mg) was placed inside a hermetic Al pan and was sealed with an Al cover. The glass transition temperature (T_g), melting temperature (T_m) and crystallization temperature (T_c) were directly obtained from the heating scan and the degree of crystallinity (X_c) was calculated using Eq. 6.2.

$$X_c = \left[\frac{\Delta H_m - \Delta H_c}{\Delta H_m^c}\right] \times \frac{100}{W_{PLA}} \quad (6.2)$$

where ΔH_m and ΔH_c represent the melting enthalpy and cold crystallization enthalpy, respectively. ΔH_m^c is the melting heat and is equal to 93.6 J/g for pure crystalline PLA [137]. W_{PLA} depicts the weight fraction of PLA in the nanocomposite sample.

6.3.9. Dynamic Mechanical Analysis (DMA)

The viscoelastic behavior of PLA and the nanocomposites were investigated using dynamic mechanical analyzer, Q800 (TA Instruments, New Castle, DE, USA). The measurements were performed in the bending mode with a frequency of 1 Hz and the strain amplitude of 0.5 %. The temperature was swept at a heating scan of 1 °C/min from 25 to 90 °C and the storage modulus (E') and the tan δ (=E″/E') of each sample were determined. For each formulation, three replicates were used, and the mean values are reported.

6.3.10. Mechanical Property

The mechanical behavior of nanocomposites are governed by microstructural parameters of matrix and nanofillers, the distribution of nanofiller through the matrix, and the interfacial bonding between nanofillers and matrix [197]. Mechanical characteristics of injection molded PLA and nanocomposites were evaluated using tensile and impact tests at room temperature (~ 25 ºC). The tensile test was conducted using a universal testing machine (Instron Model 5567, Norwood, MA, USA) following the ASTM D638 standard [136]. The Instron testing machine was equipped with a 30 KN load cell and the crosshead speed was set at 1.5 mm/min. The impact strength of samples was measured through running impact test (Tinius Olsen, Model 104, PA, USA) following ASTM D256 standard [139]. The pendulum weight and the radius were 4.497 kg and 334.949 mm, respectively. No additional load was added to the pendulum. The impact test was performed on unnotched samples with the dimension of 63.5 mm× 13 mm× 4.5 mm.

6.3.11. Statistical Analysis

The mechanical properties were statistically analyzed using one-way analysis of variance (ANOVA) and Tukey's tests to determine the significant differences in the mean values of different properties of different formulations. Minitab software (Minitab 17, State College, PA, USA) was employed to evaluate data. All statistical analyses were performed with a "α" level of 5 %. Eight replicates for test were studied.

6.4. Results and Discussion

6.4.1. Fourier Transformed Infrared Spectroscopy (FTIR)

The Fourier transform infrared (FTIR) absorption spectra were recorded for the determination of new functional groups on the surface of e-CNCs after the esterification method. The FTIR spectra of pristine CNCs and e-CNCs in Figure 6.2 show obvious differences in the

structures of CNCs as a result of the valeric acid treatment. The presence of bands around 3330-3350, 2900-2910, 1640-1650, and 1040-1059 cm^{-1} in two spectra are characteristics bands attributed to native cellulose. In Figure 6.2 the observation of the new band in the carbonyl area, at 1738 cm^{-1}, corresponds to C=O stretching vibration band of COOH group confirms the success of esterification method [225, 226]. Meanwhile, the new band around 1564 cm^{-1} corresponded to the bending vibration for aromatic C-C in the structure of e-CNCs appeared as a result of incorporating DMAP in the esterification treatment.

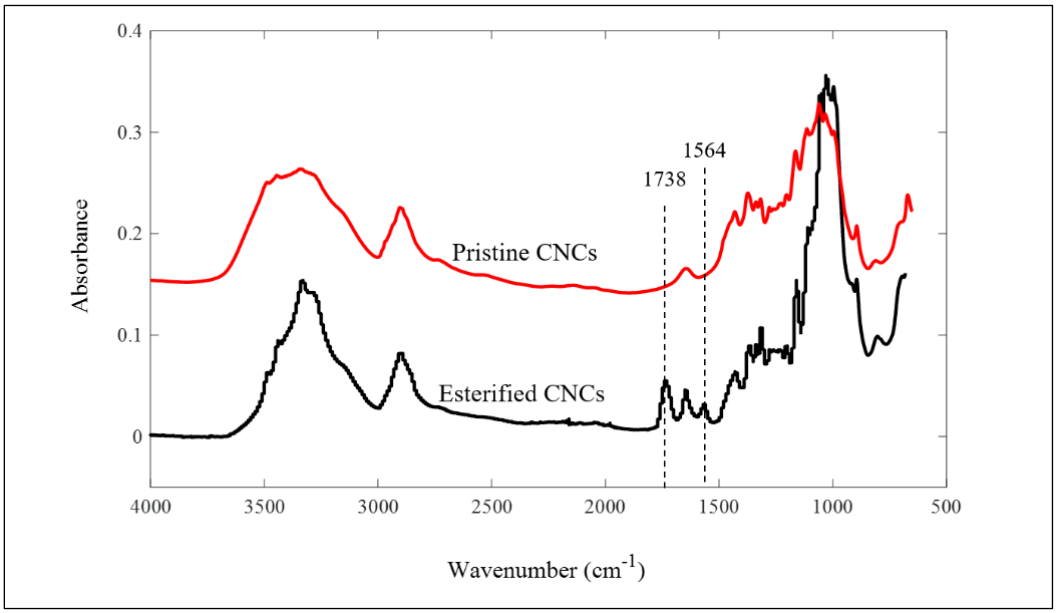

Figure 6.2. FTIR spectra of pristine CNCs and e-CNCs in the absorbance mode.

6.4.2. Morphology of CNCs and e-CNCs

The morphology of CNCs has a critical role on nanocomposite performance and dictates the mechanical properties of materials. It is an important step in nanocomposites processing technique to ensure that the morphology of modified CNCs is not affected by the application of surface modification. Figure 6.3 shows the TEM micrograph of the modified and pristine CNCs in water.

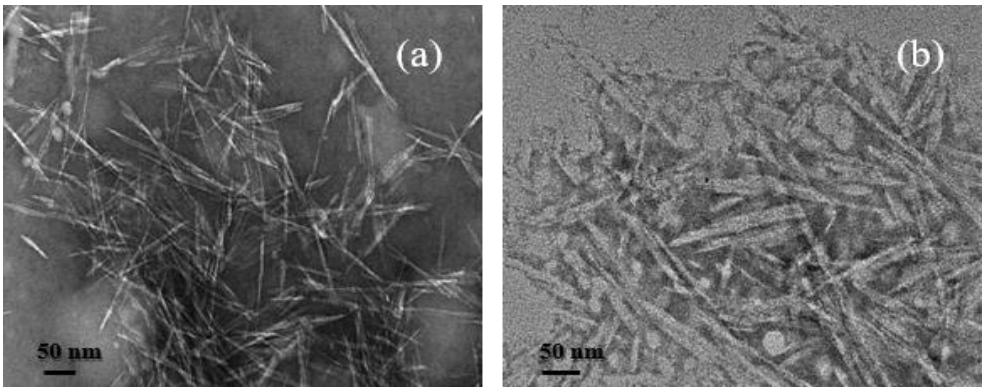

Figure 6.3. TEM micrograph of (a) pristine CNCs and (b) e-CNCs.

The needle-like and well-defined single crystals e-CNCs (Figure 6.3b) demonstrated that e-CNCs possessed the same rod shape structure as pristine CNCs. The average dimension of CNCs and e-CNCs were measured using image analysis (ImageJ software) and the average values for length and diameter of e-CNCs were 157±17 nm and 11±4 nm respectively compared to pristine CNCs with the length and diameter of 150±10 nm and 7±2 nm, respectively.

The elemental analysis of pristine CNCs exhibited the mass percentage of C: 42.20, H: 5.95, O: 51.11, and S: 0.45. The modified CNCs had the mass percentage of C, H, and O of 48.84, 6.57, and 43.86, respectively. The degree of substitution for modified CNCs was approximately calculated as 0.35.

6.4.3. Fractured Surface

The impact-fractured surface from pure PLA and nanocomposites is illustrated in Figure 6.4. The fractured surface of nanocomposites containing pristine CNCs exhibit a relatively smooth and laminated fracture surface with river-like pattern somewhat similar to that of pure PLA, indicating an inherent brittle nature. However, PLA-e-CNC nanocomposites exhibited rough and irregular pattern, suggesting higher energy required for the fracture (the impact test described later measured such energy). Meanwhile, the presence of white dots on the fractured

surface of PLA-1CNCs and PLA-3CNCs indicated the formation of CNC aggregates owing to low compatibility between PLA matrix and CNCs (Figure 6.4b and c). However, no visible aggregates were observed on the fractured surface of PLA-e-CNCs nanocomposites, representing that the introduced esterification technique helped in achieving more uniform dispersion of e-CNCs through PLA matrix (Figure 6.4d and e). The formation of CNC aggregates in the PLA-CNC nanocomposites can probably be due to the weak interaction between PLA matrix and CNCs. However, less e-CNC aggregates through PLA matrix and the strong interfacial adhesion between e-CNCs and the PLA could lead to higher impact strength in the samples. The similar results were observed in PLA filled with pristine and modified cellulose nano-whisker [51].

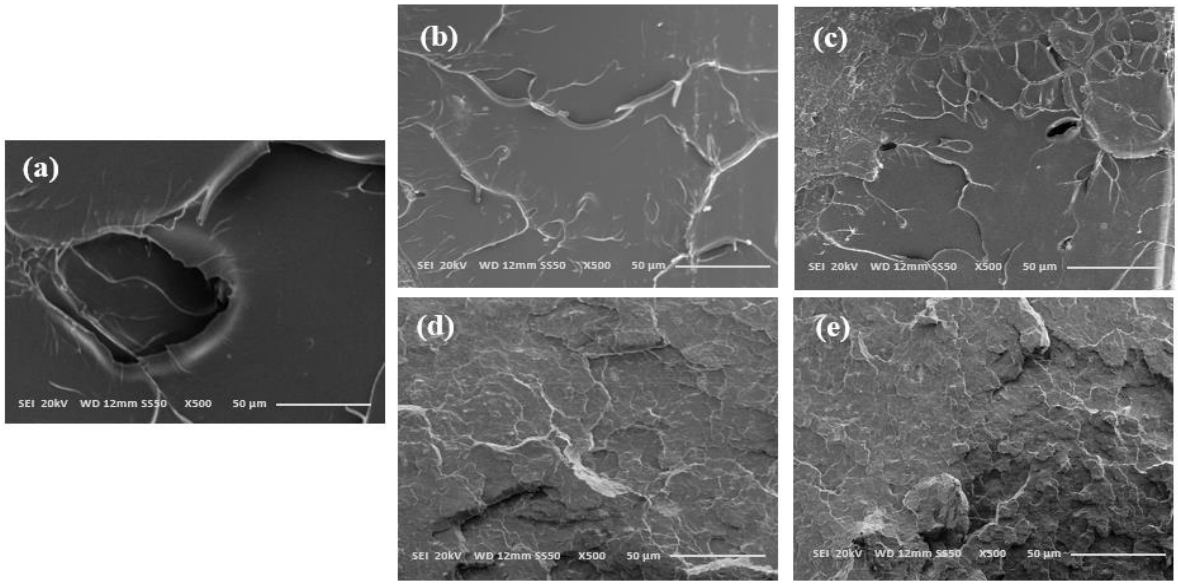

Figure 6.4. SEM micrographs of (a) pure PLA, (b) PLA-1CNCs, (c) PLA-3CNCs, (d) PLA-1e-CNCs, (e) PLA-3e-CNCs.

6.4.4. Thermogravimetric Analysis (TGA)

The thermal decomposition behavior of pure PLA and nanocomposites was studied using TGA and the corresponding TGA and DTG thermograms are illustrated in Figure 6.5. The mean values for the temperatures at which the materials start disintegrating (T_{onset}), the maximum

decomposition temperature (T_{peak}), the final degradation temperature (T_{endset}), and the residual char at degree of 600 ºC are summarized in Table 6.2.

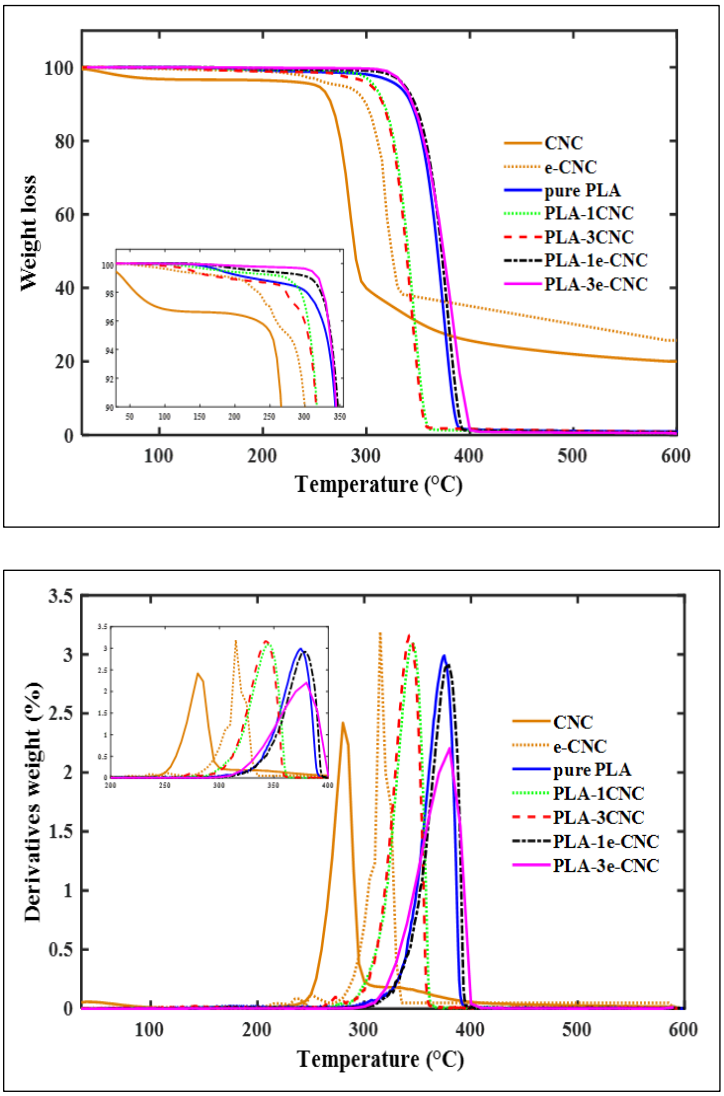

Figure 6.5. Representative (a) TGA and (b) DTG curves of CNCs, PLA and PLA-based nanocomposites.

The modified CNCs were thermally more stable compared to pristine CNCs as they exhibited slightly higher T_{onset} (3.6 %), T_{peak} (2.5 %) and less weight loss. Relatively higher amount of char was formed in e-CNCs as compared with CNCs. It was reported that thermal decomposition at relatively high temperature could closely pack the CNCs, forming a solid shell layer. The charcoal protection layer would inhibit the degradation of the inner layers and

increase the char residue in modified CNCs [227]. In addition, increase in the carbon content (~15 %, as shown in elemental analysis) increased the char residue in e-CNCs.

Table 6.2. The mean value for thermal decomposition of PLA and nanocomposites.

Sample	T_{onset} (ºC)	T_{peak} (ºC)	T_{endset} (ºC)	Weight loss%
CNCs	253.17	278.24	302.57	80.02
e-CNCs	262.34	284.96	305.17	74.15
PLA	291.21	370.10	378.87	99.75
PLA-1CNC	299.18	345.31	357.17	99.44
PLA-3CNC	296.72	342.76	360.48	99.13
PLA-1e-CNC	324.24	378.67	386.47	99.21
PLA-3e-CNC	336.73	375.74	381.17	99.08

The observed thermal differences between CNCs and e-CNCs can be attributed to the different decomposition process, more likely due to the chemical change in the structure of e-CNCs after esterification treatment. In perfect agreement with previously reported data [148, 228], the application of surface modification techniques could change the content of sulfate groups present on the surface of CNCs and less sulfate groups would result in thermally more stable sample [229]. Moreover, the addition of e-CNCs shifted T_{onset} to higher value and resulted in an enhancement in the thermal stability of the nanocomposites. However, no significant difference in T_{onset} was observed in PLA-CNCs as compared to pure PLA. The maximum decomposition temperature (T_{peak}) in PLA-e-CNC nanocomposites slightly improved, while PLA-CNCs exhibited lower T_{peak} in comparison to pure PLA. T_{endset} shifted to higher temperature in PLA-e-CNCs, in contrast, the incorporation of CNCs slightly decreased the final degradation temperature. The TGA data demonstrated higher thermal stability of PLA-e-CNCs than PLA-CNCs. In particular, the thermal stability results exhibited an improvement of 15.63 %

and 11.34 % of T_{onset} in nanocomposite containing 3 % and 1 % e-CNCs in comparison with pure PLA.

These observations were possibly due to the well-dispersed e-CNCs in PLA matrix and, the formation of a dipolar interaction between nanocomposite components. This, in turn, can hinder the decomposition of PLA-e-CNC nanocomposites at elevated temperatures, leading to thermally more stable structure [66]. In addition, the level of crystallinity is another parameter, which governs the thermal decomposition in the polymer materials. It was reported that high level of crystallinity would result in high thermal stability [230] as chains are closely packed into a highly-ordered structure and higher energy is required to break down the physical and the chemical interactions. Therefore, different observations in thermal stability in nanocomposites could probably be due to different level of crystallinity in samples at temperatures lower than 170 ºC as the polymer chains fall out of their crystal structures and become a disordered liquid after reaching the melting temperature (The level of crystallinity and melting points are described later in differential scanning calorimetry section).

Thermal characteristics of materials were also investigated using derivative thermogravimetric analysis (DTG) as shown in Figure 6.5b. Pure PLA and PLA-e-CNC nanocomposites exhibited the same single step degradation process with a main degradation peak at around 370 ºC. However, nanocomposites reinforced by pristine CNCs degraded in two distinct steps. The first degradation peak which was observed at temperatures between 250 and 300 ºC was more probably due to the decomposition of sulfate groups on the surface of CNCs [18]. The second degradation peak dominated the whole degradation process and occurred between 290 and 350 ºC. A similar observation was reported by other studies in which

unmodified CNCs, treated with sulfuric acid, exhibited the formation of two degradation peaks on DTG graph [202, 203].

6.4.5. Differential Scanning Calorimetry (DSC)

Improving the glass transition temperature and the degree of crystallinity of PLA is one of the main goals of incorporating CNCs into PLA matrix. To evaluate the application of e-CNCs in PLA, the curves corresponding to the first heating scan of pure PLA and nanocomposites are illustrated in Figure 6.6 and the related data are summarized in Table 6.3.

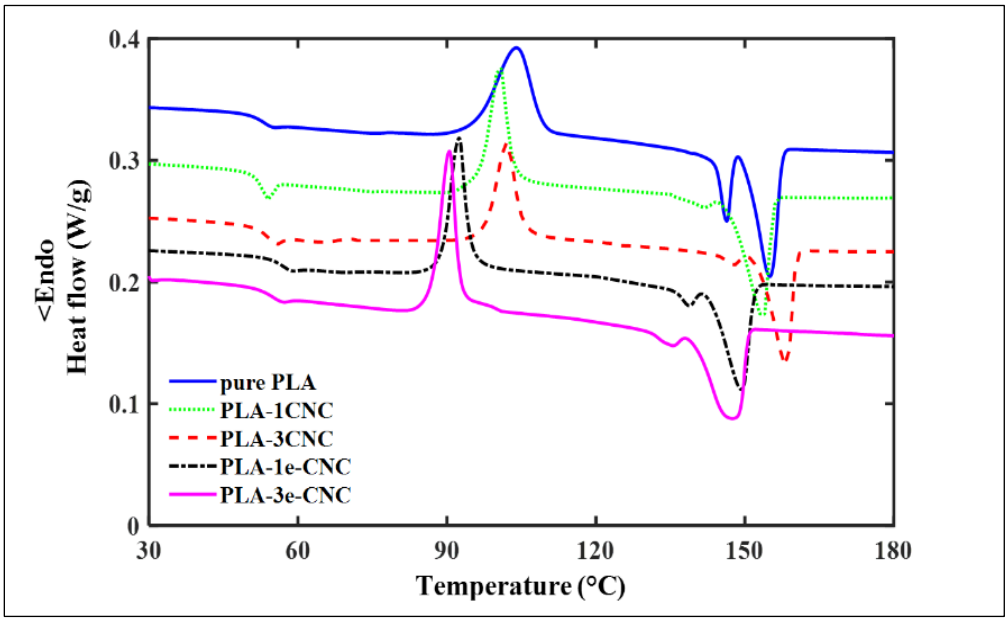

Figure 6.6. Representative DSC curves of PLA and nanocomposite.

A slight growth was observed in glass transition temperature (T_g) of PLA with the addition of CNCs and e-CNCs. The increase was more predominant in PLA-e-CNCs, reaching 56.13 °C for nanocomposite reinforced by 1 wt% e-CNC. This observation can be ascribed to the strong interfacial adhesion between e-CNC and PLA matrix which resulted in restricted polymer chain mobility. This restriction increased the energy required for the transformation of thermal behavior of PLA-e-CNC nanocomposites and resulted in an increment in T_g. Similar results were

observed by Gupta et al., in which the higher T_g was observed in PLA filled by 0.3 and 1.0 wt% lignin coated CNCs [111]. When e-CNCs content was increased from 1 to 3 wt%, the T_g was declined slightly. This is more likely to be due to the relatively poor dispersion of e-CNCs in PLA matrix and the presence of small aggregates of e-CNCs through PLA, this, in turn, can inhibit the nucleation effect of e-CNCs. A significant decline in cold crystallization temperature (Tc) was observed for all nanocomposite samples. This observation is more likely a result of the uniform dispersion of e-CNCs through PLA. The well-dispersed e-CNCs serve as heterogeneous nucleus and consequently intensify the formation of well-organized structure and lowered Tc in nanocomposites [146, 147].

Table 6.3. DSC results for PLA and its nanocomposites.

Sample	T_g (ºC)	T_c (ºC)	T_m (ºC)	X%
PLA[86]	50.16	103.98	155.06	3.99
PLA-1CNC	52.01	101.72	155.61	4.13
PLA-3CNC	52.89	100.31	160.60	5.64
PLA-1e-CNC	56.13	97.95	150.80	9.77
PLA-3e-CNC	54.24	93.55	151.14	12.53

As previously reported [231], the presence of two melting point for pure PLA and PLA-1e-CNC could be ascribed to the formation of different crystal structures in PLA formed during cooling and crystallization processes. The addition of CNCs and e-CNCs into PLA possessed different effect on melting point of nanocomposites. Slightly higher Tm was observed in PLA-CNCs, however, the incorporation of e-CNCs reduced the Tm by 5 ºC. The lower Tm in PLA-e-CNCs can be ascribed to the less stable randomly formed crystals during cold crystallization [232].

Moreover, the results for nanocomposites exhibit a significant improvement in the degree of crystallinity in PLA-e-CNCs nanocomposites as compared to pure PLA. The observed enhancement in the degree of crystallinity in PLA-e-CNCs can be ascribed to the better dispersive state of e-CNCs in PLA matrix in comparison with that of pristine CNCs. The more uniform e-CNCs dispersion through PLA enhanced the interfacial interaction between e-CNCs and PLA chain. The enhancement in network-like interaction could probably lead to the formation of more nucleation sites and an enhancement in the nucleation effect of e-CNCs. A reported study has suggested more homogenous CNCs dispersion favor the degree of crystallinity in nanocomposites [148].

6.4.6. Dynamic Mechanical Analysis (DMA)

The material response to a sinusoidal force under elevated temperatures was studied using dynamic mechanic analyzer and the corresponding storage modulus and tan δ curves as a function of temperature are illustrated in Figure 6.7. The viscoelastic behavior of materials can reveal the structure of the polymeric system. The storage modulus curve of PLA and all composite samples show the normal trend as can be seen in semi-crystalline polymers; high storage modulus at the lower temperatures and a drastic drop around glass transition temperature, reaching the second plateau corresponding to the rubbery state. For comparison, the storage modulus of all samples at two different temperature (above and below the glass transition temperature) are shown in Table 6.4.

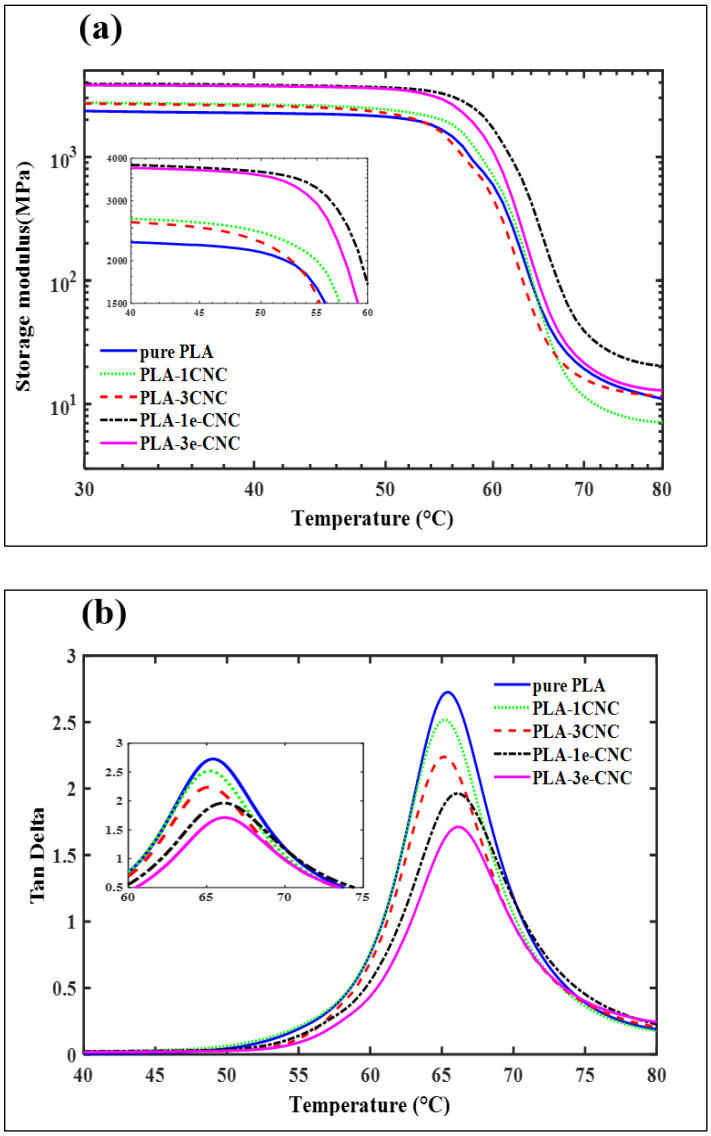

Figure 6.7. Representative DMA curves of PLA and nanocomposite: a) Storage modulus, b) Tan δ.

PLA-based nanocomposites exhibited higher storage modulus in glassy regions as compared to pure PLA, which was more prominent in PLA-e-CNC. In the rubbery state, only e-CNC resulted in higher storage modulus than that of pure PLA, which indicates the improvement of thermal-mechanical stability in PLA-e-CNC nanocomposites at elevated temperatures [233]. The improvement in storage modulus was characterized by the restricted polymer chain mobility because of the addition of cellulose nanocrystals and the higher crystallinity in nanocomposite

samples (Table 6.3). Similar behavior for PLA-based nanocomposites has been reported due to the incorporation of different concentration of cellulose nanofibers into PLA matrix [50].

Additionally, the intensity of tan δ peak is an indication of the dissipation of energy as a result of the chain mobility of the polymer segments at its corresponding temperature. Incorporating nanofillers into PLA induced a reduction in the tan δ peak value, suggesting stiffing behavior of nanofillers in nanocomposites. In both sets of nanocomposites, the peak value of tan δ exhibited a decline with the increase of nanofiller in nanocomposites.

Table 6.4. Thermo-mechanical behavior of PLA and its nanocomposites.

Sample	Tan δ peak	Storage modulus (MPa)	
		30 °C	70 °C
PLA	2.72	2353	19.33
PLA-1CNC	2.51	2740	11.54
PLA-3CNC	2.24	2708	15.99
PLA-1e-CNC	1.96	3894	39.2
PLA-3e-CNC	1.71	3807	21.53

The lower tan δ peak values for PLA-e-CNCs as compared to PLA-CNC nanocomposites can be ascribed to the existence of stronger interfacial interaction between e-CNCs and PLA matrix owing to more uniform dispersion of nanofillers [234] (Figure 6.4). The better fiber-matrix interaction can restrict the polymer chains and result in less energy dissipation [235]. This finding is corroborated by another study which reported lower tan δ intensity in PLA-based nanocomposites reinforced by cellulose nanocrystals [236]. Considering the location of the peak value of the tan δ curve as glass transition temperature of specimens, the same trend as DSC results were observed.

6.4.7. Mechanical Property

The representative stress vs strain curve for pure PLA and its corresponding nanocomposites are shown in Figure 6.8 and Table 6.5 summarized the mean values and standard deviations of the mechanical properties in the samples.

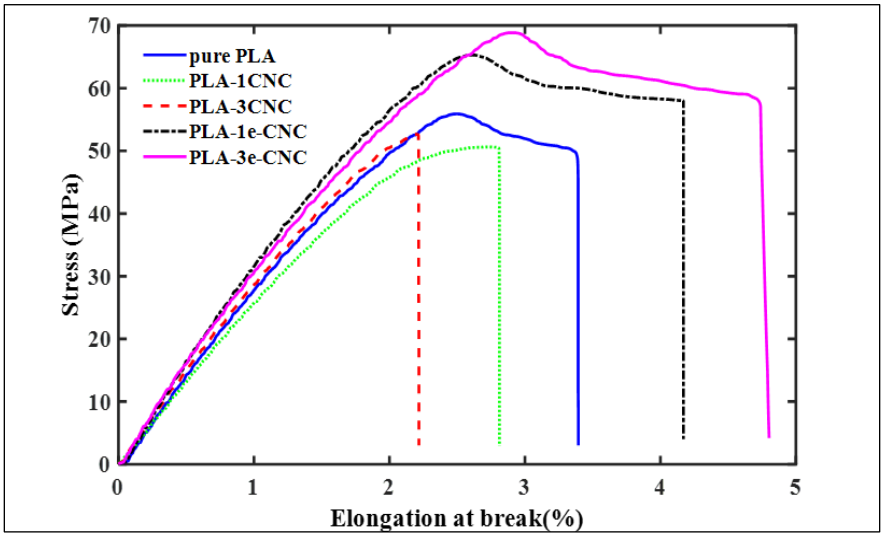

Figure 6.8. Representative stress–strain curves of PLA and the nanocomposites.

PLA-CNC nanocomposites broke without significant elongation at break, however, the elongation at break for PLA-e-CNC nanocomposites increased with increasing e-CNC contents. In addition, the presence of pristine CNCs in PLA led to a decline in the ultimate tensile strength as compared to pure PLA. However, e-CNCs acted as reinforcing phase, improving the stress-bearing capacity in nanocomposites, and increasing the ultimate tensile strength. Pure PLA samples exhibited the maximum tensile strength (σ_{max}) of 59.39 MPa and modulus of elasticity (E) of 3.33 GPa. Meanwhile, it can be observed that nanocomposite samples reinforced with e-CNCs exhibited the substantial improvement in σ_{max} (by 15.7 %) and E (by 58 %) in comparison with pure PLA, making the samples stiffer and stronger. This observation is likely supported by the fact that CNC aggregates existed in PLA-CNC nanocomposites, which were confirmed by SEM images (Figure 6.4). The CNC aggregates resulted in the weak interaction between PLA

and CNCs and consequently limited the stress transfer from matrix to nanofillers. Similar results were observed through adding unmodified CNCs into PLA [153]. In contrary, the higher σ_{max} and E in PLA-e-CNC nanocomposites were probably attributed to the better e-CNC dispersion in PLA matrix.

Table 6.5. Results of tensile and impact test of PLA and nanocomposites.

Sample	Young's modulus (GPa)	Tensile strength (MPa)	Elongation at break (%)	Impact Strength ($kJ.m^{-2}$)
PLA	$3.33\pm0.04^{b*}$	59.39 ± 1.20^{d}	3.5 ± 0.14^{d}	20.90 ± 0.63^{c}
PLA-1CNC	3.29 ± 0.19^{b}	52.76 ± 4.56^{c}	2.82 ± 0.51^{c}	21.15 ± 2.01^{c}
PLA-3CNC	3.37 ± 0.29^{b}	55.36 ± 4.21^{c}	2.23 ± 0.31^{b}	21.22 ± 1.48^{c}
PLA-1e-CNC	5.28 ± 0.34^{a}	65.00 ± 2.10^{b}	4.79 ± 0.11^{a}	27.28 ± 1.86^{b}
PLA-3e-CNC	4.85 ± 0.28^{a}	68.77 ± 0.88^{a}	5.01 ± 0.29^{a}	30.96 ± 2.03^{a}

* The different letters indicate a significant difference in the sample mean at $\alpha = 0.05$.

In general, the impact strength can be improved by incorporating individual nanofillers, since nanofiller bundles can act as crack initiation sites. The formation of relatively big CNC aggregates in PLA-CNC nanocomposites (Figure 6.4b, c) restricted the improvement of the impact strength, meaning the addition of pristine CNC into PLA matrix did not help in increasing the ductility. However, the higher impact strength in PLA-e-CNC seems therefore to be directly related to well-dispersed e-CNCs in PLA matrix (Figure 6.4d, e). PLA-1e-CNCs exhibited slightly higher Young's modulus in comparison with PLA-3e-CNC, which is statistically non-significant. However, PLA-3e-CNCs showed slightly higher elongation at break and significantly higher tensile strength and impact strength due to the higher amount of e-CNCs.

6.5. Conclusions

Chemical modification of cellulose nanocrystals was successfully performed using valeric acid and DMAP in a time-efficient procedure. Nanocomposites were prepared by diluting

spin-coated masterbatches using melt extrusion and injection molding. For the sake of comparison, pristine CNCs were used to make nanocomposites. The modified CNCs were analyzed using FTIR spectroscopy and TEM images. The FTIR spectra exhibited that chemical grafting was successfully attained. The TEM images showed that the structure of modified CNCs didn't alter to an obvious extent, compared with those of pristine CNCs. The SEM images of the fractured surface of nanocomposites containing pristine CNCs exhibited a relatively smooth fracture surface with the river-like pattern, indicating a brittle failure owing to weak bonding, however, rougher fracture surface of PLA-e-CNCs, suggested higher fracture energy required for fracture, as an indication of ductile failure. These observations were further confirmed through higher impact strength in PLA-e-CNC nanocomposites as compared to PLA-CNC samples. Meanwhile, Young's modulus and tensile strength were significantly higher in nanocomposites reinforced with e-CNCs in comparison with PLA and PLA-CNC nanocomposites, suggesting more uniform e-CNCs dispersion and stronger matrix and nanofiller interaction in PLA-e-CNC nanocomposites. The thermal stability results exhibited an improvement of 15.63 % in nanocomposite containing 3 % e-CNCs. In contrast, the incorporation of CNCs did not alter the thermal stability to an obvious extent. A considerable growth of 214 % was observed in crystallinity of PLA-3e-CNCs. The mechanical and thermal properties reported in this work demonstrated the potential application of the combination of time-efficient esterification and spin-coating masterbatches strategy for uniformly dispersing CNCs into PLA matrix.

7. CONCLUSIONS AND SUGGESTION FOR FUTURE WORK

7.1. Discussion

The main goal of this thesis dissertation was to identify and evaluate different chemical treatment methods and processing techniques that can improve the dispersion quality of cellulose nanocrystals (CNCs) in poly(lactic acid) (PLA) matrix. In particular, this thesis aimed at resolving issues such as irreversible microsized CNCs aggregation, low mechanical properties, and low thermal properties, mainly attributed to the hydrophilic nature of CNCs, presence of sulphate groups on CNCs as a result of CNCs extraction from bulk cellulose. In this work cellulose nanocrystals (CNCs) were modified though three different treatments to increase the hydrophobicity of CNCs and then incorporated into poly(lactic acid) via the application of masterbatch approach. The applied surface modification treatments were physical adsorption, green esterification and esterification. Masterbatches were prepared in the form of thin films through solvent casting and spin-coating methods. Nanocomposites were prepared using melt extrusion followed by injection molding process.

Chapter 1 and chapter 2 presented a general overview on this study, included the research hypotheses and objectives. The thesis structure also was reported in chapter 1. Chapter 2 provided an overview of previous research on CNCs modification treatment as well as mechanical preparation methods, aiming at improvement in the CNCs dispersion in PLA matrix.

In chapter 3, we have identified a facile spin-coating method for preparing high concentrated thin film masterbatches. A comparative study was conducted between solvent casting and spin-coating methods. SEM micrographs of masterbatches shown more homogenous and uniform p-CNCs dispersion in spin-coated masterbatches. This observation was described by high evaporation rate of the solvent as well as the combination of surface tension and centrifugal

force in the spin-coating method, hindering the formation of CNC aggregates. Similarly, more uniform CNC dispersion in spin-coated nanocomposites resulted in higher mechanical properties in spin-coated nanocomposites, confirming the reliability of spin-coating method as a preprocessing step in nanocomposite processing.

In chapter 4, we evaluated the influence of masterbatch preparation techniques on thermal stability, and rheological properties of nanocomposites. Furthermore, a detailed study was conducted on the molecular structure of the nanocomposites using GPC. It was observed that spin-coated nanocomposites possessed higher molecular weight with a wide distribution of chain lengths probably, due to the high injection pressure during spin-coated masterbatch production process. Higher molecular weight was observed in the spin-coated nanocomposites owing to higher molecular number in comparison with solvent cast nanocomposites. The results of this study reveal that PLA nanocomposite properties can be engineered using different mechanical processing methods. Spin-coating technique is a promising approach for masterbatch preparation, as it improves the mechanical and thermal properties of the PLA-CNC nanocomposites.

Chapter 5 focused on the application of green chemistry for cellulose nanocrystals modification. In that study benzoic acid as a nontoxic chemical was introduced on the surface of CNCs through a green esterification method. The mechanical properties as well as thermal stability of the nanocomposites prepared using modified CNCs were significantly higher than the nanocomposites reinforced by pristine CNCs. In addition, nanocomposites containing modified CNCs exhibited rough fracture surface, indicating the need of more energy for fracture. The overall improvement was observed in nanocomposites reinforced with modified CNCs, as a result of formation of smaller CNC aggregates.

In chapter 6, a time-efficient esterification technique was introduced for CNC surface modification. The nanocomposite processing time was reduced using spin-coating method for masterbatch preparation. In this study, chemical modification of CNCs was conducted using valeric acid and DMAP. The FTIR spectra exhibited the successful chemical grafting on the surface of the CNCs, however, structure of modified CNCs didn't alter to an obvious extent in comparison with pristine CNCs. The uniform fractures on the surface of nanocomposites reinforced by modified CNCs reveals the optimal CNC dispersion in this study and resulted in the higher mechanical and thermal properties.

In general, the results reported in this thesis exhibited the potential application of different surface modification treatments of CNCs along with different mechanical preparation techniques for improving the physical and mechanical properties of PLA-CNC composites.

7.2. Comparison between Esterification Techniques Identified in This Dissertation

In order to compare two esterification techniques identified in this study, different aspects such as processing time, environmental aspect, mechanical properties, and thermal characteristics should be considered.

The green esterification method which was identified in chapter five, required more processing time due to the lack of catalyzer in comparison with esterification technique introduced in chapter six. The application of DMAP as a catalyzer in esterification method using valeric acid expedited CNC' surface modification treatment and reduced the processing time to four hours. While, the solvent free green esterification technique required 20 hours to modify the surface of the CNCs.

The solvent-free green esterification method using benzoic acid with a broad application in food industry as a nontoxic and recyclable substance diminishes the environmental footprint

of the chemicals. While, the application of different chemicals even in low amount in esterification technique might reduce the potential application of the esterification method identified in chapter six.

From mechanical point of view, the higher mechanical properties were observed in nanocomposites reinforced by esterified modified CNCs in comparison with PLA and green esterified CNCs. This observation might be related to uniform dispersion of esterified CNCs through PLA matrix. In fact, the presence of well-defined peak at 1730 nm in FTIR confirmed the high efficiency of esterification technique identified in chapter six.

7.3. Alternative Solvent to Chloroform

Methylene dichloride (Dichloromethane) is a geminal organic compound with the chemical formula CH_2Cl_2. Dichloromethane as colorless and volatile liquid with a moderately sweet aroma is widely used as a solvent. Dichloromethane as a polar solvent, and miscible in a wide range of organic compounds is used in different applications such as paint and food industries. Dichloromethane is used to decaffeinate coffee and tea and it also has been used to prepare flavorings in food industry. The high evaporation rate of dichloromethane makes it as an appropriate solvent for aeosel spray propellant and blowing agent for polyurethanefoams. Dichloromethane is not recognized as an ozone-depleting material by Montreal Protocol and the US Clean Air Act. According to Environmental Protection Agency, the short lifetime of Dichloromethane accelerates the chemical decomposition before reaching the ozone layer. This solvent was introduced as an alternative for chloroform since dichloromethane is the least toxic of the simple chlorohydrocabons and it has the same chemical behavior as chloroform.

7.4. Suggestion for Future Work

Although the provided research studies and methodologies of this dissertation covered a relatively wide area of PLA reinforced by modified CNCs, future works aim at addressing PLA shortcomings explored in this chapter.

7.4.1. Spray-Coating

As mentioned earlier, the main advantage of spin-coating method was the high evaporation rate of the solvent as well as the combination of surface tension and centrifugal force. Therefore, the application of spray coating method for masterbatch preparation can be considered as a versatile and effective alternative to spin-coating method. The specific discharging process on the substrate, which could be either static or rotating at high velocity in spray coating method can further increase the solvent evaporation rate and consequently inhibits the self-assembly of CNC aggregate through highly concentrated masterbatches.

7.4.2. Electrospinning

Electrospinning is an attractive fiber production method which employs electric force to prepare polymer filaments with diameters oscillating from 2 nm to several micrometers from polymer solution. An electric field between a droplet of polymer solution at the tip of a needle and a collector plate can effectively govern the geography and orientation of the fibrous assembly. Therefore, nanocomposite nanofiber as highly concentrated masterbatches can be prepared in the form of spun nanofibers with extremely high surface-to-volume ratio and tunable permeability through the application of electrospinning method.

7.4.3. Plasma Surface Modification Treatment

Plasma treatment of fibers is a common method in fiber modification and frequently used to improve the chemical and physical structure of fibers without affecting their bulk mechanical properties. Different plasma treatments can modify the hydrophilicity character of nanofillers in good interaction with environmental worries. Plasma treatment using different carrier gasses such as hydrogen and oxygen has been commonly employed to modify surface adhesion and wetting characteristics by altering the surface chemical configuration of the fibers. The morphology of CNCs can be tailored by introducing carboxyl groups or amine groups through oxygen or ammonia gasses. Therefore, the application of plasma treatment as a CNC surface modification treatment can be explored to further improve the hydrophobicity character of CNCs.

7.4.4. Evaluating the Barrier Properties of Nanocomposite Films

In spite of PLA's success its barrier properties are often insufficient for food packaging applications. Barrier property is an important characteristic of biodegradable polymers which may impact their suitability for a specific application. Barrier properties are generally a function of degree of crystallinity, crystalline/amorphous phase ratio, structural characteristics and polarity of the polymeric chains, and processing parameters [237, 238]. PLA exhibits comparable permeability to carbon dioxide (CO_2) and oxygen (O_2) however, it is relatively permeable to small molecules such as water vapor (WV), organic vapors, and liquids [239]. The poor barrier properties in PLA as compared with selected petroleum- based polymers impose restrictions over its commercial application in packaging industry. The influence of spin-coating method on barrier properties of thin PLA nanocomposite films needs to be evaluated.

REFERENCES

[1] L.-T. Lim, R. Auras, and M. Rubino, "Processing technologies for poly (lactic acid)," *Progress in polymer science,* vol. 33, no. 8, pp. 820-852, 2008.

[2] K. Masutani and Y. Kimura, "PLA synthesis. From the monomer to the polymer," 2014.

[3] M. Hartmann and D. Kaplan, "Biopolymers from renewable resources," *Kaplan, DL, Ed,* vol. 367, pp. 629-638, 1998.

[4] T. F. Garrison, A. Murawski, and R. L. Quirino, "Bio-Based Polymers with Potential for Biodegradability," *Polymers,* vol. 8, no. 7, p. 262, 2016.

[5] A. A. Shah, F. Hasan, A. Hameed, and S. Ahmed, "Biological degradation of plastics: a comprehensive review," *Biotechnology advances,* vol. 26, no. 3, pp. 246-265, 2008.

[6] V. Taubner and R. Shishoo, "Influence of processing parameters on the degradation of poly (L-lactide) during extrusion," *Journal of applied polymer science,* vol. 79, no. 12, pp. 2128-2135, 2001.

[7] Y. Aoyagi, K. Yamashita, and Y. Doi, "Thermal degradation of poly [(R)-3-hydroxybutyrate], poly [ε-caprolactone], and poly [(S)-lactide]," *Polymer Degradation and Stability,* vol. 76, no. 1, pp. 53-59, 2002.

[8] H. Tsuji, "Autocatalytic hydrolysis of amorphous-made polylactides: effects of L-lactide content, tacticity, and enantiomeric polymer blending," *Polymer,* vol. 43, no. 6, pp. 1789-1796, 2002.

[9] L. NatureWorks, "Technology Focus Report: Blends of PLA with Other Thermoplastics," ed: USA, 2007.

[10] K. Zhu, S. Bihai, and Y. Shilin, "Super microcapsules (SMC). I. Preparation and characterization of star polymethylene oxide (PEO) polylactide (PLA) copolymers," *Journal of Polymer Science Part A: Polymer Chemistry,* vol. 27, no. 7, pp. 2151-2159, 1989.

[11] S. K. Sahoo, J. Panyam, S. Prabha, and V. Labhasetwar, "Residual polyvinyl alcohol associated with poly (D, L-lactide-co-glycolide) nanoparticles affects their physical properties and cellular uptake," *Journal of controlled release,* vol. 82, no. 1, pp. 105-114, 2002.

[12] J. Njuguna, K. Pielichowski, and S. Desai, "Nanofiller-reinforced polymer nanocomposites," *Polymers for Advanced Technologies,* vol. 19, no. 8, pp. 947-959, 2008.

[13] J. George and S. Sabapathi, "Cellulose nanocrystals: synthesis, functional properties, and applications," *Nanotechnology, science and applications,* vol. 8, p. 45, 2015.

[14] J. Jancar *et al.*, "Current issues in research on structure–property relationships in polymer nanocomposites," *Polymer,* vol. 51, no. 15, pp. 3321-3343, 2010.

[15] M. Šupová, G. S. Martynková, and K. Barabaszová, "Effect of nanofillers dispersion in polymer matrices: a review," *Science of Advanced Materials,* vol. 3, no. 1, pp. 1-25, 2011.

[16] D. Wu *et al.*, "Selective localization of nanofillers: effect on morphology and crystallization of PLA/PCL blends," *Macromolecular Chemistry and Physics,* vol. 212, no. 6, pp. 613-626, 2011.

[17] P. Qu, Y. Gao, G. Wu, and L. Zhang, "Nanocomposites of poly (lactic acid) reinforced with cellulose nanofibrils," *BioResources,* vol. 5, no. 3, pp. 1811-1823, 2010.

[18] M. Arrieta, E. Fortunati, F. Dominici, E. Rayón, J. López, and J. Kenny, "Multifunctional PLA–PHB/cellulose nanocrystal films: processing, structural and thermal properties," *Carbohydrate polymers,* vol. 107, pp. 16-24, 2014.
[19] A. Pei, Q. Zhou, and L. A. Berglund, "Functionalized cellulose nanocrystals as biobased nucleation agents in poly (l-lactide)(PLLA)–Crystallization and mechanical property effects," *Composites Science and Technology,* vol. 70, no. 5, pp. 815-821, 2010.
[20] O. J. Rojas, *Cellulose Chemistry and Properties: Fibers, Nanocelluloses and Advanced Materials*. Springer, 2016.
[21] C. Gozdecki and A. Wilczyn, "Effects of wood particle size and test specimen size on mechanical and water resistance properties of injected wood–high density polyethylene composite," *Wood and Fiber Science,* vol. 47, no. 4, pp. 365-374, 2015.
[22] G. Siqueira, S. Tapin-Lingua, J. Bras, D. da Silva Perez, and A. Dufresne, "Morphological investigation of nanoparticles obtained from combined mechanical shearing, and enzymatic and acid hydrolysis of sisal fibers," *Cellulose,* vol. 17, no. 6, pp. 1147-1158, 2010.
[23] Q. Wang, X. Zhao, and J. Zhu, "Kinetics of strong acid hydrolysis of a bleached kraft pulp for producing cellulose nanocrystals (CNCs)," *Industrial & Engineering Chemistry Research,* vol. 53, no. 27, pp. 11007-11014, 2014.
[24] P. B. Filson, B. E. Dawson-Andoh, and D. Schwegler-Berry, "Enzymatic-mediated production of cellulose nanocrystals from recycled pulp," *Green Chemistry,* vol. 11, no. 11, pp. 1808-1814, 2009.
[25] S. Ahola, X. Turon, M. Osterberg, J. Laine, and O. Rojas, "Enzymatic hydrolysis of native cellulose nanofibrils and other cellulose model films: effect of surface structure," *Langmuir,* vol. 24, no. 20, pp. 11592-11599, 2008.
[26] M. N. Angles and A. Dufresne, "Plasticized starch/tunicin whiskers nanocomposite materials. 2. Mechanical behavior," *Macromolecules,* vol. 34, no. 9, pp. 2921-2931, 2001.
[27] F. W. Herrick, R. L. Casebier, J. K. Hamilton, and K. R. Sandberg, "Microfibrillated cellulose: morphology and accessibility," in *J. Appl. Polym. Sci.: Appl. Polym. Symp.;(United States)*, 1983, vol. 37, no. CONF-8205234-Vol. 2: ITT Rayonier Inc., Shelton, WA.
[28] X. M. Dong, J.-F. Revol, and D. G. Gray, "Effect of microcrystallite preparation conditions on the formation of colloid crystals of cellulose," *Cellulose,* vol. 5, no. 1, pp. 19-32, 1998.
[29] M. Hasani, E. D. Cranston, G. Westman, and D. G. Gray, "Cationic surface functionalization of cellulose nanocrystals," *Soft Matter,* vol. 4, no. 11, pp. 2238-2244, 2008.
[30] S. Beck-Candanedo, M. Roman, and D. G. Gray, "Effect of reaction conditions on the properties and behavior of wood cellulose nanocrystal suspensions," *Biomacromolecules,* vol. 6, no. 2, pp. 1048-1054, 2005.
[31] S. Iwamoto, W. Kai, A. Isogai, and T. Iwata, "Elastic modulus of single cellulose microfibrils from tunicate measured by atomic force microscopy," *Biomacromolecules,* vol. 10, no. 9, pp. 2571-2576, 2009.
[32] C. Miao and W. Y. Hamad, "Cellulose reinforced polymer composites and nanocomposites: a critical review," *Cellulose,* vol. 20, no. 5, pp. 2221-2262, 2013.

[33] T. Abitbol *et al.*, "Nanocellulose, a tiny fiber with huge applications," *Current opinion in biotechnology,* vol. 39, pp. 76-88, 2016.
[34] A. Hebeish and J. Guthrie, "The chemistry and technology of cellulosic copolymers," S*pringer Science & Business*, 2012.
[35] M. Nagalakshmaiah, "Melt processing of cellulose nanocrystals: thermal, mechanical and rheological properties of polymer nanocomposites," Grenoble Alpes, 2016.
[36] S. Eyley and W. Thielemans, "Surface modification of cellulose nanocrystals," *Nanoscale,* vol. 6, no. 14, pp. 7764-7779, 2014.
[37] L. A. Lucia and O. Rojas, *The nanoscience and technology of renewable biomaterials*. John Wiley & Sons, 2009.
[38] V. K. Thakur, *Nanocellulose polymer nanocomposites: fundamentals and applications*. John Wiley & Sons, 2014.
[39] P. H. C. Camargo, K. G. Satyanarayana, and F. Wypych, "Nanocomposites: synthesis, structure, properties and new application opportunities," *Materials Research,* vol. 12, no. 1, pp. 1-39, 2009.
[40] C. Zhou, X. Qiu, Q. Zhuang, Z. Han, and Q. Wu, "In situ polymerization and photophysical properties of poly (p-phenylene benzobisoxazole)/multiwalled carbon nanotubes composites," *Journal of Applied Polymer Science,* vol. 124, no. 6, pp. 4740-4746, 2012.
[41] H.-M. Ng *et al.*, "Extraction of cellulose nanocrystals from plant sources for application as reinforcing agent in polymers," *Composites Part B: Engineering,* vol. 75, pp. 176-200, 2015.
[42] D. Bagheriasl, P. J. Carreau, B. Riedl, C. Dubois, and W. Y. Hamad, "Shear rheology of polylactide (PLA)–cellulose nanocrystal (CNC) nanocomposites," *Cellulose,* vol. 23, no. 3, pp. 1885-1897, 2016.
[43] C. Goussé, H. Chanzy, G. Excoffier, L. Soubeyrand, and E. Fleury, "Stable suspensions of partially silylated cellulose whiskers dispersed in organic solvents," *Polymer,* vol. 43, no. 9, pp. 2645-2651, 2002.
[44] C. Aguir and M. F. M'Henni, "Experimental study on carboxymethylation of cellulose extracted from Posidonia oceanica," *Journal of applied polymer science,* vol. 99, no. 4, pp. 1808-1816, 2006.
[45] H. Yuan, Y. Nishiyama, M. Wada, and S. Kuga, "Surface acylation of cellulose whiskers by drying aqueous emulsion," *Biomacromolecules*, vol. 7, no. 3, pp. 696-700, 2006.
[46] S. Spinella *et al.*, "Concurrent cellulose hydrolysis and esterification to prepare a surface-modified cellulose nanocrystal decorated with carboxylic acid moieties," *ACS Sustainable Chemistry & Engineering,* vol. 4, no. 3, pp. 1538-1550, 2016.
[47] G. Roggio, "Extrusion of Polylactic acid (PLA) Nanocomposites using Liquid Feeding of Cellulose Nanocrystals," ed, 2014.
[48] N. Herrera, A. P. Mathew, and K. Oksman, "Plasticized polylactic acid/cellulose nanocomposites prepared using melt-extrusion and liquid feeding: mechanical, thermal and optical properties," *Composites Science and Technology,* vol. 106, pp. 149-155, 2015.
[49] B. Lepoittevin *et al.*, "Polymer/layered silicate nanocomposites by combined intercalative polymerization and melt intercalation: a masterbatch process," *Polymer,* vol. 44, no. 7, pp. 2033-2040, 2003.

[50] M. Jonoobi, J. Harun, A. P. Mathew, and K. Oksman, "Mechanical properties of cellulose nanofiber (CNF) reinforced polylactic acid (PLA) prepared by twin screw extrusion," *Composites Science and Technology,* vol. 70, no. 12, pp. 1742-1747, 2010.
[51] L. Petersson, I. Kvien, and K. Oksman, "Structure and thermal properties of poly (lactic acid)/cellulose whiskers nanocomposite materials," *Composites Science and Technology,* vol. 67, no. 11, pp. 2535-2544, 2007.
[52] T. Mukherjee and N. Kao, "PLA based biopolymer reinforced with natural fibre: a review," *Journal of Polymers and the Environment,* vol. 19, no. 3, p. 714, 2011.
[53] A. Baier, "Nanocomposites With Biodegradable Polymers Synthesis Properties And Future Perspectives," *Synthesis,* vol. 1, p. 4, 2016.
[54] M. T. Postek, R. J. Moon, A. W. Rudie, and M. A. Bilodeau, *Production and applications of cellulose*. Tappi Press. Peachtree Corners, 2013.
[55] M. S. Peresin, Y. Habibi, J. O. Zoppe, J. J. Pawlak, and O. J. Rojas, "Nanofiber composites of polyvinyl alcohol and cellulose nanocrystals: manufacture and characterization," *Biomacromolecules,* vol. 11, no. 3, pp. 674-681, 2010.
[56] A. Pei, J.-M. Malho, J. Ruokolainen, Q. Zhou, and L. A. Berglund, "Strong nanocomposite reinforcement effects in polyurethane elastomer with low volume fraction of cellulose nanocrystals," *Macromolecules,* vol. 44, no. 11, pp. 4422-4427, 2011.
[57] H. A. Silvério, W. P. F. Neto, N. O. Dantas, and D. Pasquini, "Extraction and characterization of cellulose nanocrystals from corncob for application as reinforcing agent in nanocomposites," *Industrial Crops and Products,* vol. 44, pp. 427-436, 2013.
[58] N. Lin, J. Huang, P. R. Chang, J. Feng, and J. Yu, "Surface acetylation of cellulose nanocrystal and its reinforcing function in poly (lactic acid)," *Carbohydrate Polymers,* vol. 83, no. 4, pp. 1834-1842, 2011.
[59] H. Chang *et al.*, "Individually dispersed wood-based cellulose nanocrystals," *ACS applied materials & interfaces,* vol. 8, no. 9, pp. 5768-5771, 2016.
[60] V. Khoshkava and M. Kamal, "Effect of surface energy on dispersion and mechanical properties of polymer/nanocrystalline cellulose nanocomposites," *Biomacromolecules,* vol. 14, no. 9, pp. 3155-3163, 2013.
[61] M. Salajková, L. A. Berglund, and Q. Zhou, "Hydrophobic cellulose nanocrystals modified with quaternary ammonium salts," *Journal of Materials Chemistry,* vol. 22, no. 37, pp. 19798-19805, 2012.
[62] R. J. Moon, A. Martini, J. Nairn, J. Simonsen, and J. Youngblood, "Cellulose nanomaterials review: structure, properties and nanocomposites," *Chemical Society Reviews,* vol. 40, no. 7, pp. 3941-3994, 2011.
[63] S. Fujisawa, T. Saito, S. Kimura, T. Iwata, and A. Isogai, "Surface engineering of ultrafine cellulose nanofibrils toward polymer nanocomposite materials," *Biomacromolecules,* vol. 14, no. 5, pp. 1541-1546, 2013.
[64] B. Peng, N. Dhar, H. Liu, and K. Tam, "Chemistry and applications of nanocrystalline cellulose and its derivatives: a nanotechnology perspective," *The Canadian Journal of Chemical Engineering,* vol. 89, no. 5, pp. 1191-1206, 2011.
[65] Y. Sokolova, S. Shubanov, L. Kandyrin, and E. Kalugina, "Polymer nanocomposites and their structure and properties. A review," *Plast. Massy,* no. 3, pp. 18-23, 2009.
[66] J. Shojaeiarani, D. S. Bajwa, and N. M. Stark, "Green esterification: A new approach to improve thermal and mechanical properties of poly(lactic acid) composites reinforced by cellulose nanocrystals," *Journal of applied polymer science,* 2018.

[67] N. Lin and A. Dufresne, "Physical and/or chemical compatibilization of extruded cellulose nanocrystal reinforced polystyrene nanocomposites," *Macromolecules,* vol. 46, no. 14, pp. 5570-5583, 2013.
[68] K. Missoum, M. N. Belgacem, and J. Bras, "Nanofibrillated cellulose surface modification: a review," *Materials,* vol. 6, no. 5, pp. 1745-1766, 2013.
[69] S. A. Kedzior, H. S. Marway, and E. D. Cranston, "Tailoring Cellulose Nanocrystal and Surfactant Behavior in Miniemulsion Polymerization," *Macromolecules,* 2017.
[70] L. Carlsson, "Surface modification of cellulose by covalent grafting and physical adsorption," 2014.
[71] J. Majoinen *et al.*, "Polyelectrolyte brushes grafted from cellulose nanocrystals using Cu-mediated surface-initiated controlled radical polymerization," *Biomacromolecules,* vol. 12, no. 8, pp. 2997-3006, 2011.
[72] M. Gu, C. Jiang, D. Liu, N. Prempeh, and I. I. Smalyukh, "Cellulose Nanocrystal/Poly (ethylene glycol) Composite as an Iridescent Coating on Polymer Substrates: Structure-color and Interface Adhesion," *ACS Applied Materials & Interfaces,* 2016.
[73] A. Arias, M.-C. Heuzey, M. A. Huneault, G. Ausias, and A. Bendahou, "Enhanced dispersion of cellulose nanocrystals in melt-processed polylactide-based nanocomposites," *Cellulose,* vol. 22, no. 1, pp. 483-498, 2015.
[74] S. Spinella *et al.*, "Polylactide/cellulose nanocrystal nanocomposites: Efficient routes for nanofiber modification and effects of nanofiber chemistry on PLA reinforcement," *Polymer,* vol. 65, pp. 9-17, 2015.
[75] D. Yang *et al.*, "Fabrication of a highly elastic nanocomposite hydrogel by surface modification of cellulose nanocrystals," *RSC Advances,* vol. 5, no. 18, pp. 13878-13885, 2015.
[76] A. Dufresne, *Nanocellulose: from nature to high performance tailored materials*. Walter de Gruyter, 2013.
[77] C. Rauwendaal, *Polymer extrusion*. Carl Hanser Verlag GmbH Co KG, 2014.
[78] H. F. Giles Jr, E. M. Mount III, and J. R. Wagner Jr, *Extrusion: the definitive processing guide and handbook*. William Andrew, 2004.
[79] K. Oksman, A. P. Mathew, D. Bondeson, and I. Kvien, "Manufacturing process of cellulose whiskers/polylactic acid nanocomposites," *Composites science and technology,* vol. 66, no. 15, pp. 2776-2784, 2006.
[80] M. Pracella, M. M.-U. Haque, and D. Puglia, "Morphology and properties tuning of PLA/cellulose nanocrystals bio-nanocomposites by means of reactive functionalization and blending with PVAc," *Polymer,* vol. 55, no. 16, pp. 3720-3728, 2014.
[81] M. Mariano, N. El Kissi, and A. Dufresne, "Melt processing of cellulose nanocrystal reinforced polycarbonate from a masterbatch process," *European Polymer Journal,* vol. 69, pp. 208-223, 2015.
[82] G. Gong, A. P. Mathew, and K. Oksman, "Toughening effect of cellulose nanowhiskers on polyvinyl acetate: fracture toughness and viscoelastic analysis," *Polymer Composites,* vol. 32, no. 10, pp. 1492-1498, 2011.
[83] A. C. Corrêa *et al.*, "Obtaining nanocomposites of polyamide 6 and cellulose whiskers via extrusion and injection molding," *Cellulose,* vol. 21, no. 1, pp. 311-322, 2014.
[84] S.-H. Lee, Y. Teramoto, and T. Endo, "Cellulose nanofiber-reinforced polycaprolactone/polypropylene hybrid nanocomposite," *Composites Part A: Applied Science and Manufacturing,* vol. 42, no. 2, pp. 151-156, 2011.

[85] W. Yang *et al.*, "Synergic effect of cellulose and lignin nanostructures in PLA based systems for food antibacterial packaging," *European Polymer Journal,* vol. 79, pp. 1-12, 2016.
[86] J. Shojaeiarani, D. Bajwa, and N. Stark, "Spin-coating: A new approach for improving dispersion of cellulose nanocrytals and mechanical properties of poly(lactic acid) composites," *Carbohydrate polymers,* 2018.
[87] U. Siemann, "Solvent cast technology–a versatile tool for thin film production," *Scattering Methods and the Properties of Polymer Materials,* pp. 307-316, 2005.
[88] D. L. Chinaglia *et al.*, "Influence of the solvent evaporation rate on the crystalline phases of solution-cast poly (vinylidene fluoride) films," *Journal of applied polymer science,* vol. 116, no. 2, pp. 785-791, 2010.
[89] V. Favier, G. Canova, J. Cavaillé, H. Chanzy, A. Dufresne, and C. Gauthier, "Nanocomposite materials from latex and cellulose whiskers," *Polymers for Advanced Technologies,* vol. 6, no. 5, pp. 351-355, 1995.
[90] P. Anbukarasu, D. Sauvageau, and A. Elias, "Tuning the properties of polyhydroxybutyrate films using acetic acid via solvent casting," *Scientific reports,* vol. 5, p. 17884, 2015.
[91] S.-T. Hsu and Y. L. Yao, "Effect of Film Formation Method and Annealing on Morphology and Crystal Structure of Poly (L-Lactic Acid) Films," *Journal of Manufacturing Science and Engineering,* vol. 136, no. 2, p. 021006, 2014.
[92] M. Jonoobi, A. P. Mathew, M. M. Abdi, M. D. Makinejad, and K. Oksman, "A comparison of modified and unmodified cellulose nanofiber reinforced polylactic acid (PLA) prepared by twin screw extrusion," *Journal of Polymers and the Environment,* vol. 20, no. 4, pp. 991-997, 2012.
[93] A. Dufresne, "Nanocellulose: a new ageless bionanomaterial," *Materials Today,* vol. 16, no. 6, pp. 220-227, 2013.
[94] O. Mellbring, S. Kihlman Øiseth, A. Krozer, J. Lausmaa, and T. Hjertberg, "Spin coating and characterization of thin high-density polyethylene films," *Macromolecules,* vol. 34, no. 21, pp. 7496-7503, 2001.
[95] K. Norrman, A. Ghanbari-Siahkali, and N. Larsen, "6 Studies of spin-coated polymer films," *Annual Reports Section" C"(Physical Chemistry),* vol. 101, pp. 174-201, 2005.
[96] D. B. Hall, P. Underhill, and J. M. Torkelson, "Spin coating of thin and ultrathin polymer films," *Polymer Engineering & Science,* vol. 38, no. 12, pp. 2039-2045, 1998.
[97] J. A. Syed, H. Lu, S. Tang, and X. Meng, "Enhanced corrosion protective PANI-PAA/PEI multilayer composite coatings for 316SS by spin coating technique," *Applied Surface Science,* vol. 325, pp. 160-169, 2015.
[98] C. Brinker, A. Hurd, P. Schunk, G. Frye, and C. Ashley, "Review of sol-gel thin film formation," *Journal of Non-Crystalline Solids,* vol. 147, pp. 424-436, 1992.
[99] J. Danglad-Flores, S. Eickelmann, and H. Riegler, "Deposition of polymer films by spin casting: A quantitative analysis," *Chemical Engineering Science,* 2018.
[100] N. Sahu, B. Parija, and S. Panigrahi, "Fundamental understanding and modeling of spin coating process: A review," *Indian Journal of Physics,* vol. 83, no. 4, pp. 493-502, 2009.
[101] S.-Y. Lien, D.-S. Wuu, W.-C. Yeh, and J.-C. Liu, "Tri-layer antireflection coatings (SiO2/SiO2–TiO2/TiO2) for silicon solar cells using a sol–gel technique," *Solar Energy Materials and Solar Cells,* vol. 90, no. 16, pp. 2710-2719, 2006.

[102] A. G. Emslie, F. T. Bonner, and L. G. Peck, "Flow of a viscous liquid on a rotating disk," *Journal of Applied Physics,* vol. 29, no. 5, pp. 858-862, 1958.
[103] M. A. Herrera, J. A. Sirviö, A. P. Mathew, and K. Oksman, "Environmental friendly and sustainable gas barrier on porous materials: Nanocellulose coatings prepared using spin- and dip-coating," *Materials & Design,* vol. 93, pp. 19-25, 2016.
[104] F. Zabihi, Y. Xie, S. Gao, and M. Eslamian, "Morphology, conductivity, and wetting characteristics of PEDOT: PSS thin films deposited by spin and spray coating," *Applied Surface Science,* vol. 338, pp. 163-177, 2015.
[105] Y. Cheng, S. Deng, P. Chen, and R. Ruan, "Polylactic acid (PLA) synthesis and modifications: a review," *Frontiers of chemistry in China,* vol. 4, no. 3, pp. 259-264, 2009.
[106] M. Jamshidian, E. A. Tehrany, M. Imran, M. Jacquot, and S. Desobry, "Poly-Lactic Acid: production, applications, nanocomposites, and release studies," *Comprehensive Reviews in Food Science and Food Safety,* vol. 9, no. 5, pp. 552-571, 2010.
[107] J. Y. Nam, S. Sinha Ray, and M. Okamoto, "Crystallization behavior and morphology of biodegradable polylactide/layered silicate nanocomposite," *Macromolecules,* vol. 36, no. 19, pp. 7126-7131, 2003.
[108] R. E. Drumright, P. R. Gruber, and D. E. Henton, "Polylactic acid technology," *Advanced materials,* vol. 12, no. 23, pp. 1841-1846, 2000.
[109] S. Domenek and V. Ducruet, "Characteristics and Applications of PLA," *Biodegradable and Biobased Polymers for Environmental and Biomedical Applications,* pp. 171-224, 2016.
[110] K. Oksman, M. Skrifvars, and J.-F. Selin, "Natural fibres as reinforcement in polylactic acid (PLA) composites," *Composites science and technology,* vol. 63, no. 9, pp. 1317-1324, 2003.
[111] A. Gupta, W. Simmons, G. T. Schueneman, D. Hylton, and E. A. Mintz, "Rheological and thermo-mechanical properties of poly (lactic acid)/lignin-coated cellulose nanocrystal composites," *ACS Sustainable Chemistry & Engineering,* vol. 5, no. 2, pp. 1711-1720, 2017.
[112] N. Ljungberg and B. Wesslén, "Preparation and properties of plasticized poly (lactic acid) films," *Biomacromolecules,* vol. 6, no. 3, pp. 1789-1796, 2005.
[113] X. Li *et al.,* "Impact behaviors of poly-lactic acid based biocomposite reinforced with unidirectional high-strength magnesium alloy wires," *Progress in Natural Science: Materials International,* vol. 24, no. 5, pp. 472-478, 2014.
[114] X. Shi, J. Jiang, L. Sun, and Z. Gan, "Hydrolysis and biomineralization of porous PLA microspheres and their influence on cell growth," *Colloids and Surfaces B: Biointerfaces,* vol. 85, no. 1, pp. 73-80, 2011.
[115] C. S. Yoon and D. S. Ji, "The effects of blend composition and blending time on the ester interchange reaction and tensile properties of PLA/LPCL/HPCL blends," *Fibers and Polymers,* vol. 4, no. 2, pp. 59-65, 2003.
[116] K. J. De France, K. J. Chan, E. D. Cranston, and T. Hoare, "Enhanced mechanical properties in cellulose nanocrystal–poly (oligoethylene glycol methacrylate) injectable nanocomposite hydrogels through control of physical and chemical cross-linking," *Biomacromolecules,* vol. 17, no. 2, pp. 649-660, 2016.

[117] Q. Shi, C. Zhou, Y. Yue, W. Guo, Y. Wu, and Q. Wu, "Mechanical properties and in vitro degradation of electrospun bio-nanocomposite mats from PLA and cellulose nanocrystals," *Carbohydrate polymers*, vol. 90, no. 1, pp. 301-308, 2012.
[118] M. Martínez-Sanz, A. Lopez-Rubio, and J. M. Lagaron, "Optimization of the dispersion of unmodified bacterial cellulose nanowhiskers into polylactide via melt compounding to significantly enhance barrier and mechanical properties," *Biomacromolecules*, vol. 13, no. 11, pp. 3887-3899, 2012.
[119] H.-Y. Yu, Z.-Y. Qin, Y.-N. Liu, L. Chen, N. Liu, and Z. Zhou, "Simultaneous improvement of mechanical properties and thermal stability of bacterial polyester by cellulose nanocrystals," *Carbohydrate polymers*, vol. 89, no. 3, pp. 971-978, 2012.
[120] E. M. Sullivan, R. J. Moon, and K. Kalaitzidou, "Processing and characterization of cellulose nanocrystals/polylactic acid nanocomposite films," *Materials*, vol. 8, no. 12, pp. 8106-8116, 2015.
[121] L. Brinchi, F. Cotana, E. Fortunati, and J. Kenny, "Production of nanocrystalline cellulose from lignocellulosic biomass: technology and applications," *Carbohydrate Polymers*, vol. 94, no. 1, pp. 154-169, 2013.
[122] N. Duran, A. Paula Lemes, and A. B Seabra, "Review of cellulose nanocrystals patents: preparation, composites and general applications," *Recent patents on nanotechnology*, vol. 6, no. 1, pp. 16-28, 2012.
[123] D. Klemm *et al.*, "Nanocelluloses: A new family of nature-based materials," *Angewandte Chemie International Edition*, vol. 50, no. 24, pp. 5438-5466, 2011.
[124] W. Hamad, "On the development and applications of cellulosic nanofibrillar and nanocrystalline materials," *The Canadian Journal of Chemical Engineering*, vol. 84, no. 5, pp. 513-519, 2006.
[125] C. López de Dicastillo, L. Garrido, N. Alvarado, J. Romero, J. L. Palma, and M. J. Galotto, "Improvement of Polylactide Properties through Cellulose Nanocrystals Embedded in Poly (Vinyl Alcohol) Electrospun Nanofibers," *Nanomaterials*, vol. 7, no. 5, p. 106, 2017.
[126] N. S. Cetin *et al.*, "Acetylation of cellulose nanowhiskers with vinyl acetate under moderate conditions," *Macromolecular Bioscience*, vol. 9, no. 10, pp. 997-1003, 2009.
[127] M. Andresen, L.-S. Johansson, B. S. Tanem, and P. Stenius, "Properties and characterization of hydrophobized microfibrillated cellulose," *Cellulose*, vol. 13, no. 6, pp. 665-677, 2006.
[128] H.-Y. Yu, R. Chen, G.-Y. Chen, L. Liu, X.-G. Yang, and J.-M. Yao, "Silylation of cellulose nanocrystals and their reinforcement of commercial silicone rubber," *Journal of Nanoparticle Research*, vol. 17, no. 9, p. 361, 2015.
[129] C. Aulin, E. Johansson, L. Wågberg, and T. Lindström, "Self-organized films from cellulose I nanofibrils using the layer-by-layer technique," *Biomacromolecules*, vol. 11, no. 4, pp. 872-882, 2010.
[130] H. S. Yang, D. J. Gardner, and J. W. Nader, "Morphological properties of impact fracture surfaces and essential work of fracture analysis of cellulose nanofibril-filled polypropylene composites," *Journal of Applied Polymer Science*, vol. 128, no. 5, pp. 3064-3076, 2013.
[131] E. Kontturi, P. Thüne, A. Alexeev, and J. Niemantsverdriet, "Introducing open films of nanosized cellulose—atomic force microscopy and quantification of morphology," *Polymer*, vol. 46, no. 10, pp. 3307-3317, 2005.

[132] M. A. Herrera, A. P. Mathew, and K. Oksman, "Gas permeability and selectivity of cellulose nanocrystals films (layers) deposited by spin coating," *Carbohydrate polymers,* vol. 112, pp. 494-501, 2014.
[133] K. Ben Azouz, E. C. Ramires, W. Van den Fonteyne, N. El Kissi, and A. Dufresne, "Simple method for the melt extrusion of a cellulose nanocrystal reinforced hydrophobic polymer," *ACS Macro Letters,* vol. 1, no. 1, pp. 236-240, 2011.
[134] J. Huang, Y. Chen, and P. R. Chang, "Surface ModIfIcatIon of celluloSe nanocryStalS for nanocoMpoSIteS," *Surface Modification of Biopolymers,* p. 258, 2015.
[135] D. ASTM, "790-03," *Standard test methods for flexural properties of unreinforced and reinforced plastics and electrical insulating materials,* vol. 11, 2003.
[136] D. ASTM, "638-03: Standard Test Method for Tensile Properties of Plastics," *Current edition approved Apr,* vol. 1, pp. 1-16, 2008.
[137] E. Quero, A. J. Müller, F. Signori, M. B. Coltelli, and S. Bronco, "Isothermal Cold-Crystallization of PLA/PBAT Blends With and Without the Addition of Acetyl Tributyl Citrate," *Macromolecular Chemistry and Physics,* vol. 213, no. 1, pp. 36-48, 2012.
[138] I. ASTM D, "Standard practice for plastics: Dynamic mechanical properties: Determination and report of procedures," ed: ASTM International, 2012.
[139] A. D256, "Standard test method for determining the Izod pendulum impact resistance of plastics," *Philadelphia, PA: American Society for Testing Materials International,* 2005.
[140] A. B. Strong, D. Yarnell, Ed. *Plastics: materials and processing,* Third ed. New Jersey, Columbus, Ohio: Prentice Hall, 2006, p. 917.
[141] H. Gao and T. Qiang, "Fracture Surface Morphology and Impact Strength of Cellulose/PLA Composites," *Materials,* vol. 10, no. 6, p. 624, 2017.
[142] M. Todo and T. Takayama, "Fracture mechanisms of biodegradable PLA and PLA/PCL blends," in *Biomaterials-Physics and Chemistry*: InTech, 2011.
[143] M. Yasuniwa, K. Sakamo, Y. Ono, and W. Kawahara, "Melting behavior of poly (l-lactic acid): X-ray and DSC analyses of the melting process," *Polymer,* vol. 49, no. 7, pp. 1943-1951, 2008.
[144] A. Nijenhuis, E. Colstee, D. Grijpma, and A. Pennings, "High molecular weight poly (L-lactide) and poly (ethylene oxide) blends: Thermal characterization and physical properties," *Polymer,* vol. 37, no. 26, pp. 5849-5857, 1996.
[145] O. Martin and L. Averous, "Poly (lactic acid): plasticization and properties of biodegradable multiphase systems," *Polymer,* vol. 42, no. 14, pp. 6209-6219, 2001.
[146] K. Halász and L. Csóka, "Plasticized biodegradable poly (lactic acid) based composites containing cellulose in micro-and nanosize," *Journal of Engineering,* vol. 2013, 2013.
[147] Y. Du, T. Wu, N. Yan, M. T. Kortschot, and R. Farnood, "Fabrication and characterization of fully biodegradable natural fiber-reinforced poly (lactic acid) composites," *Composites Part B: Engineering,* vol. 56, pp. 717-723, 2014.
[148] E. Fortunati *et al.*, "Multifunctional bionanocomposite films of poly (lactic acid), cellulose nanocrystals and silver nanoparticles," *Carbohydrate polymers,* vol. 87, no. 2, pp. 1596-1605, 2012.
[149] M. Tyona, "A theoritical study on spin coating technique," *Advances in materials Research,* vol. 2, no. 4, pp. 195-208, 2013.
[150] R. P. Chartoff, J. D. Menczel, and S. H. Dillman, "Dynamic mechanical analysis (DMA)," *Thermal analysis of polymers: fundamentals and applications,* pp. 387-495, 2009.

[151] L. A. Pothan, Z. Oommen, and S. Thomas, "Dynamic mechanical analysis of banana fiber reinforced polyester composites," *Composites Science and Technology,* vol. 63, no. 2, pp. 283-293, 2003.
[152] E. Hassan, Y. Wei, H. Jiao, and Y. Muhuo, "Dynamic mechanical properties and thermal stability of poly (lactic acid) and poly (butylene succinate) blends composites," *Journal of Fiber Bioengineering and Informatics,* vol. 6, no. 1, pp. 85-94, 2013.
[153] E. Fortunati *et al.*, "Microstructure and nonisothermal cold crystallization of PLA composites based on silver nanoparticles and nanocrystalline cellulose," *Polymer Degradation and Stability,* vol. 97, no. 10, pp. 2027-2036, 2012.
[154] D. V. Plackett *et al.*, "Characterization of l-polylactide and l-polylactide–polycaprolactone co-polymer films for use in cheese-packaging applications," *Packaging Technology and Science,* vol. 19, no. 1, pp. 1-24, 2006.
[155] R. Al-Itry, K. Lamnawar, and A. Maazouz, "Reactive extrusion of PLA, PBAT with a multi-functional epoxide: Physico-chemical and rheological properties," *European Polymer Journal,* vol. 58, pp. 90-102, 2014.
[156] M. Hernández-Alamilla and A. Valadez-Gonzalez, "The effect of two commercial melt strength enhancer additives on the thermal, rheological and morphological properties of polylactide," *Journal of Polymer Engineering,* vol. 36, no. 1, pp. 31-41, 2016.
[157] E. Espino-Pérez *et al.*, "Designed cellulose nanocrystal surface properties for improving barrier properties in polylactide nanocomposites," *Carbohydrate Polymers,* vol. 183, pp. 267-277, 2018.
[158] S. Huan, G. Liu, W. Cheng, G. Han, and L. Bai, "Electrospun Poly (lactic acid)-Based Fibrous Nanocomposite Reinforced by Cellulose Nanocrystals: Impact of Fiber Uniaxial Alignment on Microstructure and Mechanical Properties," *Biomacromolecules,* 2018.
[159] M. R. Kamal and V. Khoshkava, "Effect of cellulose nanocrystals (CNC) on rheological and mechanical properties and crystallization behavior of PLA/CNC nanocomposites," *Carbohydrate polymers,* vol. 123, pp. 105-114, 2015.
[160] E. Fortunati, W. Yang, F. Luzi, J. Kenny, L. Torre, and D. Puglia, "Lignocellulosic nanostructures as reinforcement in extruded and solvent casted polymeric nanocomposites: an overview," *European Polymer Journal,* vol. 80, pp. 295-316, 2016.
[161] Y. C. Ching *et al.*, "Rheological properties of cellulose nanocrystal-embedded polymer composites: a review," *Cellulose,* vol. 23, no. 2, pp. 1011-1030, 2016.
[162] M. Majid, E.-D. Hassan, A. Davoud, and M. Saman, "A study on the effect of nano-ZnO on rheological and dynamic mechanical properties of polypropylene: experiments and models," *Composites Part B: Engineering,* vol. 42, no. 7, pp. 2038-2046, 2011.
[163] W. M. Chávez-Montes, G. González-Sánchez, E. I. López-Martínez, P. de Lira-Gómez, L. Ballinas-Casarrubias, and S. Flores-Gallardo, "Effect of artificial weathering on PLA/nanocomposite molecular weight distribution," *Polymers,* vol. 7, no. 4, pp. 760-776, 2015.
[164] M. Murariu, L. Bonnaud, P. Yoann, G. Fontaine, S. Bourbigot, and P. Dubois, "New trends in polylactide (PLA)-based materials:“Green” PLA–Calcium sulfate (nano) composites tailored with flame retardant properties," *Polymer Degradation and Stability,* vol. 95, no. 3, pp. 374-381, 2010.
[165] L. Zaidi, M. Kaci, S. Bruzaud, A. Bourmaud, and Y. Grohens, "Effect of natural weather on the structure and properties of polylactide/Cloisite 30B nanocomposites," *Polymer Degradation and Stability,* vol. 95, no. 9, pp. 1751-1758, 2010.

[166] Y. Fujimoto, S. S. Ray, M. Okamoto, A. Ogami, K. Yamada, and K. Ueda, "Well-Controlled Biodegradable Nanocomposite Foams: From Microcellular to Nanocellular," *Macromolecular Rapid Communications,* vol. 24, no. 7, pp. 457-461, 2003.
[167] S. S. Ray and M. Okamoto, "Biodegradable polylactide and its nanocomposites: opening a new dimension for plastics and composites," *Macromolecular Rapid Communications,* vol. 24, no. 14, pp. 815-840, 2003.
[168] K. Fukushima, D. Tabuani, C. Abbate, M. Arena, and L. Ferreri, "Effect of sepiolite on the biodegradation of poly (lactic acid) and polycaprolactone," *Polymer Degradation and Stability,* vol. 95, no. 10, pp. 2049-2056, 2010.
[169] K. King, "Changes in the functional properties and molecular weight of sodium alginate following γ irradiation," *Food hydrocolloids,* vol. 8, no. 2, pp. 83-96, 1994.
[170] N. Karak, *Fundamentals of polymers: raw materials to finish products*. PHI Learning Pvt. Ltd., 2009.
[171] F. Panzer, H. Bässler, R. Lohwasser, M. Thelakkat, and A. Köhler, "The impact of polydispersity and molecular weight on the order–disorder transition in poly (3-hexylthiophene)," *The journal of physical chemistry letters,* vol. 5, no. 15, pp. 2742-2747, 2014.
[172] A. J. Crosby and J. Y. Lee, "Polymer nanocomposites: the "nano" effect on mechanical properties," *Polymer reviews,* vol. 47, no. 2, pp. 217-229, 2007.
[173] A. Pinheiro and J. F. Mano, "Study of the glass transition on viscous-forming and powder materials using dynamic mechanical analysis," *Polymer Testing,* vol. 28, no. 1, pp. 89-95, 2009.
[174] L. Priya and J. Jog, "Poly (vinylidene fluoride)/clay nanocomposites prepared by melt intercalation: crystallization and dynamic mechanical behavior studies," *Journal of Polymer Science Part B: Polymer Physics,* vol. 40, no. 15, pp. 1682-1689, 2002.
[175] T. G. Fox and P. J. Flory, "The glass temperature and related properties of polystyrene. Influence of molecular weight," *Journal of Polymer Science Part A: Polymer Chemistry,* vol. 14, no. 75, pp. 315-319, 1954.
[176] D. Hill, M. Perera, P. Pomery, and H. Toh, "Dynamic mechanical properties of networks prepared from siloxane modified divinyl benzene pre-polymers," *Polymer,* vol. 41, no. 26, pp. 9131-9137, 2000.
[177] P. Kucharczyk, A. Pavelková, P. Stloukal, and V. Sedlarík, "Degradation behaviour of PLA-based polyesterurethanes under abiotic and biotic environments," *Polymer Degradation and Stability,* vol. 129, pp. 222-230, 2016.
[178] J. Wang, H. Huang, and X. Huang, "Molecular weight and the Mark-Houwink relation for ultra-high molecular weight charged polyacrylamide determined using automatic batch mode multi-angle light scattering," *Journal of Applied Polymer Science,* vol. 133, no. 31, 2016.
[179] E. Morris, A. Cutler, S. Ross-Murphy, D. Rees, and J. Price, "Concentration and shear rate dependence of viscosity in random coil polysaccharide solutions," *Carbohydrate polymers,* vol. 1, no. 1, pp. 5-21, 1981.
[180] A. Franck, "Understanding rheology of thermoplastic polymers," *TA Instruments,* vol. 118, pp. 1-8, 2004.
[181] J. J. Cooper-White and M. E. Mackay, "Rheological properties of poly (lactides). Effect of molecular weight and temperature on the viscoelasticity of poly (l-lactic acid),"

Journal of Polymer Science Part B: Polymer Physics, vol. 37, no. 15, pp. 1803-1814, 1999.
[182] L. Le Pluart, J. Duchet, H. Sautereau, P. Halley, and J.-F. Gerard, "Rheological properties of organoclay suspensions in epoxy network precursors," *Applied clay science,* vol. 25, no. 3-4, pp. 207-219, 2004.
[183] H. Li and M. A. Huneault, "Effect of nucleation and plasticization on the crystallization of poly (lactic acid)," *Polymer,* vol. 48, no. 23, pp. 6855-6866, 2007.
[184] R. Al-Itry, K. Lamnawar, and A. Maazouz, "Improvement of thermal stability, rheological and mechanical properties of PLA, PBAT and their blends by reactive extrusion with functionalized epoxy," *Polymer Degradation and Stability,* vol. 97, no. 10, pp. 1898-1914, 2012.
[185] R. Bhardwaj and A. K. Mohanty, "Modification of brittle polylactide by novel hyperbranched polymer-based nanostructures," *Biomacromolecules,* vol. 8, no. 8, pp. 2476-2484, 2007.
[186] A. Abdulkhani, J. Hosseinzadeh, A. Ashori, S. Dadashi, and Z. Takzare, "Preparation and characterization of modified cellulose nanofibers reinforced polylactic acid nanocomposite," *Polymer testing,* vol. 35, pp. 73-79, 2014.
[187] J.-G. Gwon *et al.*, "Mechanical and thermal properties of toluene diisocyanate-modified cellulose nanocrystal nanocomposites using semi-crystalline poly (lactic acid) as a base matrix," *RSC Advances,* vol. 6, no. 77, pp. 73879-73886, 2016.
[188] L. Valentini, M. Cardinali, E. Fortunati, L. Torre, and J. Kenny, "A novel method to prepare conductive nanocrystalline cellulose/graphene oxide composite films," *Materials Letters,* vol. 105, pp. 4-7, 2013.
[189] Y. Habibi, L. A. Lucia, and O. J. Rojas, "Cellulose nanocrystals: chemistry, self-assembly, and applications," *Chemical reviews,* vol. 110, no. 6, pp. 3479-3500, 2010.
[190] M. Mariano *et al.*, "Preparation of Cellulose Nanocrystal-Reinforced Poly (lactic acid) Nanocomposites through Noncovalent Modification with PLLA-Based Surfactants," *ACS Omega,* vol. 2, no. 6, pp. 2678-2688, 2017.
[191] J. Yang, C.-R. Han, X.-M. Zhang, F. Xu, and R.-C. Sun, "Cellulose nanocrystals mechanical reinforcement in composite hydrogels with multiple cross-links: correlations between dissipation properties and deformation mechanisms," *Macromolecules,* vol. 47, no. 12, pp. 4077-4086, 2014.
[192] R. Prathapan, J. D. Berry, A. Fery, G. Garnier, and R. F. Tabor, "Decreasing the wettability of cellulose nanocrystal surfaces using wrinkle-based alignment," *ACS Applied Materials & Interfaces,* vol. 9, no. 17, pp. 15202-15211, 2017.
[193] Y. Yoo and J. P. Youngblood, "Green one-pot synthesis of surface hydrophobized cellulose nanocrystals in aqueous medium," *ACS Sustainable Chemistry & Engineering,* vol. 4, no. 7, pp. 3927-3938, 2016.
[194] S. Gazzotti *et al.*, "Polylactide/cellulose nanocrystals: The in situ polymerization approach to improved nanocomposites," *European Polymer Journal,* vol. 94, pp. 173-184, 2017.
[195] E. Espino-Pérez, S. Domenek, N. Belgacem, C. c. Sillard, and J. Bras, "Green process for chemical functionalization of nanocellulose with carboxylic acids," *Biomacromolecules,* vol. 15, no. 12, pp. 4551-4560, 2014.

[196] D. O. de Castro, J. Bras, A. Gandini, and N. Belgacem, "Surface grafting of cellulose nanocrystals with natural antimicrobial rosin mixture using a green process," *Carbohydrate polymers,* vol. 137, pp. 1-8, 2016.
[197] F. H. Gojny, M. H. Wichmann, B. Fiedler, and K. Schulte, "Influence of different carbon nanotubes on the mechanical properties of epoxy matrix composites–a comparative study," *Composites Science and Technology,* vol. 65, no. 15, pp. 2300-2313, 2005.
[198] B. B. Mandelbrot, D. E. Passoja, and A. J. Paullay, "Fractal character of fracture surfaces of metals," *Nature,* vol. 308, no. 5961, pp. 721-722, 1984.
[199] K. Okubo, T. Fujii, and E. T. Thostenson, "Multi-scale hybrid biocomposite: processing and mechanical characterization of bamboo fiber reinforced PLA with microfibrillated cellulose," *Composites Part A: Applied Science and Manufacturing,* vol. 40, no. 4, pp. 469-475, 2009.
[200] X. Xu, F. Liu, L. Jiang, J. Zhu, D. Haagenson, and D. P. Wiesenborn, "Cellulose nanocrystals vs. cellulose nanofibrils: a comparative study on their microstructures and effects as polymer reinforcing agents," *ACS applied materials & interfaces,* vol. 5, no. 8, pp. 2999-3009, 2013.
[201] J. Gong, J. Li, J. Xu, Z. Xiang, and L. Mo, "Research on cellulose nanocrystals produced from cellulose sources with various polymorphs," *RSC Advances,* vol. 7, no. 53, pp. 33486-33493, 2017.
[202] N. Yildirim and S. Shaler, "A study on thermal and nanomechanical performance of cellulose nanomaterials (CNs)," *Materials,* vol. 10, no. 7, p. 718, 2017.
[203] M. Parit, "Thermoplastic polymer nanocomposites," 2016.
[204] P. Dhar, D. Tarafder, A. Kumar, and V. Katiyar, "Effect of cellulose nanocrystal polymorphs on mechanical, barrier and thermal properties of poly(lactic acid) based bionanocomposites," *RSC Advances,* vol. 5, no. 74, pp. 60426-60440, 2015.
[205] Y. W. Chen, T. H. Tan, H. V. Lee, and S. B. Abd Hamid, "Easy Fabrication of Highly Thermal-Stable Cellulose Nanocrystals Using Cr (NO3) 3 Catalytic Hydrolysis System: A Feasibility Study from Macro-to Nano-Dimensions," *Materials,* vol. 10, no. 1, p. 42, 2017.
[206] L. Chen, J. Zhu, C. Baez, P. Kitin, and T. Elder, "Highly thermal-stable and functional cellulose nanocrystals and nanofibrils produced using fully recyclable organic acids," *Green Chemistry,* vol. 18, no. 13, pp. 3835-3843, 2016.
[207] M. Grunert and W. T. Winter, "Nanocomposites of cellulose acetate butyrate reinforced with cellulose nanocrystals," *Journal of Polymers and the Environment,* vol. 10, no. 1, pp. 27-30, 2002.
[208] T. Yamanobe, K. Ueki, T. Komoto, and H. Uehara, "Structure and molecular mobility of nascent isotactic polypropylene powders," *Polymer journal,* vol. 44, no. 8, pp. 764-771, 2012.
[209] R. P. Babu, K. O'connor, and R. Seeram, "Current progress on bio-based polymers and their future trends," *Progress in Biomaterials,* vol. 2, no. 1, p. 8, 2013.
[210] S. A. Kedzior, H. S. Marway, and E. D. Cranston, "Tailoring cellulose nanocrystal and surfactant behavior in miniemulsion polymerization," *Macromolecules,* vol. 50, no. 7, pp. 2645-2655, 2017.
[211] R. M. Rasal, A. V. Janorkar, and D. E. Hirt, "Poly (lactic acid) modifications," *Progress in polymer science,* vol. 35, no. 3, pp. 338-356, 2010.

[212] J.-M. Raquez, Y. Habibi, M. Murariu, and P. Dubois, "Polylactide (PLA)-based nanocomposites," *Progress in Polymer Science*, vol. 38, no. 10, pp. 1504-1542, 2013.
[213] Y. Li and H. Shimizu, "Toughening of polylactide by melt blending with a biodegradable poly (ether) urethane elastomer," *Macromolecular bioscience*, vol. 7, no. 7, pp. 921-928, 2007.
[214] Y.-I. Hsu, K. Masutani, T. Yamaoka, and Y. Kimura, "Strengthening of hydrogels made from enantiomeric block copolymers of polylactide (PLA) and poly (ethylene glycol)(PEG) by the chain extending Diels–Alder reaction at the hydrophilic PEG terminals," *Polymer*, vol. 67, pp. 157-166, 2015.
[215] H.-M. Ng, L. T. Sin, S.-T. Bee, T.-T. Tee, and A. Rahmat, "Review of Nanocellulose Polymer Composite Characteristics and Challenges," *Polymer-Plastics Technology and Engineering*, vol. 56, no. 7, pp. 687-731, 2017.
[216] H. Sehaqui, T. Zimmermann, and P. Tingaut, "Hydrophobic cellulose nanopaper through a mild esterification procedure," *Cellulose*, vol. 21, no. 1, pp. 367-382, 2014.
[217] C. Fraschini, G. Chauve, and J. Bouchard, "TEMPO-mediated surface oxidation of cellulose nanocrystals (CNCs)," *Cellulose*, pp. 1-16, 2017.
[218] H. de la Motte, M. Hasani, H. Brelid, and G. Westman, "Molecular characterization of hydrolyzed cationized nanocrystalline cellulose, cotton cellulose and softwood kraft pulp using high resolution 1D and 2D NMR," *Carbohydrate polymers*, vol. 85, no. 4, pp. 738-746, 2011.
[219] F. Hoeng, A. Denneulin, C. Neuman, and J. Bras, "Charge density modification of carboxylated cellulose nanocrystals for stable silver nanoparticles suspension preparation," *Journal of Nanoparticle Research*, vol. 17, no. 6, p. 244, 2015.
[220] E. L. d. Paula, V. Mano, E. A. R. Duek, and F. V. Pereira, "Hydrolytic degradation behavior of PLLA nanocomposites reinforced with modified cellulose nanocrystals," *Química Nova*, vol. 38, no. 8, pp. 1014-1020, 2015.
[221] P. Tingaut, T. Zimmermann, and G. Sèbe, "Cellulose nanocrystals and microfibrillated cellulose as building blocks for the design of hierarchical functional materials," *Journal of Materials Chemistry*, vol. 22, no. 38, pp. 20105-20111, 2012.
[222] L.-L. Dong, L. He, G.-H. Tao, and C. Hu, "High yield of ethyl valerate from the esterification of renewable valeric acid catalyzed by amino acid ionic liquids," *RSC Advances*, vol. 3, no. 14, pp. 4806-4813, 2013.
[223] W. H. Organization. (1997, 2/16/2018). *Evaluations of the Joint FAO/WHO Expert Commitee on Food Additives (JECFA)*.
[224] H. Rosilo, E. Kontturi, J. Seitsonen, E. Kolehmainen, and O. Ikkala, "Transition to reinforced state by percolating domains of intercalated brush-modified cellulose nanocrystals and poly (butadiene) in cross-linked composites based on thiol–ene click chemistry," *Biomacromolecules*, vol. 14, no. 5, pp. 1547-1554, 2013.
[225] L. Tang *et al.*, "Ultrasonication-assisted manufacture of cellulose nanocrystals esterified with acetic acid," *Bioresource technology*, vol. 127, pp. 100-105, 2013.
[226] S. X. Peng, H. Chang, S. Kumar, R. J. Moon, and J. P. Youngblood, "A comparative guide to controlled hydrophobization of cellulose nanocrystals via surface esterification," *Cellulose*, vol. 23, no. 3, pp. 1825-1846, 2016.
[227] Y. Peng, D. J. Gardner, Y. Han, A. Kiziltas, Z. Cai, and M. A. Tshabalala, "Influence of drying method on the material properties of nanocellulose I: thermostability and crystallinity," *Cellulose*, vol. 20, no. 5, pp. 2379-2392, 2013.

[228] N. Wang, E. Ding, and R. Cheng, "Surface modification of cellulose nanocrystals," *Frontiers of Chemical Engineering in China,* vol. 1, no. 3, pp. 228-232, 2007.
[229] W. Du, J. Guo, H. Li, and Y. Gao, "Heterogeneously Modified Cellulose Nanocrystals-Stabilized Pickering Emulsion: Preparation and Their Template Application for the Creation of PS Microspheres with Amino-Rich Surfaces," *ACS Sustainable Chemistry & Engineering,* vol. 5, no. 9, pp. 7514-7523, 2017.
[230] M. Poletto, V. Pistor, and A. J. Zattera, "Structural characteristics and thermal properties of native cellulose," in *Cellulose-fundamental aspects*: InTech, 2013.
[231] M. Yasuniwa, S. Tsubakihara, Y. Sugimoto, and C. Nakafuku, "Thermal analysis of the double-melting behavior of poly (L-lactic acid)," *Journal of Polymer Science Part B: Polymer Physics,* vol. 42, no. 1, pp. 25-32, 2004.
[232] A. Gupta, W. Simmons, G. T. Schueneman, and E. A. Mintz, "Lignin-coated cellulose nanocrystals as promising nucleating agent for poly (lactic acid)," *Journal of Thermal Analysis and Calorimetry,* vol. 126, no. 3, pp. 1243-1251, 2016.
[233] Y. Di, S. Iannace, E. D. Maio, and L. Nicolais, "Poly (lactic acid)/organoclay nanocomposites: thermal, rheological properties and foam processing," *Journal of Polymer Science Part B: Polymer Physics,* vol. 43, no. 6, pp. 689-698, 2005.
[234] S. Singh and A. Mohanty, "Wood fiber reinforced bacterial bioplastic composites: Fabrication and performance evaluation," *Composites Science and Technology,* vol. 67, no. 9, pp. 1753-1763, 2007.
[235] T. Yu, J. Ren, S. Li, H. Yuan, and Y. Li, "Effect of fiber surface-treatments on the properties of poly (lactic acid)/ramie composites," *Composites Part A: Applied Science and Manufacturing,* vol. 41, no. 4, pp. 499-505, 2010.
[236] D. Bondeson and K. Oksman, "Dispersion and characteristics of surfactant modified cellulose whiskers nanocomposites," *Composite Interfaces,* vol. 14, no. 7-9, pp. 617-630, 2007.
[237] J. Muller, C. González-Martínez, and A. Chiralt, "Combination of Poly (lactic) Acid and Starch for Biodegradable Food Packaging," *Materials,* vol. 10, no. 8, p. 952, 2017.
[238] K. Müller *et al.*, "Review on the processing and properties of polymer nanocomposites and nanocoatings and their applications in the packaging, automotive and solar energy fields," *Nanomaterials,* vol. 7, no. 4, p. 74, 2017.
[239] M. Montemor, "Smart Composite Coatings and Membranes: Transport, Structural, Environmental, and Energy Applications," 2016.